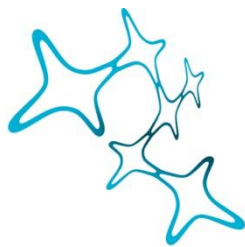


---

# VISUO-VESTIBULAR SENSORIMOTOR PLASTICITY IN XENOPUS AND AXOLOTL LARVAE

---



Graduate School of  
Systemic Neurosciences

LMU Munich



Parthena Schneider-Soupiadis

Dissertation at the  
Graduate School of Systemic Neurosciences  
Ludwig-Maximilians-Universität München

February, 2024



Supervisors

Prof. Dr. Hans Straka

Faculty of Biology

Ludwig-Maximilians-Universität München

Prof. Dr. med. Andreas Zwergal

Department of Neurology

Ludwig-Maximilians-Universität München

First Reviewer: Prof. Dr. med. Andreas Zwergal

Second Reviewer: Prof. Dr. Oliver Behrend

External Reviewer: Prof. Dr. Ansgar Büschges

Date of Submission: 06.02.2024

Date of Defense: 02.07.2024



*To my mom, who left us too soon and whose courage gave me the chance for a better life,  
and to my dad for his endless love.*

---

## SUMMARY

---

Locomotion causes disrupting consequences for sensory perception, which requires concurrent gaze stabilization to maintain visual acuity. Visuo-vestibular reflexes along with spinal efference copy signalling generate motor commands that enable the eyes to perceive a stable image during body/head movement. In vertebrates, these short-latency motor behaviors work synergistically and are evolutionarily well conserved. However, the underlying neural and circuit components must remain plastic and adapt to accommodate the eco-physiological requirements and locomotor characteristics of each species. This dissertation aimed to explore such adaptations of the oculomotor system ensuring gaze stabilization during self-motion. The following chapters focused on understanding how motor performances may be altered or improved in phylogenetically related species that share many similarities but also clear differences. This exploration got extended to pathological conditions, acutely after a severe loss of vestibular sensory input. For this, I profiled and compared the locomotion pattern of two amphibian species, the salamander Axolotl, and the frog *Xenopus laevis*. To ensure that potential differences were biologically meaningful I used similarly aged and sized animals of both species, at comparable developmental stages which were validated by comparing external morphological features. While *Xenopus* move more or less continuously, Axolotls exhibit interspersed, short bouts of locomotion followed by a passive glide. Moreover, *Xenopus* have longer bouts, while Axolotls display higher velocity bouts. *In vitro* whole-head recordings of the angular vestibulo-ocular reflex (VOR) in Axolotl were significantly lower in gain compared to *Xenopus* at identical stimulus conditions. Older staged Axolotls show an increase in gain but did only reach the level of stage 49 *Xenopus* hinting at a delayed developmental onset of angular gaze compensation. Further experiments on fictive locomotion revealed no compensation through efference copy derived eye motions. In addition, the capacity to stabilize gaze is critically dependent on the morphological parameters of inner ear structures. A comparative investigation of the horizontal canals revealed distinct differences in various parameters between *Xenopus* and Axolotl. These differences favor the dynamic of endolymph flow and, consequently, the capacity of semicircular canals to detect angular head accelerations in *Xenopus*.

In an additional set of experiments, I investigated the plasticity potential during pathological conditions, after the complete loss of unilateral vestibular input in *Xenopus*. Such a loss generates severe symptoms related to posture, eye movements, and higher-order perceptual deficits. While compensation of such injuries has been explored already extensively in various species, the novelty of my experiments involved *in vitro* whole head preparations. Such an approach enables a targeted nerve transection with a direct evaluation of its impact within minutes after the surgery, without the influence of anesthesia. Indeed, a severe impairment of the VOR could be observed after the lesion. However, a delayed further decline of both visual and vestibular reflexes persisted and did

not show any signs of compensation. This led to the conclusion that the sensory loss was intensified by secondary neuronal effects that likely involve plasticity mechanisms evoked by the ongoing asymmetric activity in the shared visuo-vestibular circuits.

---

## TABLE OF CONTENTS

---

<b>SUMMARY</b> .....	<b>IV</b>
<b>LIST OF ABBREVIATIONS</b> .....	<b>VII</b>
<b>CHAPTER I:</b> .....	<b>1</b>
<b>INTRODUCTION</b> .....	<b>1</b>
GENERAL INTRODUCTION AND AIMS .....	1
SELF-MOTION: IMPORTANCE & PROCESSING .....	2
VESTIBULAR MOTION SENSORS: ANATOMY, PHYSIOLOGY & CIRCUITRY .....	3
VISUAL MOTION SENSORS: ANATOMY, PHYSIOLOGY & CIRCUITRY .....	4
GAZE STABILIZATION: FUNCTION, COMPONENTS & CIRCUITRIES .....	5
<i>The vestibulo-ocular reflex (VOR)</i> .....	6
<i>The optokinetic reflex (OKR)</i> .....	7
<i>Spinal efference copy (EC) signaling</i> .....	8
PLASTICITY OF GAZE STABILIZING REFLEXES .....	9
<i>Phylogenetic adaptive plasticity</i> .....	9
<i>Lesion induced plasticity</i> .....	10
EXPERIMENTAL RATIONALE & AMPHIBIAN ANIMAL MODELS.....	11
<b>CHAPTER II:</b> .....	<b>13</b>
<b>A FUNCTIONAL COMPARISON BETWEEN INNER EAR MORPHOLOGY, GAZE STABILIZATION, AND LOCOMOTION IN LARVAL AMPHIBIANS</b> .....	<b>13</b>
<b>CHAPTER III:</b> .....	<b>36</b>
<b>ACUTE CONSEQUENCES OF A UNILATERAL VIIIITH NERVE TRANSECTION ON VESTIBULO-OCULAR AND OPTOKINETIC REFLEXES IN <i>XENOPUS LAEVIS</i> TADPOLES</b> .....	<b>36</b>
<b>CHAPTER IV:</b> .....	<b>53</b>
<b>DISCUSSION &amp; FUTURE DIRECTIONS</b> .....	<b>53</b>
<i>XENOPUS LAEVIS</i> & <i>AXOLOTL</i> LARVAE: IDEAL EXPERIMENTAL MODELS FOR STUDYING PLASTICITY IN SENSORIMOTOR CIRCUITS .....	54
SELF-MOTION & ITS CONSEQUENCES .....	55
VISUO-VESTIBULAR & EC PLASTICITY UNDER HEALTHY CONDITIONS .....	56
SEMICIRCULAR CANAL SENSITIVITY IS CONSTRAINED BY MORPHOLOGY .....	58
VISUO-VESTIBULAR PLASTICITY UNDER PATHOLOGICAL CONDITIONS .....	59
CONCLUSIONS & FUTURE DIRECTIONS .....	61
<b>REFERENCES</b> .....	<b>64</b>
<b>ACKNOWLEDGMENTS</b> .....	<b>77</b>
<b>LIST OF PUBLICATIONS</b> .....	<b>79</b>
<b>AI DISCLOSURE</b> .....	<b>80</b>
<b>AFFIDAVIT/EIDESTÄTLICHE ERKLÄRUNG</b> .....	<b>81</b>
<b>DECLARATION OF AUTHOR CONTRIBUTIONS</b> .....	<b>82</b>

---

## LIST OF ABBREVIATIONS

---

AOS	accessory optic system
CNS	central nervous system
CPG(s)	central pattern generator(s)
EC	efference copy
EOM(s)	extraocular muscle(s)
DTN	dorsal terminal nucleus
IO	inferior oblique
IR	inferior rectus
LR	lateral rectus
LTN	lateral terminal nucleus
MR	medial rectus
MTN	medial terminal nucleus
nII	optic nerve
nIII	oculomotor nerve
nVI	abducens nerve
nIV	trochlear nerve
nBOR	nucleus of the basal optic root
NLM	nucleus lentiformis mesencephali
NOT	nucleus of the optic tract
(a,g,l)VOR	(angular, gravitational, linear) vestibulo-ocular reflex
(h,t)OKR	(horizontal, torsional) optokinetic reflex
RGC(s)	retinal ganglion cell(s)
SO	superior oblique
SR	superior rectus

---

## CHAPTER I: INTRODUCTION

---

### GENERAL INTRODUCTION AND AIMS

Sensory systems have evolved over millions of years to allow individuals to interact and respond to changes in their environments (Linford et al., 2011). Based on the location and characteristics of their peripheral receptors, sensory systems have been grouped into the sense of hearing, vision, olfaction, touch, and taste. Apart from these classic sensory divisions in humans, more specialized modalities exist (Hodos and Butler, 1997) that enable the detection of different ranges of the same physical input, like infrared vision in rattlesnakes (Schroeder and Loop, 1976) or completely different physical stimuli such as detecting the magnetic field of the earth present in migrating birds (Mouritsen, 2015). Among those sensory modalities, one of the most underestimated and widespread senses in the animal kingdom is the vestibular system without the existence of which common everyday activities would be unfeasible. The vestibular system allows us, amongst a wide variety of other capabilities, to navigate in space, control our posture, and keep our gaze stable by generating appropriate motor commands compensating for head and/or body movements during self-motion (Day and Fitzpatrick, 2005). From an evolutionary perspective, animals could only undergo a transition from a sessile lifestyle to free locomotion due to the emergence of vestibular endorgans (Straka and Gordy, 2020). Due to its major importance in freely moving animals, the vestibular system is one of the most evolutionarily conserved senses among vertebrates (Lipovsek and Wingate, 2018). This high conservation is, with a few exceptions in some species, applicable to all the components of its circuitry (Fritzsche, 1998; Straka et al., 2014). Despite this hard-wired nature of the vestibular system, it is nevertheless able to adapt to varying degrees and mechanisms, which is, among others, manifested in changes in its output (Miles and Lisberger, 1981). This adaptability, called plasticity, allows for the generation of appropriate motor outputs to the same stimulus under varying internal and environmental conditions.

This thesis aims to explore plasticity in visuo-vestibular ocular reflexes ensuring visual acuity during locomotion. As mentioned above, plasticity enables a species to respond optimally to changing and complex environments, beyond developmentally defined functionalities. This can manifest in varying ways and levels within the nervous system. Studying plasticity and its impact on oculomotor systems maintaining gaze stability is therefore a multifaceted undertaking. My experiments aimed at investigating how different neuronal and anatomical elements contribute to plasticity, both in the context of evolution as well as in response to a sudden absence of unilateral sensory input. The experimental model organisms I used to shed more light on this question are two amphibian species, the African clawed frog *Xenopus laevis*, and the Mexican salamander *Ambystoma mexicanum*,

colloquially called Axolotl. Both species share various similarities and allow the employment of *in-vitro* preparations, providing many experimental advantages, which I will elaborate on more in the following parts of this chapter. My first study (Schneider-Soupiadis et al., unpublished manuscript), constituting chapter II, aimed to investigate plasticity within evolutionarily related species by correlating and comparing the locomotion pattern, gaze stabilizing performance, and morphology of vestibular sensors in *Xenopus* and Axolotl. The focus of my second research project, presented in chapter III, focused on elucidating plasticity within a single species after an acute loss of peripheral vestibular function and its functional impact on gaze stabilization in *Xenopus* tadpoles. In my final chapter, I discuss the implication of these two studies to the current field of research.

## SELF-MOTION: IMPORTANCE & PROCESSING

The awareness of our own movement in space is an essential sensory perception used in everyday life. Tasks such as orientation and navigation in space, posture control, obstacle avoidance, and spatial memory generation are dependent on accurate discernment of self-motion (Campos and Bühlhoff, 2012). Moreover, the capability to perceive and interpret self-motion is a fundamental trait shared by all vertebrates. This ability plays a crucial role for an animal's survival, especially when detecting an approaching predator or pursuing escaping prey, for instance. Self-motion is typically experienced during active locomotion (e.g. swimming, walking, running) within the environment, but also during passive motion (e.g. being displaced by an external medium), and relies strongly on various motion detecting sensory systems (Campos and Bühlhoff, 2012). Despite the considerable importance of auditory inputs (Tanahashi et al., 2015) and proprioceptive information allowing for approximations of positional changes of our body and limbs (Cullen and Zobeiri, 2021), the major sensory input for self-motion detection is provided by vestibular and visual receptor cells (DeAngelis and Angelaki, 2012). As mentioned above, the vestibular system encodes positional changes of our head/body through acceleration sensors located in the inner ear (Angelaki and Cullen, 2008), while the visual system provides information on the relative motion of an observer (self-motion) or object (Barnes, 1983). In order to have a holistic and reliable estimation of the extent, speed, and direction of either self-and/or object motion, visual and vestibular inputs are integrated together, maintaining a high level of visual acuity. Since this visuo-vestibular interaction is a major aspect of this thesis, I will elaborate more on the functional connectivity of these two sensory systems in the following sections.

## VESTIBULAR MOTION SENSORS: ANATOMY, PHYSIOLOGY & CIRCUITRY

Motion detection through the vestibular system arises from dedicated bilateral inner ear organs constituting a complex network of ducts and pouches. These endorgans are composed of motion sensitive elements, the mechanoreceptive hair cells, embedded in direction specific structures to encode all vectors of a three-dimensional movement (Mackowetzky et al., 2021). More precisely, jawed vertebrates possess on each cranial side three fluid filled circular tubes, the semicircular canals, which sense rotational movements of the head/body (Angelaki and Cullen, 2008; Groves and Fekete, 2012). These ducts are almost perpendicular to each other and are named after their predominant plane of sensitivity horizontal, anterior-vertical, and posterior-vertical canal (Platt and Straka, 2020). Rotation of the head induces motion of the fluid, the endolymph, the inertia of which deflects the cupula (Straka et al., 2021). The cupula is a gelatinous structure in which the motion sensitive hair cell bundles are embedded and is located at one terminal end of each canal (Goyens et al., 2019). Depending on the dimension of rotation only the semicircular canal pair of the matching dimensional plane will result in either excitation or inhibition of the innervating sensory neuron (Blanks et al., 1975; Deans, 2021). Moreover, based on the direction of acceleration, only the semicircular canal towards which the head is moving will lead to the facilitation/activation of its downstream circuit connections. Conversely, the opposite effect occurs in its coplanar semicircular canal pair, operating in a “push-pull” mode (Fetter, 2016). On the other hand, translational movements as well as positional changes within the earth’s gravitational field are sensed by otolith organs (Platt and Straka, 2020). Unlike the canals, otolith organs are more diverse with respect to their occurrence and function. There are at least two otolith organs found in jawed vertebrates, the utricle and saccule (Lysakowski and Goldberg, 2004). In non-mammals and some monotremes a third endorgan exists, the lagena (de Burlet, 1929) as well as a few further, more specialized, which are not relevant to the context of this thesis. However, each otolith organ is filled with endolymph and consists of a sensory epithelium, the macula that contains hair cells. Their stereocilia bundles are surrounded by a gelatinous matrix, which in turn is covered by calcium carbonate crystals, called otoconia (Popper et al., 2005). During displacements of the head, the inertia of this crystal mass induces the displacement of stereocilia and thus determines the synaptic vesicle release on the afferent neuron (elucidated in the following paragraph). Similar to the motion encoding properties of the canals, orientation of the otoliths in the head is key for their sensitivity (Lindeman, 1969) and allows them to decompose the full range of linear acceleration vectors along three-dimensional space (Platt and Straka, 2020). The general principle of how motion transduction works on the hair cell level, for both types of vestibular endorgans, will be explained in the following paragraph.

Motion transduction originates at the hair cell level, each of which is composed of a large kinocilium followed by multiple stereocilia organized in a staircase fashion with a mechanical link along their dorsal tips (Fritzsche and Straka, 2014). These hair cells have their apical parts surrounded by endorgan specific structures which either contain a potassium

(K<sup>+</sup>)-rich fluid, the endolymph, or a gelatinous membrane. Mechanical displacements of the hair cell bundles toward the kinocilium, open ion channels (K<sup>+</sup> and Ca<sup>2+</sup>) leading to a depolarization of the membrane, while deflection in the opposite direction causes a hyperpolarization, thereby converting sensory information into a receptor potential (Hudspeth, 2005; Meredith and Rennie, 2016). Subsequently, upon depolarization, neurotransmitter vesicles are released at the synapse between the hair cell and afferent neuron which leads to changes in its spontaneous firing rate (Mukhopadhyay and Pangrsic, 2022). Afferent/primary vestibular neurons are bipolar, connecting hair cells placed in the different endorgans on one end to hindbrain second-order vestibular neurons on the other end via the vestibular/8<sup>th</sup> nerve (Maklad and Fritzsich, 2003). Their cell bodies are located between the sensory periphery and brain, close to auditory neurons, and constitute the ganglion of Scarpa (Curthoys, 1981; Koundakjian et al., 2007). Information about linear and angular acceleration is further processed in different groups of central vestibular neurons which are classified according to their anatomical location along the vertebrate hindbrain and constitute the later-, medial-, superior-, and inferior-vestibular nucleus (Branoner et al., 2016; Horn, 2020). Moreover, the nuclei on both brainstem hemispheres are interconnected by commissural pathways, ensuring a balanced activity at rest (Malinvaud et al., 2010). Aside from vestibular information, vestibular nuclei receive proprioceptive and visual inputs as well as motor signals (Angelaki et al., 2009; Cullen, 2019). This is another unique feature of the vestibular system. Unlike other sensory systems, it is composed of multimodal integrating nuclei that converge information about self-motion in space. As to the outputs of central vestibular neurons, their projections range from the thalamus and hippocampus (navigation and orientation in space) to the cerebellum (adaptive plasticity), and spinal cord (posture stabilization) (Straka and Grody, 2020). The most relevant projection though in the context of this thesis is the vestibular-ocular connectivity responsible for gaze stabilization which is going to be elaborated on further after the introduction of the basic principles of the visual system.

## VISUAL MOTION SENSORS: ANATOMY, PHYSIOLOGY & CIRCUITRY

As indicated earlier, the visual system serves as the second significant processor of self-motion. The motion sensitive elements are located in the retina of each vertebrate eye, a multilayered structure composed of various cell types (Stenkamp, 2015). The physical stimulus of this sensory system, light/photons, is absorbed by specialized cells known as photoreceptors. There are two kinds of light sensitive cells, rods and cones, each composed of an outer membrane segment that houses the phototransduction machinery (Sung et al., 1994). These two cell types complement one another to adjust vision to varying intensities of light. Thus, rods have a high sensitivity for low light intensities, able to detect single photons, and are therefore the abundant cell type in nocturnal/night-vision animals (Ingram et al., 2016). In contrast to rods, cones are less sensitive to light but operate at bright light conditions with high spatial acuity and mediate colour vision (Kawamura and Tachibanaki,

2022). Moreover, the number and type of cones determines the visual spectrum sensitivity of each animal, which can range from ultraviolet to infrared vision.

Unlike the typical depolarization of a receptor cell, photoreceptors hyperpolarize upon photon absorption and convert light energy into a chemical signal (Kawamura, 1994). Following the first layer of light transduction, photoreceptors connect to the spike generating neurons, the retinal ganglion cells (RGCs) via an intermediate layer of bipolar cells (Erskine and Herrera, 2014). The interconnection between photoreceptor and bipolar cells, as well as between bipolar and RGCs, is influenced and refined by inhibitory horizontal and amacrine cells (Gollisch and Meister, 2010). The final stage of retinal signal is conveyed by the axons of RGCs, collectively forming the optic nerve, to the brain. In amphibians, this signal mostly crosses to the contralateral hemisphere, ultimately reaching the pretectal nuclei before ending up in the optic tectum, while in mammals this information travels through the thalamus to reach the primary visual cortex (Benfey et al., 2022).

Returning to the mechanism of motion detection, during self-motion the entire visual scene is shifted together with the head/body. This shift, commonly referred to as "optic flow," serves as a source of estimation of bodily motion through space (Mauss and Borst, 2019). The process of computing motion operates by analyzing the spatial and temporal brightness changes of a visual scene or object, which occurs as motion takes place (Borst and Egelhaaf, 1993). These brightness fluctuations are perceived by photoreceptors, with each receptor cell corresponding to a specific position of the visual field. Furthermore, motion selective populations of RGCs have been found to respond preferentially to specific directions of motion (Barlow and Hill, 1963; Matsumoto et al., 2019). However, bipolar and amacrine cells also play a significant role in visual motion processing (Taylor and Smith, 2012; Hellmer et al., 2021). Taken together, the main principle of motion computation is determined by calculating the difference between the spatial alteration of brightness and the temporal change occurring at a particular point within the image (Mauss et al., 2017). It is worth noting that relying solely on optic flow and therefore visual input is not always sufficient to accurately perceive self-motion. Illusions of motion can be generated despite being physically stationary as experienced when e.g. a neighboring train begins to move (Dichgans and Brandt, 1978). Hence, the integration of visual and vestibular information, among other inputs, is essential for the correct interpretation and response to self-motion.

## GAZE STABILIZATION: FUNCTION, COMPONENTS & CIRCUITRIES

The generated optic flow accompanied by the displacements of the head/eyes during self-motion would render many visuomotor behaviors impossible. Thus, an important function of the CNS is to ensure visual acuity through gaze stabilization. Motion sensors of the ear and eye transform the relevant sensory information into motor commands, ultimately pulling the eyes in the appropriate direction to counteract the disruptive

consequences of locomotion (Straka et al., 2014). These concurrent stabilizing eye movements are mainly achieved through short-latency neural circuitries, the vestibulo-ocular reflex (VOR) and optokinetic reflex (OKR; Schweigart et al., 1997; Huterer and Cullen, 2002). These reflexes work synergistically and complement each other in the velocity domain as the OKR is most efficient at slow movements of a visual stimulus, while the VOR operates best at mid-to-high head rotation frequencies (Schweigart et al., 1995; França de Barros et al., 2020). Consequently, their combined operation ensures coverage of a large dynamic working range during self-motion.

One important component of the oculomotor system driving gaze stabilization are the extraocular eye muscles (EOMs). These muscles are the effector organs of the reflexes that transform the sensory input regarding motion of the head or visual scene into a motor command to pull the eyes in the appropriate direction. Jawed vertebrates possess six EOMs that work together in antagonistic pairs to facilitate a wide range of eye movements, encompassing horizontal, vertical, and rotational directions (Straka et al., 2014; Branoner et al., 2016). Two oblique muscles, the inferior (IO) and superior oblique (SO), enable intorsional (inward) and extorsional (outward) movements. From the remaining four recti muscles, the superior (SR) and inferior rectus (IR) elevate and depress the eye, while the medial (MR) and lateral rectus (LR) facilitate leftward and rightward movements in the horizontal plane (Büttner-Ennever, 2006; Horn, 2020). The precise and effective execution of these different movements is achieved through innervation provided by three dedicated cranial nerves (Spencer and Porter, 2006). To elaborate further, the SR, IR, MR, and IO muscles receive their innervation from motoneurons located within the oculomotor nucleus (nIII). On the other hand, the LR and SO are innervated by axon bundles originating from two brainstem nuclei, the abducens (nVI) and trochlear (nIV) respectively (Horn, 2020). Interconnections between motor nuclei innervating antagonistic muscle pairs facilitate conjugated movements of both eyes in the same direction (Baker and Highstein, 1975). Moreover, the spatial arrangement of these muscles is aligned with the orientation of the semicircular canals and coordinate system of visual motion detectors (Cohen et al., 1964; Curthoys, 2021; Horn and Straka, 2021). The functional importance of this will become more evident in the following subsections.

In this thesis, both the VOR and OKR were employed as a functional readout to better understand plasticity mechanisms within the CNS. Subsequently, I will provide a more comprehensive introduction to each of these mechanisms leading to gaze stabilization in the following subsections.

## THE VESTIBULO- OCULAR REFLEX (VOR)

The functional principle of how the VOR ensures gaze stability is to elicit compensatory eye movements in the opposite direction of the head displacement. Its fast response latency of only 7 ms is owed to a three-neuron circuit involving vestibular afferents, central vestibular neurons, and extraocular motoneurons (Baker et al., 1981;

Huterer and Cullen, 2002). Sensory information detected by the three semicircular canals, responsible for detecting angular accelerations, govern the angular VOR (aVOR) circuit. On the contrary, otolith derived sensory input about linear acceleration, drives the linear VOR pathway (IVOR; Anastasopoulos, 1996). This thesis exclusively encompasses experimental paradigms conducted in the horizontal rotational axis. This choice is driven by experimental simplicity and the consideration that tilt or roll axis rotations would not activate only canal driven gaze stabilization but also involve otolithic components, thus engaging more than one circuit. Therefore, in order to restrict complexity and facilitate drawing conclusions about potential plasticity events, I will focus solely on the aVOR and provide a more comprehensive description of its circuitry.

The aVOR, also often referred to as a “simple reflex-arc” (Straka et al., 2014) operates as follows: Counterclockwise vestibular stimulation/head rotation for instance depolarizes the hair cells of the left horizontal semicircular canal and thus stimulates ipsilateral second-order vestibular neurons in the hindbrain. These in turn excite the contralateral abducens neurons and interneurons (Baker and Highstein, 1975). Abducens neurons synapse onto the LR of the right eye while projections from abducens interneurons cross the midline to reach the contralateral oculomotor nucleus, which innervates the MR of the left eye. Concurrently, ipsilateral second-order vestibular neurons also inhibit ipsilateral abducens neurons and interneurons, thereby reducing the motor drive of the left LR and right MR muscles. Simultaneously, the spontaneous resting activity of vestibular afferents decreases in the right horizontal canal, coupled with an increased commissural inhibition from the activated side, resulting in the disfacilitation/silencing of any contribution from the right side (Fetter, 2016). Collectively, these processes ensure conjugated eye movements towards the right side to counteract leftward head rotations (Branoner et al., 2016). Nonetheless, no internal feedback about the accuracy of corrective eye movements exists and therefore the VOR acts as an open-loop control system (Miles and Lisberger, 1981). This lack of feedback combined with the VOR’s optimal working range at mid-to-high frequencies underlies the importance of cooperation with the OKR that closes the feedback loop (Precht, 1979).

## THE OPTOKINETIC REFLEX (OKR)

As previously mentioned, despite large field optic flow displacing the eyes, a stable image is nonetheless maintained on the retina by the OKR. This is achieved through eye movements that follow the direction and velocity of the visual image flow (Büttner and Büttner-Ennever, 2006). As soon as the eyes reach their most eccentric position, oppositely directed fast-resetting movements are made facilitating the continuation of their preceding motion (Distler and Hoffmann, 2011). Consequently, the OKR consists of a slow following and rapid resetting eye motion. The OKR can be categorized into three subtypes depending on the stimulus direction: vertical/oblique (vOKR) elicited by upward/downward vertical stimulation, horizontal (hOKR), and torsional OKR (tOKR) evoked by stimuli in the roll plane. Similar to the VOR, this thesis primarily focuses on the hOKR.

Panoramic shift in the horizontal plane is encoded by direction selective RGCs which project via the optic nerve (nII) to dedicated midbrain and diencephalic regions. A cluster of nuclei that comprises the accessory optic system (AOS) and a corresponding pretectal nucleus underlie the neural substrate of the OKR (Masseck and Hoffmann, 2009). The mammalian AOS encompasses the dorsal-, medial-, and lateral terminal nucleus (DTN, MTN, LTN; Simpson et al., 1988) while in birds and amphibians these neural clusters are referred to as the nuclei of the basal optic root (nBOR; Gruberg and Grasse, 1984; McKenna and Wallman, 1985). The additionally involved pretectal nucleus is called the nucleus of the optic tract (NOT) or nucleus lentiformis mesencephali in amphibians and reptiles (nLM; McKenna and Wallman, 1985). While the DTN and NOT of mammals process the horizontal OKR, only the nLM of amphibians, birds, and reptiles relays this information (Masseck and Hoffmann, 2009). Moreover, efferent projections from the nLM, as e.g. in the case of frogs, terminate in the ipsilateral abducens nucleus as well as in the contralateral oculomotor nucleus via abducens internuclear neurons leading to a contraction of the MR and LR muscles to move the eyes in the horizontal plane (Cochran et al., 1984; Straka and Dieringer, 1991). Further synaptic relays from the AOS and pretectal centers include the inferior olive, cerebellum, and vestibular nuclei (Masseck and Hoffmann, 2009; Horn and Straka, 2021). Taken together, elucidating the circuitries of the VOR and OKR highlights even more their shared convergence and cooperative nature.

### SPINAL EFFERENCE COPY (EC) SIGNALING

Apart from sensory induced gaze stabilization, predictive motor signaling originating in the spinal cord is also an important contributor to gaze stabilization during locomotor activity (Lambert et al., 2012; Straka et al., 2022). Any type of rhythmic locomotion such as walking or swimming is driven by central pattern generators which produce motor outputs in the absence of sensory feedback (CPGs; Marder and Calabrese, 1996). Motor commands, such as the CPGs, generate intrinsic neural representations known as efference copies (ECs), allowing an organism to anticipate the sensory outcomes of its actions (Straka et al., 2018). This capability helps to distinguish between sensations arising from one's own behavior and those triggered by external factors, facilitating the selective processing of relevant stimuli. For instance, fish use their lateral line system for prey detection by perceiving alterations in water movement in their surroundings (Ghysen and Dambly-Chaudière, 2004). However, during fish locomotion sinusoidal movements of the trunk and tail generate water turbulences that also stimulate their lateral line system, potentially leading to overstimulation without the existence of predictive signaling (Roberts and Russell, 1972).

To gain a deeper understanding of the functional relevance of predictive motor signaling, *in vitro* experimental conditions have been extensively employed where the CNS component of interest is isolated from its sensory input and muscle targets (e.g. in lampreys (Grillner, 2003); in mice (Meehan et al., 2012); in locusts (Rillich et al., 2013)). These *in vitro* model systems, which will be discussed in more detail in the following section, permit the study of neural circuits responsible for locomotion by recording from cranial or spinal nerves

under ‘fictive’ conditions, with actual physical movement not taking place (‘fictive’ locomotion). Research conducted in frogs has emphasized the importance of spinal ECs in maintaining a stable gaze during tail or limb based propulsion (Lambert et al., 2023). The predictability of head displacements and associated retinal perturbations of an animal’s rhythmic locomotion constitute a reliable signal for predicting the sensory outcomes of locomotor actions (Straka et al., 2022). *In vitro* experiments in tadpoles have further revealed that gaze stabilizing eye movements occur during ‘fictive’ locomotion by coordinated neuronal activities of spinal ventral roots and extraocular motor nerves, leading to alternate contractions of LR/MR muscle pairs (Stehouwer, 1987). Likewise, spinal ECs have been shown to project to the same targets of the aVOR circuit and suppress vestibular evoked signaling during fast, horizontal undulatory locomotion while showing an additive effect in slower, older staged animals (Lambert et al., 2012; Bacqué-Cazenave et al., 2022). Overall, as spinal ECs have been demonstrated to be a crucial component of gaze stabilization during locomotion, I have included investigations on this topic in chapter II of this thesis.

## PLASTICITY OF GAZE STABILIZING REFLEXES

A core characteristic of the vertebrate nervous system is its capacity to adapt and restructure to both internal and external stimuli (Mateos-Aparicio and Rodríguez-Moreno, 2019). This adaptability, widely known as plasticity, can occur across a range of systemic levels, including adjustments to circuit anatomy, synaptic modifications, alterations in individual cell properties, and changes in behavior (Pascual-Leone et al., 2005). Gaining a more profound understanding of these mechanisms, as well as their limitations, is fundamental for advancing basic and clinical research, ultimately facilitating their translation to various disciplines (Cramer et al., 2011). As evident from the preceding section, the relative simplicity of gaze stabilizing circuits makes them an excellent model system for bridging the gap between the function of neuronal circuits, behavior, and plasticity. Despite the remarkably preserved nature of these reflexes across vertebrate phylogeny, which highlights the significance of their motor outputs, some flexibility exists to adapt to species-specific needs, lifestyles, and pathological conditions (Straka et al., 2016). This thesis endeavors to address these aspects of plasticity through comparative analyses of two amphibian species, and under acute, pathological conditions within a species (Chapters II and III correspondingly).

## PHYLOGENETIC ADAPTIVE PLASTICITY

As locomotion increases in speed and becomes more intricate across the various vertebrate groups, the efficacy of visuo-vestibular reflexes must adapt to cope with the disruptions induced by self-motion (Dieringer, 1995). The OKR and VOR, jointly or in

isolation, were studied in a variety of vertebrates, revealing numerous species-specific and/or eco-physiological adaptations (Straka and Dieringer, 2004; Masseck and Hoffmann, 2009). For instance, comparative investigations in bony fish have tried to establish a connection between their oculomotor responses and speed of locomotion during feeding and escape behaviors. Bottom-dwellers, such as the toadfish, known for slow and sporadic swimming, exhibit lower OKR and VOR performances compared to fish living in fast-flowing waters (Dieringer et al., 1992). Morphological data of the semicircular canals also shows variations in features like size, curvature, and orientation among vertebrate groups, having led to different hypotheses on their functionality (Platt and Straka, 2020). A causal link between the presence of a robust angular VOR and sufficiently sized semicircular canals has been shown to exist (Jones and Spells, 1963; Muller, 1994, 1999; Hullar, 2006), as during the ontogeny of small fish and amphibian larvae it often represents a critical issue and thus determines the onset and subsequent performance of the aVOR (Lambert et al., 2008). Moreover, correlations between the locomotor style/capacity of a particular species, semicircular canal dimensions, and behavioral repertoire were often used to infer causality in paleontological studies (Spoor et al., 2002; Hullar, 2006). Semicircular canals are frequently well-maintained in cranial fossil records and can be reconstructed by high-resolution computed tomography scans. Such scans are used for assumptions to be made regarding the motion capacities and maneuverability of a particular species. In this regard, it has been found that primates and other mammals with fast and more agile locomotion tend to have significantly larger canals relative to their body mass than animals with slower locomotion (Spoor et al., 2007).

## LESION INDUCED PLASTICITY

The presence of the vestibular system along with its vital role in everyday activities may go unnoticed under healthy physiological conditions. Damage to the vestibular system through an accident or disease can lead to a wide spectrum of symptoms, encompassing issues related to eye movements, posture, as well as higher-order perceptual deficits and neurodegenerative disorders (Lacour and Tighilet, 2010). These symptoms are traditionally divided into two categories based on their association with head motion: static deficits, which manifest without head movements, and dynamic deficits, which emerge in the presence of head motion by stimulating the vestibular labyrinth (Smith and Curthoys, 1989). Static symptoms include postural asymmetries of the head and body towards the affected side as well as involuntary ocular displacements (such as spontaneous nystagmus in mammals), and typically subside within hours or days (Smith and Curthoys, 1989; Curthoys, 2000; Cullen et al., 2009). As for the dynamic symptoms, these include disruptions in amplitude and timing of the VOR and their restoration is slow, incomplete, and restricted to low- and middle-frequency range stimuli (Paterson et al., 2005; Straka et al., 2005).

Unilateral disruptions of peripheral vestibular signaling have been employed under experimental settings to gain a deeper insight into the plasticity mechanisms leading to either of the previously mentioned outcomes. The observed behavioral improvement

following unilateral labyrinthectomy (UL) or neurectomy is commonly referred to as “vestibular compensation” and has been found to vary in its degree and timeline for the different symptoms in the various vertebrate species examined so far (Curthoys, 2000; Lambert and Straka, 2012). Moreover, researchers have explored the neural underpinnings of vestibular compensation using a variety of approaches, including anatomical, electrophysiological, and molecular methods, and have identified these mechanisms within different parts of the VOR circuitry (Dutia, 2010). Common ground of UL symptoms is the generated imbalance in activity levels within the vestibular nuclei. As mentioned earlier, the vestibular endorgans exist as bilateral pairs on either side of the head, arranged in a mirror-symmetry to each other (Platt and Straka, 2020). Consequently, rotational movements excite the hair cells in the cristae of one ear, while at the same time suppressing the activity in the complementary cristae of the opposite ear. Unilateral loss of vestibular input results therefore in a sudden inequality of resting activity levels in the vestibular nuclei, which is enhanced by inhibitory commissural pathways from the intact side (Dutia, 2010). While the restoration of static deficits lies in the amelioration of this inequality, the partial substitution of dynamic deficits is attributed to plastic changes within the visuo-vestibular circuit as any regeneration of peripheral neurosensory elements has not been observed (Beraneck et al., 2003; Straka et al., 2005; Lambert and Straka, 2012). These include a reduction of motor deficits through multifactorial and individualistic behavioral strategies as well as through input from other sensory systems that bypass or supplement vestibular control (Paterson et al., 2005; Sadegh et al., 2012).

## EXPERIMENTAL RATIONALE & AMPHIBIAN ANIMAL MODELS

The scientific objective of this dissertation is to delve deeper into the extents and constraints of visuo-vestibular sensorimotor plasticity. To do so, I made use of two amphibian animal models, the frog *Xenopus laevis*, and the salamander, *Ambystoma mexicanum* (Axolotl). Both species undergo comparable larval stages and growth rates during development, which are well characterized and supplemented by morphological characteristics (Schreckenber and Jacobson, 1975; Nieuwkoop and Faber, 1994; Nye et al., 2003). Moreover, both species allow the employment of semi-intact *in vitro* experimental preparations which come along with a number of advantages (Straka and Simmers, 2012; Knorr et al., 2018). These include a long survival time, tissue transparency, easy accessibility of desired CNS and sensory elements for different kinds of manipulations (e.g. lesions of cranial nerves), and most importantly, controlled experimental conditions. The evolutionarily conserved nature of visuo-vestibular reflexes (Masseck and Hoffmann, 2009; Straka and Baker, 2013), together with their well-defined behaviors, provides powerful neurobiological insights into neuronal processing. In the following data chapter (Chapter II, Schneider-Soupiadis et al., unpublished manuscript) I made use of the shared aquatic larval stages of *Xenopus* and Axolotl larvae in which both utilize undulatory tail-based swimming. This comparative analysis aimed to identify correlations between their locomotion patterns and

their impact on gaze stability and semicircular canal morphology. The second data chapter (Chapter III, Soupiadou et al., 2020) had its focus on challenging visuo-vestibular processing to further understand the acute impacts of a unilateral loss of vestibular input. The unique possibility of observing the immediate and initial-hour impacts of such an insult without the influence of anesthesia, which is provided by amphibian *in vitro* preparations, aimed at identifying potential compensatory mechanisms. Overall, both studies intended to investigate, under distinct experimental frameworks, using behavioral and anatomical techniques, different aspects of hindbrain sensorimotor plasticity.

---

## CHAPTER II:

### A FUNCTIONAL COMPARISON BETWEEN INNER EAR MORPHOLOGY, GAZE STABILIZATION, AND LOCOMOTION IN LARVAL AMPHIBIANS

---

**Parthena Schneider-Soupiadis**<sup>1,2</sup>, Michael Forsthofer<sup>1,2,4</sup>, Gilles Courtand<sup>3</sup>, Rosario Sanchez-Gonzales<sup>1</sup>, François M. Lambert<sup>3,\*</sup> and Hans Straka<sup>1</sup>

<sup>1</sup> Faculty of Biology, Ludwig-Maximilians-University Munich, Großhaderner Str. 2, 82152 Planegg, Germany

<sup>2</sup> Graduate School of Systemic Neurosciences, Ludwig-Maximilians-University Munich, Großhaderner Str. 2, 82152 Planegg, Germany

<sup>3</sup> Institut de Neurosciences Cognitives et Intégratives d'Aquitaine (INICIA), CNRS UMR 5287, Université de Bordeaux, 33076 Bordeaux, France

<sup>4</sup> School of Life Sciences, University of Sussex, BN1 9QG Brighton, UK

\*Correspondence: [francois.lambert@u-bordeaux.fr](mailto:francois.lambert@u-bordeaux.fr) (FML)

#### Contribution of authors:

Conceptualization: PS, MF, RSG, FML, HS; Methodology: PS, MF, GC, FML, HS; Investigation: PS, MF, FML, HS; Formal analysis: PS, MF, GC, FML; Software: MF, GC, FML; Visualization: PS, FML; Writing-original draft: PS, MF, FML, HS; Writing-review & editing: PS, MF, RSG, FML; Funding acquisition: FML, HS.

#### My contributions to this manuscript:

I contributed to the design of experiments and the conceptualization of analysis scripts. I performed all experiments and analyzed the anatomical comparisons of *Xenopus* and *Axolotl* larvae, visuo-vestibular eye tracking data, and 2D canal injection data. I created initial versions of the figures and contributed to revisions on all figures. I wrote the initial version of the manuscript and contributed to the editing process.

The following manuscript is unpublished.

## **A functional comparison between inner ear morphology, gaze stabilization, and locomotion in larval amphibians**

Parthena Schneider-Soupiadis<sup>1,2</sup>, Michael Forsthofer<sup>1,2,4</sup>, Gilles Courtand<sup>3</sup>, Rosario Sanchez-Gonzales<sup>1</sup>, François M. Lambert<sup>3,§</sup> and Hans Straka<sup>1,&</sup>

<sup>1</sup> Faculty of Biology, Ludwig-Maximilians-University Munich, Großhaderner Str. 2, 82152 Planegg, Germany

<sup>2</sup> Graduate School of Systemic Neurosciences, Ludwig-Maximilians-University Munich, Großhaderner Str. 2, 82152 Planegg, Germany

<sup>3</sup> Institut de Neurosciences Cognitives et Intégratives d'Aquitaine (INCIA), CNRS UMR 5287, Université de Bordeaux, 33076 Bordeaux, France

<sup>4</sup> School of Life Sciences, University of Sussex, BN1 9QG Brighton, UK

**Key words:** vestibulo-ocular reflex, optokinetic reflex, semicircular canal, eye movements, locomotion, *xenopus*, axolotl

**Conflict of interest statement:** The authors declare no competing financial interests.

<sup>§</sup>To whom correspondence should be addressed:

**Dr. François M. Lambert**

Institut de Neurosciences Cognitives et Intégratives d'Aquitaine (INCIA),

CNRS UMR 5287, Université de Bordeaux

France

Tel: +33 5 57 57 47 73

Email: [francois.lambert@u-bordeaux.fr](mailto:francois.lambert@u-bordeaux.fr)

<sup>&</sup>We dedicate this article to the memory of our mentor Prof. Dr. Hans Straka, who sadly and unexpectedly passed away in December 2022. He left a big hole in our research community and is greatly missed by all of us.

### **Acknowledgments**

This research was funded by the German Science Foundation (CRC 870; STR 478/3-1; RTG 2175), the German Federal Ministry of Education and Research under the Grant code 01 EO 0901, and the Agence Nationale de la Recherche (ANR-22-CE37-0002-01LOCOGATE and ANR-22-CE16-0004-02 MOTOC) supported by the Centre National de la Recherche Scientifique, Université de Bordeaux. The authors would like to thank the Rupp lab and Hörmanseder lab for the supply of *Xenopus* embryos and PD Dr. Steffen Dietzel, Dr. Thomae Andreas, and Brigitte Bergner from the Core Facility Bioimaging at the Biomedical Center of the LMU for support and access to microscopes. Special thanks go to Dr. Clayton Gordy for scientific guidance and great support.

## ABSTRACT

Achieving efficient locomotion requires effective gaze stabilization and, therefore, accurate sensory detection of both passive and active head movements. Arguably the main component of fast motion detection is the vestibular system, the sensory transduction of which critically relies on the morphology of inner ear endorgans. An evolutionary relationship between locomotion and gaze stabilizing capacities on the one hand, and semicircular canal morphology on the other hand, exists in vertebrates as an adaptation to eco-physiological and species-specific needs. Here, we study this link by comparing two amphibian species, the salamander Axolotl and the frog *Xenopus laevis*. We found that *Xenopus* preferentially swim continuously, while Axolotls swim in short bouts, and exhibit a wider angular head acceleration range. Moreover, *in vitro* recordings of the angular vestibulo-ocular reflex (aVOR) show a significantly lower gain in stage 54 Axolotl with a much larger time delay. Older Axolotls (stage 56) show an increased gain, comparable to stage 54 *Xenopus*, hinting at a delayed developmental onset of aVOR derived gaze compensation. To investigate whether the delayed functional onset is linked to inner ear development as it is in frogs, we conducted morphological comparisons of the semicircular canals of both species. These revealed that the horizontal canal in Axolotl is thinner, less curved and has a less even trajectory along the horizontal plane compared to *Xenopus*. Additionally, the ampulla of *Xenopus* is rounder and less elongated than in Axolotl. All these parameters are critical for endolymph flow and consequently for the capacity of semicircular canals to perceive head motion. Altogether our results demonstrate that semicircular canal morphology is clearly linked to vestibular sensitivity, affecting the aVOR performance, but also locomotor capacity.

## INTRODUCTION

Locomotion in all vertebrates is accompanied by reflexive gaze-stabilizing eye movements that minimize the deteriorating consequences of the head/body motion on retinal image stability (Angelaki and Cullen, 2008). The dominating components are provided by visuo- and vestibulo-motor behaviors, which act synergistically through the vestibulo-ocular (VOR) and the optokinetic (OKR) reflexes. Their associated sensory components and neuronal circuits have been evolutionarily well conserved over the last 500 million years (Masseck and Hoffmann, 2009; Straka and Baker, 2013; Straka et al., 2014; Lipovsek and Wingate, 2018). Nevertheless, both sensory systems maintain a dynamic range of plasticity to respond to changing environments and demands. This adaptability has been studied in a variety of vertebrates and found to exhibit a number of species-specific and/or eco-physiological adaptations (Straka and Dieringer, 2004; Masseck and Hoffmann, 2009). In any case, a robust angular VOR clearly requires sufficiently sized semicircular canals (Mayne, 1950; Jones and Spells, 1963; Curthoys and Oman, 1986; Oman et al., 1987; Muller and Verhagen, 2002a, 2002b; Muller, 1994, 1999; for review see Lambert and Bacqué-Cazenave, 2020), which during the ontogeny of small fish and amphibian larvae often represents a critical issue and thus determines the onset and subsequent performance of the reflex (Beck et al., 2004; Lambert et al., 2008). Not only duct size is of particular importance for the capacity to sense head motion, but also other parameters of the labyrinth which influence endolymph flow (Lambert and Bacqué-Cazenave, 2020). Moreover, the detection of head movements through the vestibular endorgans contributes to an optimization of locomotor parameters. Accordingly, labyrinth geometry is believed to have a strong impact on locomotor as well as vestibular capacity. As a general rule, it appears that animals with fast and agile locomotion exhibit large semicircular canals with elongated ducts whereas smaller ducts are more common for slower locomotor regimes (Spoor et al., 2007). Various studies have tried to demonstrate a phylogenetic link in vertebrate evolution between locomotor style/capacity of a particular species, semicircular canal dimensions, and behavioral repertoire (Spoor et al., 1994, 2002, 2007; Rogers, 2005; Hullar, 2006; Malinzak et al., 2012; Pfaff et al., 2015; Benson et al., 2017; Le Maitre et al., 2017; Schwab et al., 2018; Capshaw et al., 2019; Essner et al., 2022). However, deciphering this causal relationship remains a challenging task, primarily due to the difficulty of identifying comparable species with similar developmental patterns as well as locomotor, and vestibular systems that are easily experimentally accessible. Moreover, the difficult accessibility of the inner ear, typically situated within the head and covered by bone in

most vertebrates, complicates morphological comparisons.

In addressing this challenge, we conducted a study characterizing the locomotion profiles as well as visuo- vestibular performances, and labyrinth morphology in two related amphibian species: the toad *Xenopus laevis* and the salamander Axolotl (*Ambystoma mexicanum*). *Xenopus* belongs to the anuran group, amphibian species that lose their tail after metamorphosis, whereas Axolotls are part of the urodela group, with the tail conserved after metamorphosis. Both species exhibit a similar developmental pattern until mid-larval stages, have transparent tissue with the inner ear being visually exposed, and utilize undulatory tail-based swimming during their aquatic larval stages. Locomotor performances were recorded from free swimming sequences of both amphibian larvae while *in vitro* preparations were used to address their gaze stabilization capacities during passive head motion. Herein, the well-studied OKR and VOR dynamics of the behavioral performance of *Xenopus laevis* larvae (Gravot et al., 2017; Lambert et al., 2008, 2020; Soupiadou et al., 2020; Bacqué-Cazenave et al., 2022) was compared to the respective profiles of these gaze-stabilizing reflexes in Axolotl. The observed inferior execution of the VOR together with the lower locomotor performances in Axolotl compared to *Xenopus* larvae prompted us to quantify the morphology of the horizontal semicircular canals. By combining these approaches, we provide cumulative evidence that ties the locomotor performances, vestibular sensitivity, and capacity with the morphology of the inner ear sensor responsible for the detection of head rotations in the horizontal plane.

## MATERIAL AND METHODS

### Experimental Model and Subject Details

Behavioral and anatomical experiments were conducted on *Xenopus laevis* tadpoles ( $n = 85$ ) and Axolotl (*Ambystoma mexicanum*) larvae ( $n = 67$ ) of either sex at developmental stages 48-56. Developmental stages were determined based on the description by Nieuwkoop and Faber (1994) for *Xenopus* and by Nye et al. (2003) for Axolotl. Axolotl larvae were obtained from the in-house breeding facility at the Biocenter-Martinsried of the Ludwig-Maximilians-University Munich (LMU) while *Xenopus* embryos were obtained from the Biomedical Center of the LMU and transferred to the in-house animal facility. Larvae of both species were maintained in separate tanks with filtered water (17-19°C) at a 12 hour/12 hour light/dark cycle. All experiments were performed in compliance with the “Principles of animal care” publication No. 86–23, revised 1985, of the National Institutes of Health and were carried out in accordance with the ARRIVE guidelines and regulations. Permission for the experiments was granted by the government of Upper Bavaria (Regierung von Oberbayern) under the license codes ROB-55.2.2532.Vet\_03-17-24 and ROB-55.2.2532.Vet\_02-22-54. In addition, all experiments were performed in accordance with the relevant guidelines and regulations of the LMU Munich.

### Method Details

#### Video tracking and analysis of swimming/locomotor behaviors

Freely swimming animals were filmed to extract and quantify locomotor kinematic parameters in *Xenopus* ( $n=13$ ) and Axolotl ( $n=12$ ) larvae. Animals were placed in a circular dish (diameter 18.8 cm, water height ~2 cm; Fig. 2A) and illuminated from below with an illumination box (Kaiser 2450 slimlite LED). Animals were video-recorded from above with a color camera (Basler ace, acA1300-200uc, 106754), mounted on a tripod (Manfrotto 290 xtra, MH804-3W) using pylon viewer (5.0.12.11830, Basler). Videos were recorded for one minute at a framerate of 30 FPS with a resolution of 1200 x 1200 px and were stored in the avi-file format. Recorded sequences consisted of either spontaneous swimming or were induced by a gentle water flow produced with a plastic pipette at the tip of tail.

Video recordings were analyzed offline. The avi files were converted into mp4-file formats using ffmpeg (Tomar, 2006), and the spatial position of the animals was extracted using the SLEAP framework

(Pereira et al., 2022). In brief, a model was trained for each species to identify external anatomical landmarks of the animal comprising the eyes, center of the skull, and body center of mass as well as 3 tail points (Fig. 2A). This was subsequently used to infer the position of the landmarks across different videos. Videos of the motion-tracked animals were exported with the respective markers for visualization purposes. Marker coordinates were exported as time series in the hdf5-format and were further analyzed in Python (python 3.7) using the Spyder 4 IDE. The position of the body center of mass over time was plotted for visualization of the swim path, and to calculate changes in distance. The differentiation of this yielded the swim velocity of animals, and the integral the total swim distance within a recording. Finally, the angle between the brain-center of mass axis and the center of mass – tail axis was calculated and differentiated to calculate the tail deflection velocity. Swim and tail velocity traces were then smoothed with a Savitzky-Golay filter (window length 15, order 3). Active swim bouts were identified by finding periods where animals crossed a velocity threshold (3mm/s) and a tail velocity threshold (3°/s) (i.e. the animal moved its tail while moving forward, eliminating either tail movements without locomotion, or passive horizontal motions). The duration of such swimming events was then used to calculate the time animals spent actively locomoting. For the calculation of swim kinematics, the angle of the line between the left eye and right eye was measured relative to the horizontal axis of the video and was differentiated twice to obtain the angular acceleration of the head during swimming.

For statistical comparison of swim kinematics in Python, head angular acceleration and swim velocity during active swim episodes were pooled across animals within each species and plotted as histograms, either in absolute values (head angular acceleration) or probability densities (swim velocity). Data were tested for belonging to the same distribution with a Kolmogorov-Smirnov test (scipy toolbox). To compare the contribution of swim bouts to overall swimming, rather than mere occurrence of bouts (which would bias towards shorter bouts due to their statistically higher occurrence within a recording), swim bouts were weighted according to their relative contribution to overall locomotion within a recording. For this, the duration of each swim bout was calculated, and the resulting value added to an array as many times as its length in data points. This pooled array was then plotted as a histogram of the probability density per species, and the two distributions were compared with a Kolmogorov-Smirnov test. Additionally, swim bouts were visualized as a heatmap displaying active swimming as black bars (matplotlib toolbox).

### Experimental preparation for eye and tail tracking

Semi-intact preparations for *in vitro* eye motion tracking experiments were produced according to a previously described protocol (Özugur et al., 2022; Bacqué-Cazenave et al., 2022). Accordingly, Axolotl and *Xenopus* larvae were deeply anesthetized in 0.05% 3-aminobenzoic acid ethyl ester methanesulfonate at room temperature (MS-222; Pharmaq Ltd. UK) for 3 minutes (Ramlochansingh et al., 2014), transferred to a petri dish (Ø 5 cm) containing ice-cold Ringer solution (75 mM NaCl, 25 mM NaHCO<sub>3</sub>, 2 mM CaCl<sub>2</sub>, 2 mM KCl, 0.1 mM MgCl<sub>2</sub>, and 11 mM glucose, pH 7.4) and decapitated at experiment-dependent levels of the spinal cord. Following removal of the lower jaws and visceral organs, the head was mechanically secured dorsal side-up with insect pins (0.2 mm, Fine Science Tools) onto the Sylgard-lined floor of the petri dish. Thereafter, the skin directly above the skull and bilateral otic capsules was taken off and the cartilaginous tissue until the first 5-8 spinal segments was opened. The forebrain was disconnected and the choroid plexus covering the fourth ventricle was removed to allow access of the Ringer solution. The remaining central nervous system, visual, and vestibular sensory periphery with afferent connections, and extraocular motor nerves remained functionally preserved. This allowed prolonged recordings of robust eye movements during application of visual and vestibular motion stimuli and spontaneous tail undulations (Soupiadou et al., 2020; Lambert et al., 2020; Bacqué-Cazenave et al., 2022). After the surgery, all preparations were allowed to recover for ~3 hours at 17°C before commencing with the recording session. During a recording session, preparations were mechanically secured in the center of the Sylgard-lined recording chamber (Ø 5 cm) and were continuously supplied with oxygenated (Carbogen: 95% O<sub>2</sub>, 5% CO<sub>2</sub>) Ringer solution at a constant temperature of 17.5 ± 0.5°C.

## Visual and vestibular motion stimulation, recording, and analysis

The preserved neuronal innervation of all extraocular muscles in semi-intact preparations allowed activation and video-recording of eye movements in response to vestibular and visual motion stimulation. In order to comply with the 3R regulation, OKR and VOR measurements from larval *Axolotl* ( $n=10$  at stage 54;  $n=5$  at stage 56) were compared to data from larval *Xenopus* previously obtained in the same experimental conditions in Soupiadou et al., 2020 and Bacqué-Cazenave et al., 2022 ( $n=6$  at stage 54,  $n=4$  at stage 56). Activation of the vestibular endorgans was performed with a six degrees of freedom motion stimulator (PI H-840, Physik Instrumente, Karlsruhe, Germany). Motion stimuli consisted of sinusoidal horizontal rotations at 0.5 Hz and a positional excursion of  $\pm 10^\circ$  with a peak rotational velocity of  $\pm 31.4^\circ/\text{s}$ . Large-field visual pattern motion was provided in an open-loop virtual reality setting consisting of an open cylindrical screen surrounding the recording chamber horizontally by encompassing  $275^\circ$  of the visual field with a diameter of 8 cm and a height of 5 cm (Gravot et al., 2017; Soupiadou et al., 2020; Forsthofer and Straka, 2022). Three digital light processing (DLP) video projectors (Aiptek V60, Aiptek International GmbH, Willich, Germany), installed in  $90^\circ$  angles to each other were affixed around the motion platform and projected a visual pattern at a refresh rate of 60 Hz onto the screen. The pattern consisted of equally spaced vertical, black and white stripes with a spatial size of  $16^\circ/16^\circ$ . The horizontal pattern motion consisted of sinusoidal oscillations at 0.1 Hz and positional excursions of  $\pm 10^\circ$  ( $\pm 6.28^\circ/\text{s}$  peak velocity). For all experiments, the Sylgard-lined recording chamber with the affixed preparation was centered inside the cylindrical screen that co-aligned with the vertical rotation axis of the vestibular motion stimulator. Visuo-vestibular motion stimuli were applied separately to evoke a VOR in darkness, VOR in light (in the presence of the world-stationary vertical black and white stripes) or an OKR response.

The movements of both eyes were captured non-invasively with a camera (Grasshopper 0.3 MP Mono Fire-Wire 1394b, PointGrey, Vancouver, BC, Canada) equipped with an objective lens (Optem Zoom 70XL, Qioptiq Photonics GmbH & Co. KG, Germany; M25 x 0.75 + 0.25) and infrared-filter (800 nm long pass) at a frame rate of 30 FPS (see Soupiadou et al., 2020; Forsthofer and Straka, 2023 for details), while the preparation was illuminated from above by an infrared light source (840 nm). Eye position was extracted in real time from the video by automated fitting of an ellipse around each eye (Gravot et al., 2017). The angle between the major axis of each ellipse and the vertical image axis was calculated in a frame-by-frame manner by a custom-written software (Beck et al., 2004) and was recorded and stored for off-line analysis along with the visual-vestibular motion stimulus (Spike2 version 7.04, Cambridge Electronic Design Ltd.).

Visuo-vestibular evoked eye motion data were acquired in Spike2, subsequently exported as .mat files (The MathWorks Inc.) and analyzed off-line with custom-written Python 3 scripts. Prior to this procedure, stimulus and eye motion recordings were resampled at 200 Hz and filtered with a 4 Hz low-pass Butterworth filter as implemented previously (Forsthofer and Straka, 2023; Gordy and Straka 2022). For better visualization of species-specific differences, left and right eye conjugated positions were averaged (Knorr et al., 2018; Gordy and Straka, 2022). Eye movement and corresponding stimulus profiles were further segmented into individual stimulus cycles from peak-to-peak positions, and averaged across multiple, uninterrupted (15-20) cycles within each animal. Sporadic cycles with either stimulus-evoked resetting fast-phases or spontaneous jerking movements were manually identified and excluded from further analysis. Eye movements were quantitatively assessed by calculating the response gain (peak-to-peak eye position/peak-to-peak stimulus position) and by determining the phase relation of the motion-induced eye movements with respect to the stimulus position. Phase calculations were obtained by comparing the timing of the average response peak with the timing of the maximal table position or visual motion pattern excursion (Gordy and Straka, 2022).

## Locomotor-induced eye movements, recording and analysis

Horizontal eye movements were recorded during spontaneous swimming episodes in head-fixed *in vitro* semi-intact preparations with intact tails. Like for the OKR/VOR measurements, locomotor-induced ocular activity from larval *Axolotl* ( $n=7$  at stage 53-54) were compared to data from larval *Xenopus* previously obtained in the same experimental conditions in Bacqué-Cazenave et al., 2022 ( $n=7$  at stage 53-54), in

accordance with the 3R regulation. Both optic nerves were transected and the head was firmly secured to the Sylgard floor to exclude any visual and vestibular sensory input during the recording session. Movements of the eyes and tail were recorded at 250 frames per second with a high-speed digital camera (Basler ace, acA1300-200uc, 106754) equipped with a micro-lens (Optem MVZL macro video zoom lens, QIOPTIQ). The camera was placed above the center of the preparations and videos were recorded at a shutter speed of 3000  $\mu$ s and a resolution of 1200 x 800 px, stored in an avi-file format. The position of both eyes and the tail was offline analyzed using an automated, custom-written software in Python 3.5 (AniMotion collaborative core facility, INCIA CNRS UMR5287, Université de Bordeaux, <http://www.incia.ubordeaux1.fr/spip.php?rubrique193>). Angles between the major axis of the elliptically shaped eyes as well as the angles of the positional deviation of the first five tail myotomes relative to the longitudinal head axis were calculated frame-by-frame.

### Semicircular canal injections and analysis

The dimensions of the horizontal semicircular canals were determined in a subset of semi-intact preparations of Axolotl (stage 54,  $n = 8$ ; stage 56,  $n=3$ ) and *Xenopus* larvae (stage 54,  $n = 8$ ; stage 56,  $n=2$ ). Each specimen was mechanically secured to a Sylgard-lined Petri dish ( $\varnothing$  5 cm), carefully cleaned from connective and muscle tissue attached to the exterior of the inner ear capsule and photographed with bright-field illumination using a camera (Axiocam 305 color, Carl Zeiss Microscopy GmbH) mounted onto a stereoscope (SteREO Discovery.V20, Carl Zeiss Microscopy GmbH).

To visualize and analyze the morphology of the horizontal semicircular canal within the inner ear compartment, a small volume of dextran conjugated Tetramethylrhodamine (10.000 MW; Invitrogen, D1817) was injected into the endolymphatic compartment. Microelectrodes for the injections were fabricated from borosilicate glass (diameter: 1.5 mm GB150-8P, Science Products, Hofheim, Germany) with a horizontal puller (Sutter Instrument, P-87 Brown/ Flaming). Thereafter, tips were broken under visual control and beveled (Micropipette Grinder EG-45, Narishige) to a diameter of  $\sim 30$   $\mu$ m ( $30^\circ$  angle). Microelectrodes were filled with a 20% solution of the fluorescent dye, inserted into an electrode holder connected to a pressure injection device (PDES-01 AM, napi electronic GmbH, Tamm, Germany) and mounted onto a 3-axis micromanipulator (Bachhofer, Reutlingen). Microelectrodes were inserted into the endolymphatic cavity of the *common crus*, where the anterior and posterior vertical semicircular canals merge dorso-medially (see Miller Bever et al., 2003). The fluorescent dye ( $\sim 0.5$   $\mu$ l) was injected with 2-6 pressure pulses of 1 bar and 100 ms duration over a period of  $\sim 5$  minutes followed by a period of  $\sim 2$  hours to allow the fluorescent dye to spread and label the entire endolymphatic space. Fluorescent images of the inner ear were captured on a stereomicroscope (SteReo Lumar.V12, NeoLumar S 0.8x objective equipped with an AxioCam MRm camera, Carl Zeiss Microscopy GmbH) to quantify the endolymphatic lumen- and circuit radius (circuit radius =  $\sqrt{\frac{Ra^2 + Rb^2}{2}}$ ) of each semicircular canal (ZEN lite, CZI, Zeiss, Germany).

In an additional set of animals, 30 min post injection, preparations were mounted in PBS using a custom metal spacer for confocal imaging to 3D reconstruct the structure of the horizontal semicircular canal. Images were taken at the Core Bioimaging Facility of the Biomedical Center of the LMU on a Leica SP8 upright microscope, using solid state laser excitation at 552 nm. Images were acquired with a 10x objective (HC PL FLUOTAR, 10x/0.30; WD 11 mm, dry), image pixel size was 1.47  $\mu$ m. TMR fluorescent images were recorded with external, non-descanned hybrid detectors (HyDs) and recording was sequentially to avoid bleed-through. 3D analysis of the imaged horizontal canals was performed in Fiji (Schindelin et al., 2012). First a region of interest (ROI) was manually selected around the horizontal canal, cropped, and smoothed with a Gaussian blur filter (4). Then the image threshold was adjusted, and a new black and white stack created. For the 3D measurements, the 3D manager plugin was used (Ollion et al., 2013). After 3D segmentation was applied, the volume, elongation ratio, and flatness of the canal was measured. For the measurement of canal cross section areas, the thresholded images were imported from Fiji in the 3DSlicer 5.2 (Fedorov et al., 2012). A center line within the canal was defined using the Vascular Modeling Toolkit (<https://github.com/NeuroMorph-EPFL/NeuroMorph/wiki/Centerlines-and-Cross-Sections>) and from this diameter values were measured from one end of the canal to the other.

## Statistics and Software

Statistical analysis and individual plots were performed in Prism 9 (Graph- Pad Software Inc. USA) or Python 3.7. Data were plotted as column scatter plots with mean  $\pm$  standard deviation or standard error of the mean (SD; SEM). Statistical differences between experimental groups were calculated with the non-parametric Mann-Whitney *U*-test for unpaired parameters, the Wilcoxon signed-rank test for paired parameters, and the Kruskal-Wallis-test and a Dunn's test (unpaired parameters) for multiple comparisons and indicated as p-values (\*  $p < 0.05$ ; \*\*  $p < 0.001$ ; \*\*\*  $p < 0.0001$ ). Circular statistics for phase relationships of eye movements were calculated in Oriana (Version 4; Kovach Computing Services). A mean vector was computed from phase values, providing both the mean direction and the vector's strength, serving as an indicator of data clustering on a scale from 0-1. Differences in phase values were identified with a Watson-Williams-F test. Figures were compiled in Affinity (Version 1.9.3., Serif, UK).

## RESULTS

### *Xenopus* and Axolotl larvae show a comparable developmental pattern

In this project, we set out to investigate how differences in sensory systems and corresponding behaviors correlate with locomotion within the class of amphibians. For this, we assessed swim kinematics and eye movements of the anuran *Xenopus laevis* and the urodele *Ambystoma mexicanum* (Axolotl), which share a common Ichthyostegid ancestor in the middle Paleozoic era (Feller and Hedges, 1998; Fig.1A). While both species can be maintained under very similar conditions in a laboratory environment, our initial aim was to verify the comparability of both species concerning anatomical features and developmental timepoints (Fig.1B-F). In both species, developmental stage identification is based on morphological features such as limb growth during ontogeny (Fig.1B; Nieuwkoop and Faber, 1994; Nye et al., 2003). *Xenopus* and Axolotl showed a similar hindlimb bud growth (Fig.1B) as well as a similar body size growth over time with no significant difference across the examined stages (Fig.1C) and demonstrated a highly comparable developmental pattern along the larval period. Critical for our question, otic capsule length and area were not significantly different between both species at a given stage (Fig.1D, F), validating that variations in inner ear endorgan morphology were not due to general size differences of the head or otic capsule size themselves. Thus, both species are similar in developmental patterns, environmental requirements, and size parameters, reducing external sources of behavioral variability and allowing a more specific correlation of the visuo-vestibular physiology with semicircular canal geometry between *Xenopus* and Axolotl.

### *Xenopus* and Axolotl exhibit different swimming kinematics

We recorded the swimming activity of freely moving animals in a circular dish from the top (Fig.2A) and tracked the x-y position of body parts across time using SLEAP (Pereira et al. 2022). This allowed us to extract several locomotor kinematic parameters like the swim distance, speed, bout length, tail deflection, and angular head acceleration across time. This revealed key differences in swim strategy between the two species, concerning both frequency and mode of locomotion. *Xenopus* swim rather continuously with a relatively constant swim speed (see examples in Fig. 2B, D), whereas Axolotl exhibit interspersed, short bouts of locomotion with high speeds followed by a short passive glide until stationary (Fig. 2C, E). Active swimming activity was identified as times where animals moved while also deflecting their tail, (Fig.2F, G, black bars) and quantified for each animal (Fig. 2H). *Xenopus* spent significantly more time locomoting than Axolotl, with 28.8 as opposed to 10.7 seconds on average (Fig. 2H  $p = 0.0188$ , Mann Whitney U-test, two-tailed). This manifested in two ways, which was: 1) overall more swim events in *Xenopus* and, more importantly, significantly longer bouts in *Xenopus* as indicated by the weighted length of swim bouts (Fig.2I,  $p < 0.0001$ , Kolmogorov-Smirnov test). Each swim bout was weighted relative to their contribution to total swimming, i.e. a 50 second swim bout counted 50x more than a 1 second bout. This showed that the mean swim bout duration of *Xenopus* was 6.98 s, while Axolotl swam mostly short bouts of 0.92 s duration. Thus overall, *Xenopus* spends more time actively locomoting, and does so in longer consecutive swim periods, than Axolotl.

As active locomotion necessitates gaze stabilization, this may indicate a stronger need for *Xenopus* to maintain a stable gaze. However, perhaps more important than the amount of motion is its characteristics to be compensated, and we thus looked next at the main parameter detected by vestibular-based gaze stabilization. During undulatory swimming, the head rotates mainly in the horizontal plane, which is mostly picked up by the horizontal semicircular canals as angular acceleration (Hänzi and Straka, 2017; Lambert et al., 2020). Quantification of the angular head acceleration profiles were found to be different (Fig.2J,  $p=0.012$ , Kolmogorov-Smirnov test) with less swimming of Axolotl as indicated by the overall amount of data. However, *Xenopus* exhibited lower mean accelerations of  $192.32^\circ/s^2$  with a narrower distribution in contrast to Axolotl, which showed average head accelerations of  $202.01^\circ/s^2$  with a wider spread. Altogether, these results suggest that larval *Xenopus* exhibit more locomotor events, with longer durations and lower, more consistent velocities, while Axolotl at comparable developmental stages performed rare, short, and high velocity swim events.

*Xenopus* exhibit better vestibular- and locomotor-induced gaze-stabilizing eye movements than Axolotl

*Xenopus* tadpoles perform a robust angular vestibulo-ocular reflex (aVOR) after reaching developmental stage 53 (Lambert et al., 2008; Gordy and Straka, 2022; Bacqué-Cazenave et al., 2022). Therefore, we directly assessed the visuo-vestibular ocular reflexes in whole head *in vitro* preparations of *Xenopus* and Axolotl at larval stage 54 to compare the dynamics of gaze-stabilizing behavior of both species. In complete darkness, stimulation of the horizontal semicircular canal, elicited during sinusoidal head rotations at 0.5 Hz with a peak velocity of  $\pm 31.4^\circ/s$  ( $\pm 10^\circ$  positional excursion), evoked robust reflexive compensatory eye movements in *Xenopus* which were oppositely directed to the stimulus position (Fig.3A, B, green), with an average gain (eye motion amplitude/stimulus amplitude) of  $0.29 \pm 0.1$  (Fig.3C, green; mean  $\pm$  SD,  $n=6$ ). They also exhibited a phase lead of  $-54.3^\circ \pm 12.34^\circ$  (Fig.3D, green;  $r = 0.98$ ) relative to the peak stimulus position at  $0^\circ$ . This aVOR response was similar to previous findings reported in larval *Xenopus* (Lambert et al., 2008, Gensberger et al., 2016; Gordy and Straka, 2022; Bacqué-Cazenave et al., 2022). Inversely, Axolotl larvae subjected to the same stimulus exhibited comparatively poor aVOR performances (Fig.3A, B, orange) with an average gain of only  $0.05 \pm 0.02$  (Fig.3C, orange; mean  $\pm$  SD,  $n=10$ ). Apart from a significantly reduced gain ( $p < 0.0001$ , Mann-Whitney *U*-test, two-tailed), the aVOR exhibited a phase-lag *re* the stimulus ( $p < 0.0001$ , Watson-Williams F-test) by  $47.06^\circ \pm 24.48^\circ$  (Fig.3D, orange;  $r = 0.91$ ). Comparison of gain values across various developmental stages revealed that in both species the gain follows a linear increase, albeit with a major difference in the onset of the aVOR. While semicircular canal-driven eye motions become functional at stage 49 (gain  $\geq 0.12$ ) in *Xenopus* (Lambert et al., 2008), this lower threshold was equivalent to our recorded gain in Axolotl at stage 54, indicating that the aVOR in this species only becomes sustainable at stage 56 ( $0.15 \pm 0.04$ , mean  $\pm$  SD; Fig.3E, orange). However, the aVOR performed in Axolotl at stage 56 remained much lower than in *Xenopus* at the same stage (Fig.3E).

Undulatory swimming results in large field visual scene motion that, in addition to the VOR, co-activates the optokinetic reflex through activation of motion sensitive retinal ganglion cells (França de Barros et al., 2020). The OKR works in synergy with the VOR, as it detects preferentially slow visual motion, and thus lower frequencies than the VOR. It also serves as a feedback loop and corporately both reflexes ensure appropriate gaze stabilization (Collewijn and Grootendorst, 1979). Therefore, we next investigated the potential contribution of the OKR to compensation of undulatory locomotion either in isolation, or conjointly activated with the VOR.

Horizontal, sinusoidal rotation of a black and white vertical striped pattern at 0.1 Hz and  $\pm 6.28^\circ/s$ , corresponding to positional excursions of  $\pm 10^\circ$ , resulted in stimulus-following ocular motor responses for both species. Conversely to VOR responses, the OKR was stronger in Axolotl at a gain of  $0.25 \pm 0.09$  (mean  $\pm$  SD,  $p=0.011$ , Mann-Whitney *U*-test, two-tailed) compared to *Xenopus* at  $0.14 \pm 0.04$  (Fig.3I, J, K, green,  $n=6$ , Gravot et al., 2017; Knorr et al., 2018). In both cases, the average eye positions faithfully followed the stimulus (Fig.3I, J) and were nearly in phase with the peak stimulus position at  $13.4^\circ \pm 10.1^\circ$  (Fig.3L, green,  $r = 0.99$ ) for *Xenopus*

and at  $6.03^\circ \pm 13.9^\circ$  (Fig.3L, orange; mean  $\pm$  SD,  $r = 0.97$ ) for Axolotl. We next tested whether under naturalistic conditions where usually simultaneous activation of OKR and VOR takes place, the improved OKR could compensate for the lack of VOR in Axolotl.

For the joint activation of the aVOR and OKR, animals of both species were subjected to horizontal sinusoidal head rotation at 0.5 Hz ( $\pm 31.4^\circ/s$ ) in front of a world-stationary black and white striped pattern (Fig.3F-H). Under these conditions, *Xenopus* tadpoles exhibited VOR and OKR-driven compensatory eye motion profiles with a higher gain of  $0.32 \pm 0.08$  (Fig.3F, G, green, mean  $\pm$  SD,  $n=6$ ) than VOR or OKR alone and an improved phase lead *re* stimulus ( $-29.4^\circ \pm 18.2^\circ$ ; Fig.3H, green,  $r = 0.96$ ) compared to vestibular-only condition, but still lower than during OKR stimulation alone. For Axolotl, co-activation of the OKR and VOR resulted in gains slightly higher than in VOR conditions but lower than OKR conditions (Fig. 3F, G;  $p=0.002$ , Wilcoxon matched-pairs signed rank test) but was still significantly lower compared to *Xenopus* ( $p=0.0002$ , Mann-Whitney *U*-test, two-tailed) with an average gain of  $0.14 \pm 0.06$  (Fig.3G, orange, mean  $\pm$  SD,  $n=10$ ). Quantifications of phase relative to peak stimulus position were similar to exclusive VOR stimulation, leading by  $41.52^\circ \pm 18.62^\circ$  *re* stimulus (Fig.3H, orange,  $r = 0.95$ ). These results indicate that joint activation of OKR and VOR leads to better gaze-stabilization than either reflex alone, yet the improved OKR performance is not able to completely compensate for the missing vestibular component.

During rhythmic locomotion, reflexive gaze stabilizing eye movements as measured above are additionally complemented by an efference copy feedforward signal from spinal central pattern generators, and accordingly, these could further compensate for the lack of vestibular input during swimming (Lambert et al., 2012; França de Barros et al., 2022; Dietrich and Wühr, 2019; Wibble et al., 2022; for review see Lambert et al., 2023). However, the maturation and efficiency of locomotor-induced gaze stabilizing eye movement rely on the onset and maturation of semicircular canal sensitivity during larval development in *Xenopus* (Bacqué-Cazenave et al., 2022). Taking into consideration this conjoint maturation, we next quantified locomotor-induced ocular activity in larval Axolotl in comparison to *Xenopus* to see whether vestibular signalling is sufficient to enable efference-copy driven eye motions, and if these could drive compensatory eye motions during locomotion (Fig.3M-O). In the absence of any visuo-vestibular sensory input (see methods), undulatory swimming in semi-intact *in vitro* head fixed preparations of stage 54 Axolotl produced conjugated eye movements, phase-coupled to the tail movement but in the opposite direction (Fig. 3M) comparable to those previously described in larval stage 54 *Xenopus* (Bacqué-Cazenave et al., 2018, 2022). In both species the spino-ocular gain gradually decreased with large tail amplitudes but with a more pronounced tendency in Axolotl than in *Xenopus* even if the difference was not significant (Fig. 3N;  $p=0.43$ , simple linear regression). However, the spino-ocular motor coupling was much less efficient to produce compensatory eye movements correlated to each tail cycle in Axolotl than in *Xenopus*, with an eye/tail cycle ratio of  $56.49\% \pm 19.76\%$  in Axolotl and  $90.31\% \pm 4.15\%$  in *Xenopus* (Fig. 3O, mean  $\pm$  SD,  $p=0.0023$ , Mann-Whitney *U*-test, two-tailed).

All together, these results demonstrated that Axolotl exhibit a less efficient aVOR and spino-ocular motor coupling than *Xenopus* at a comparable larval stage, with the OKR being larger but insufficient for complete compensation. However, the aVOR performance increases with development strongly suggesting a semicircular canal dependent sensitivity during ontogeny.

### Semicircular canal geometry induced constraints for endolymph flow in Axolotl

Canal geometry is critical for the endolymph flow dynamics and consequently for the capacity of semicircular canals to detect angular head accelerations (Lambert and Bacqué-Cazenave, 2020). In particular, canal circuit ( $R$ , Fig. 4A) and duct ( $r$ , Fig. 4A) radii appear to be the two major morphological components determining the onset of the aVOR during vertebrate development (Beck et al., 2004; Lambert et al., 2008; for theoretical aspects see Muller, 1999). The late aVOR appearance in larval Axolotl development (at stage 54, Fig. 3E), compared to *Xenopus*, led to the hypothesis that horizontal semicircular canal circuit and duct radii at this stage are insufficient to detect angular head motion, and only at this point or later reach the same critical size threshold to trigger a functional VOR response, comparable to stage 49 in *Xenopus*. Therefore, we examined the canal circuit and lumen radius in both species at stage 54. A fluorescent tracer (see methods section) was

injected into the *common crus* of the anterior and posterior canal allowing for visualization of the canal morphology in 2- and 3- dimensions following fluorescence microscopy (Fig.4-5). Fitting an ellipse on the z stack of the horizontal semicircular canal imaged from dorsal (Fig.4A) revealed that the circuit radius was smaller in Axolotl ( $582.91 \pm 22.05$ ) than in *Xenopus* ( $634.09 \pm 33.73$ ) (Fig.4D,  $p= 0.0104$ , Mann Whitney U-test, two-tailed). Moreover, the canal radius ( $r$ ) was also significantly smaller in Axolotl ( $66.32 \pm 1.95$ ;  $77.11 \pm 1.2$ ; Fig.4E,  $p= 0.0002$ , Mann Whitney U-test, two-tailed). As hypothesized, canal radii measurements of Axolotl at stage 54 were comparable to values found in *Xenopus* stage 49 ( $R \sim 600 \mu\text{m}$ ,  $r \sim 70 \mu\text{m}$ ; Lambert et al., 2008), indicating that semicircular canal morphology limits vestibular performance prior to this stage.

Another difference between both species is the shape of the ampulla, the enlarged region at one extremity of each canal, which houses the hair cells (Fig.4A). A less round ampulla limits endolymph flow detection by hair cells and thus canal sensitivity (Oman et al., 1987; Lambert and Bacqué-Cazenave, 2020). Quantification of ampulla roundness by calculating the linear regression and the ratio between the major and minor semi-axis (Fig.4B, C) indeed revealed a more elliptical ampulla for Axolotl (Fig.4F, G, orange,  $n= 8$ ) than in *Xenopus* (Fig.4 F, G, green,  $n=8$ ; a ratio of 1 in the Y axis corresponds to a perfect circle), which likely contributes to comparatively lower canal sensitivity in Axolotl.

For a more comprehensive morphological distinction, we reconstructed 3D models of the entire horizontal semicircular canal from confocal scans (see methods; Fig. 4B, C). This revealed significant differences in the overall shape of *Xenopus* and Axolotl horizontal canals (Fig.5A, B respectively). Ellipsoid fitting on the HC canal in 3 dimensions allowed measuring a true semi-major (blue axis “a” in Fig. 5C) and semi-minor axis (green axis “b” in Fig. 5C), allowing to measure the elongation of the canal as the elongation ratio (major axis (a)/minor axis(b), lower = rounder, Fig. 5D). Additionally, the depth axis (red axis “c” in Fig. 5C) which shows vertical displacement of the canal trajectory, was measured to calculate the flatness ratio (Fig. 5E) as the minor axis (b) / vertical displacement(c), showing how planar the canal is (higher = more planar). Elongation and flatness ratio calculations showed that HC canals in Axolotl were less curved (Fig.5D,  $p=0.0043$ , Mann-Whitney U-test, two-tailed) and less flat (Fig.5E,  $p=0.0043$ , Mann-Whitney U-test, two-tailed) than in *Xenopus*, both of which likely restrict endolymph motion and further contribute to reduced sensitivity. Finally, plotting of the canal cross section (yellow disk “cs” in Fig. 5C) across the entire length of the canal (Fig. 5 F, G) revealed a constricted area/stenosis of the duct just at the entrance of the ampulla in Axolotl (Fig. 5G, arrow) which was absent in *Xenopus*. Overall, results from 2D and 3D analyses demonstrated that Axolotl exhibited a horizontal semicircular canal with morphological characteristics that tend to restrain the biomechanical activation of hair cells by the endolymph flow.

## DISCUSSION

The results of this paper provide evidence for the functional correlation of semicircular canal morphology which constrains head motion detection, thereby restricting vestibular based gaze stabilization. We further show that such restrictions in vestibular sensitivity go hand in hand with differences in locomotion strategy.

### Consequences of low vestibular sensitivity on visuo-vestibular and EC-derived ocular reflex

Our experiments demonstrate that the onset of the aVOR in Axolotl is delayed compared to *Xenopus*. In *Xenopus* larvae, robust and reliable eye motions of spino-ocular, optokinetic, and gravitational VOR are first observed at stage 42, concomitant with the activation of a complex swimming behavior (Bacqué-Cazenave et al., 2022). Responses to angular head rotations first emerge at stage 49, with an increase in performance until the maximum gain is reached around stage 55. We show that Axolotl have effectively no functional VOR up to stage 54, with severe limitations in both magnitude and timing of eye motions. Only at later stages (56) do they display a functional VOR comparable to *Xenopus* at stage 54, indicating that this reduced vestibular performance is caused by delayed development. We nonetheless tested whether, at these limited stages, the OKR can compensate for this lack of vestibular input during naturalistic stimulation. While indeed, Axolotl

display a larger OKR at these stages than *Xenopus*, that may serve to compensate, it does so incompletely, as conjoint activation of OKR and VOR still produce comparatively worse eye movements. Such improved OKR performances in absence of vestibular signals may be mediated by plasticity mechanisms that have been previously reported in other vertebrates in response to changes in visuo-vestibular sensation. In mice and rabbits, adaptive stimuli that cause a reduction in VOR gain lead to an increased OKR gain (Collewijn and Grootendorst, 1979; Faulstich et al., 2004). Common ground for this type of adaptive plasticity in the shared VOR-OKR pathway seems to be the cerebellum and the vestibular nuclei (du Lac et al., 1995; Highstein et al., 1997; Forsthofer and Straka, 2023).

We also investigated another source of potential compensation: spino-ocular motor coupling, which produces compensatory eye movements based on efference copy signalling of the spinal locomotor central pattern generator, independently of any sensory inputs (for review see Straka et al., 2022). This efference copy intrinsic signal is known to gate the aVOR during swimming either by a complete cancelling of the canal input or by a summative processing and could thus operate without vestibular input (Lambert et al., 2012; Bacqué-Cazenave et al., 2022). However, despite while such coupling was present, it appeared to be less efficient to produce repetitive locomotor-induced compensatory eye movements in Axolotl, likely due to a lack of vestibular tuning of this reflex which has been shown to play a critical role in maturation of locomotor-induced oculomotor behaviour (Bacqué-Cazenave et al., 2022).

Overall, the increased gain during visual-only stimulation which is not sufficient to compensate for the missing VOR component during co-activation of both reflexes, along with the severe phase-lagged peak eye motion response suggests an issue with vestibular sensation. In addition, even after the onset, the aVOR performance remained lower in Axolotl than in *Xenopus*, suggesting not only a delay in VOR onset but an overall lower functionality thereof. This led us to investigate the sensory organ itself where variations in canal geometry could induce a different sensitivity to head rotations between urodele salamanders and anuran toads.

### Semicircular canal morphology constrains vestibular sensitivity

Prior to reaching developmental stages 49-50, *Xenopus* employs solely a gVOR and an OKR, as semicircular canals are not functional due to insufficiently sized duct diameters (Lambert et al., 2008; Bacqué-Cazenave et al., 2022). Our results showed that the minimum canal size necessary to trigger an aVOR onset in stage 49 *Xenopus* (Lambert et al., 2008) was not reached at larval Axolotl at stage 54 suggesting that this biomechanical rule seems to be a common feature in VOR ontogeny throughout vertebrates. Indeed, similar findings were made in Zebrafish and miniaturized frogs (Beck et al., 2004; Essner et al., 2022). The variation in canal radius along with the more elliptical shape of the Axolotl ampulla suggests that endolymph flow is more favorable in *Xenopus* (Muller and Verhagen, 1988; Muller, 1994). Furthermore, in the 3D analysis of Axolotl, the semicircular canal exhibits a low circularity, a substantial distortion from a single spatial plane, and a stenosis of the duct just near the entrance of the ampulla. These features contribute to a perturbation of the endolymph flow within the canal, leading to a deceleration of the input fluid force into the ampulla and, consequently, a reduction in hair cell activation (Lambert and Bacqué-Cazenave, 2020). Accordingly, a HC with such geometrical parameters would be less efficient in detecting head acceleration during both active and passive motion.

### Consequences of low vestibular sensitivity on swimming patterns

By detecting passive and active head movements, and thereby ensuring a stable posture which is required for efficient locomotion, vestibular endorgans contribute to an optimization of locomotor parameters (gait, speed, trajectory) by producing the necessary postural adjustments (Angelaki and Cullen, 2008). Consequently, there is a strong likelihood that vestibular function is tightly correlated with locomotor activity and modes across vertebrate species. Our locomotor style analysis showed that swimming instances in both species were characterized by swim speed ranges that were consistent with values reported from other aquatic larvae and fish (Budick and O'Malley, 2000; Hänzi and Straka, 2017). Yet, a notable difference was observed in the swimming style. Axolotls exhibit distinct swimming events, with a high-velocity forward thrust/propulsion followed by a passive glide, commonly referred to as a bout (Fig.2E, G). This swimming mode is in high contrast

to *Xenopus*, which show an almost continuous locomotion as indicated by a larger percentage of time allocated to swimming throughout the recording session and much longer bouts (Fig. 2H, I). This type of swimming mode distinction has also been observed and characterized in two related fish species, zebrafish and *Danionella cerebrum* (Rajan et al., 2022). Larval zebrafish demonstrated bouts of swimming whereas *Danionella cerebrum* exhibited continuous swimming sequences and a very late aVOR onset during the development, around 35dpf, compared to some other fish species like medaka (around 20dpf; Beck et al., 2004). Even if additional experiments need to be done in larval fishes to confirm this hypothesis, these partial data suggest that a lifestyle-dependent phenotypic distinction of vestibular endorgans could exist in larval fish as described here in larval amphibians.

Undulatory swimming, in the absence of a flexible neck, produces rhythmic oscillations of the head, thereby activating lateral semicircular canals through the resultant angular rotations. In *Xenopus*, semicircular canals are exposed to average peak angular accelerations of around  $150\text{-}200^\circ/\text{s}^2$  (Lambert et al., 2020). In comparison, the average angular head acceleration was higher in Axolotl at  $202.01^\circ/\text{s}^2$ . The discontinuous, bout-like swimming activity could be a locomotor adaptation in Axolotl imposed by the low vestibular sensitivity due to the non-optimal semicircular canal morphology: Higher, but less variable accelerations may reduce the error or mismatch signal between an ineffective capacity to detect head rotations and a weak angular VOR, while subsequent straightforward glides and overall reduced swimming events would reduce head deflections, minimizing the need for self-motion detection overall. Such reduced but fast locomotion in Axolotl indeed fits with their ecological niche. Axolotls even in juvenile stages are sit-and-wait predators and are paedomorphic retaining an aquatic lifestyle throughout life (Hoff et al., 1989). In contrast, the anuran *Xenopus laevis* tadpoles are filter feeders, almost continuously in motion, feeding herbivore material in the surrounding water (Sillar et al., 2008; Currie and Sillar, 2018). Previous investigations also observed less efficient swimming in adult Axolotl compared to anuran tadpoles and most fishes and was speculated to be an adjustment to living in shallow lakes with dense vegetation (D'août and Aerts, 1997). From this angle, reduced necessity for swimming may lead to less evolutionary pressure to rapidly develop functional inner ears, providing an alternative link between our morphological and behavioral data.

## Conclusions

Altogether our findings reinforce the idea of an ecology-dependent relationship between semicircular canal morphology, locomotor, and vestibular functional capacity. A causative demonstration of whether lifestyle depends on vestibular performance, or whether vestibular performance causes lifestyle adaptations is challenging to show. Nonetheless, it is clear that both vestibular sensation and locomotion require a co-adaptation, and this co-adaptation can be observed in many vertebrates' taxa. On this purpose, aquatic species like fish and amphibians, appeared to be of particular interest to continue exploring this question along the line developed in the present study.

## AUTHOR CONTRIBUTIONS

Conceptualization: PS, MF, RSG, FML, HS; Investigation: PS, MF, FML, HS; Formal analysis: PS, MF, GC, FML; Software: MF, GC, FML; Visualization: PS, FML; Writing-original draft: PS, MF, FML, HS; Writing-review & editing: PS, MF, GC, RSG, FML; Funding acquisition: FML, HS.

## DISCLOSURE

The authors declare no competing interests.

## DATA AND CODE AVAILABILITY

All data included in this article will be shared by the corresponding author(s) and all analysis codes will be shared in GitHub.

## REFERENCES

- Angelaki, D.E., and Cullen, K. E. (2008). Vestibular system: the many facets of a multimodal sense. *Annu Rev Neurosci* 31, 125-150.
- Bacqué-Cazenave, J., Courtand, G., Beraneck, M., Lambert, F.M., and Combes, D. (2018). Temporal Relationship of Ocular and Tail Segmental Movements Underlying Locomotor-Induced Gaze Stabilization During Undulatory Swimming in Larval *Xenopus*. *Front Neural Circuits* 12, 95.
- Bacqué-Cazenave, J., Courtand, G., Beraneck, M., Straka, H., Combes, D., and Lambert, F.M. (2022). Locomotion-induced ocular motor behavior in larval *Xenopus* is developmentally tuned by visuo-vestibular reflexes. *Nat Commun* 13, 2957.
- Beck, J.C., Gilland, E., Tank, D.W., and Baker, R. (2004). Quantifying the ontogeny of optokinetic and vestibuloocular behaviors in zebrafish, medaka, and goldfish. *J Neurophysiol* 92, 3546-3561.
- Benson, R.B.J., Starmer-Jones, E., Close, R.A., and Walsh, S.A. (2017). Comparative analysis of vestibular ecomorphology in birds. *J Anat* 231, 990-1018.
- Budick, S.A., and O'Malley, D.M. (2000). Locomotor repertoire of the larval zebrafish: swimming, turning and prey capture. *J Exp Biol* 203, 2565-2579.
- Capshaw, G., Soares, D., and Carr, C.E. (2019). Bony labyrinth morphometry reveals hidden diversity in lungless salamanders (Family Plethodontidae): structural correlates of ecology, development, and vision in the inner ear. *Evolution* 73, 2135-2150.
- Collewijn, H., and Grootendorst, A.F. (1979). Adaptation of optokinetic and vestibulo-ocular reflexes to modified visual input in the rabbit. *Pro Brain Res* 50, 771-781.
- Currie, S.P., and Sillar, K.T. (2018). Developmental changes in spinal neuronal properties, motor network configuration, and neuromodulation at free-swimming stages of *Xenopus* tadpoles. *J Neurophysiol* 119, 786-795.
- Curthoys, I.S., and Oman, C.M. (1986). Dimensions of the horizontal semicircular duct, ampulla and utricle in rat and guinea pig. *Acta Otolaryngol* 101, 1-10.
- D'août, K., and Aerts, P. (1997). Kinematics and Efficiency of Steady Swimming in Adult Axolotls (*Ambystoma Mexicanum*). *J Exp Biol* 200, 1863-1871.
- Dietrich, H., and Wühr, M. (2019). Strategies for Gaze Stabilization Critically Depend on Locomotor Speed. *Neuroscienc* 408, 418-429.
- du Lac, S., Raymond, J.L., Sejnowski, T.J., and Lisberger, S.G. (1995). Learning and memory in the vestibulo-ocular reflex. *Annu Rev Neurosci* 18, 409-441.
- Essner, R.L., Pereira, R.E., Blackburn, D.C., Singh, A.L., Stanley, E.L., Moura, M.O., Confetti, A.E., and Pie, M.R. (2022). Semicircular canal size constrains vestibular function in miniaturized frogs. *Sci Adv* 8, eabn1104.
- Faulstich, B.M., Onori, K.A., and du Lac, S. (2004). Comparison of plasticity and development of mouse optokinetic and vestibulo-ocular reflexes suggests differential gain control mechanisms. *Vision Res* 44, 3419-3427.
- Fedorov, A., Beichel, R., Kalpathy-Cramer, J., Finet, J., Fillion-Robin, J.C., Pujol, S., Bauer, C., Jennings, D., Fennessy, F., Sonka, M., Buatti, J., Aylward, S., Miller, J.V., Pieper, S., and Kikinis, R. (2012). 3D Slicer as an image computing platform for the Quantitative Imaging Network. *Magn Reson Imaging* 30, 1323-12-41.
- Feller, A.E., and Hedges, S.B. (1998). Molecular evidence for the early history of living amphibians. *Mol Phylogenet Evol* 9, 509-516.
- Forsthofer, M., and Straka, H. (2023). Homeostatic plasticity of eye movement performance in *Xenopus* tadpoles following prolonged visual image motion stimulation. *J Neurol* 270, 57-70.
- França de Barros, F., Schenberg, L., Tagliabue, M., and Beraneck, M. (2020). Long term visuo-vestibular mismatch in freely behaving mice differentially affects gaze stabilizing reflexes. *Sci Rep* 10, 20018.

- Gensberger, K. D., Kaufmann, A.K., Dietrich, H., Branoner, F., Banchi, R., Chagnaud, B.P., and Straka, H. (2016). Galvanic Vestibular Stimulation: Cellular Substrates and Response Patterns of Neurons in the Vestibulo-Ocular Network. *J Neurosci* 36, 9097-9110.
- Gordy, C., and Straka, H. (2022). Developmental eye motion plasticity after unilateral embryonic ear removal in *Xenopus laevis*. *iScience* 25, 105165.
- Gravot, C.M., Knorr, A.G., Glasauer, S., and Straka, H. (2017). It's not all black and white: Visual scene parameters influence optokinetic reflex performance in *Xenopus laevis* tadpoles. *J Exp Biol* 220, 4213-4224.
- Hänzi, S., and Straka, H. (2017). Developmental changes in head movement kinematics during swimming in *Xenopus laevis* tadpoles. *J Exp Biol* 220, 227-236.
- Highstein, S.M., Partsalis, A., and Arikan, R. (1997). Role of the Y-group of the vestibular nuclei and flocculus of the cerebellum in motor learning of the vertical vestibulo-ocular reflex. *Rog Brain Res* 114, 383-397.
- Hoff, K.V., Hug, N., King, V.A., and Wassersug, R.J. (1989). The kinematics of larval salamander swimming (Ambystomatidae: Caudata). *Can J Zool* 67, 2756-2761.
- Hullar, T.E. (2006). Semicircular canal geometry, afferent sensitivity, and animal behavior. *Anat Rec A* 288, 466–472.
- Jones, G.M., and Spells, K.E. (1963). A theoretical and comparative study of the functional dependence of the semicircular canal upon its physical dimensions. *Proc R Soc Lond B Biol Sci* 157, 403–419.
- Knorr, A.G., Gravot, C.M., Gordy, C., Glasauer, S., and Straka, H. (2018). I spy with my little eye: a simple behavioral assay to test color sensitivity on digital displays. *Biol Open* 7, bio035725.
- Lambert, F.M., and Bacqué-Cazenave, J. (2020). Rules and Mechanistic Principles for the Ontogenetic Establishment of Vestibular Function. In *The Senses: A Comprehensive Reference*, Vol 6, Fritzsche, B., Straka, H., eds (Elsevier), pp. 162-172.
- Lambert, F.M., Bacqué-Cazenave, J., Le Seach, A., Arama, J., Courtand, G., Tagliabue, M., Eskiizmirliiler, S., Straka, H., and Beranek, M. (2020). Stabilization of gaze during early *Xenopus* development by swimming-related utricular signals. *Curr Biol* 30, 1-8.
- Lambert, F.M., Beck, J.C., Baker, R., and Straka, H. (2008). Semicircular canal size determines the developmental onset of angular vestibuloocular reflexes in larval *Xenopus*. *J Neurosci* 28, 8086-8095.
- Lambert, F.M., Beranek, M., Straka, H., and Simmers, J. (2023). Locomotor efference copy signaling and gaze control: An evolutionary perspective. *Curr Opin Neurobiol* 82, 102761.
- Lambert, F.M., and Straka, H. (2012). The Frog Vestibular System as a Model for Lesion-Induced Plasticity: Basic Neural Principles and Implications for Posture Control. *Front Neurol* 3, 42.
- Le Maitre, A., Schuetz, P., Vignaud, P., and Brunet, M. (2017). New data about semicircular canal morphology and locomotion in modern hominoids. *J Anat* 231, 95-109.
- Lipovsek, M., and Wingate, R.J. (2018). Conserved and divergent development of brainstem vestibular and auditory nuclei. *elife* 7, e40232.
- Malinzak, M.D., Kay, R.F., Hullar, T.E. (2012). Locomotor head movements and semicircular canal morphology in primates. *Proc Natl Acad Sci U S A* 109, 17914-17919.
- Masseck, O.A., and Hoffmann, K.P. (2009). Comparative neurobiology of the optokinetic reflex. *Ann N Y Acad Sci* 1164, 430-439.
- Mayne, R. (1950). The dynamic characteristics of the semicircular canals. *J Comp Physiol Psychol* 43, 309-319.
- Miller Bever, M., Jean, Y.Y., and Fekete, D.M. (2003). Three-dimensional morphology of inner ear development in *Xenopus laevis*. *Dev Dyn* 227, 422-430.
- Muller, M. (1994). Semicircular duct dimensions and sensitivity of the vertebrate vestibular system. *J Theor Biol* 167, 239-256.

- Muller, M. (1999). Size limitations in semicircular duct systems. *J Theor Biol* 198, 405-437.
- Muller, M., and Verhagen, J.H. (1988). A new quantitative model of total endolymph flow in the system of semicircular ducts. *J Theo Biol* 134, 473-501.
- Muller, M., and Verhagen, J.H. (2002a). Optimization of the mechanical performance of a two-duct semicircular duct system—part1: dynamics and duct dimensions. *J Theor Biol* 216, 409-424.
- Muller, M., and Verhagen, J.H. (2002b). Optimization of the mechanical performance of a two-duct semicircular duct system—part 2: excitation of endolymph movements. *J Theor Biol* 216, 425-442.
- Nieuwkoop, P.D., and Faber, J. (1994). *Normal Table of *Xenopus laevis* (Daudin): A Systematical and Chronological Survey of the Development from the Fertilized Egg Till the End of Metamorphosis*. Garland Pub., New York.
- Nye, H.L., Cameron, J.A., Chernoff, E.A., and Stocum, D.L. (2003). Extending the table of stages of normal development of the axolotl: limb development. *Dev. Dynam.*, 226, 555–560.
- Ollion, J., Cochennec, J., Loll, F., Escudé, C., Boudier, T. (2013). TANGO: a generic tool for high-throughput 3D image analysis for studying nuclear organization. *Bioinformatics* 29, 1840-1841.
- Oman, C.M., Marcus, E.N., and Curthoys, I.S. (1987). The influence of semicircular canal morphology on endolymph flow dynamics. An anatomically descriptive mathematical model. *Acta Otolaryngol* 103, 1–13.
- Özugur, S., Chávez, M.N., Sanchez-Gonzalez, R., Kunz, L., Nickelsen, J., and Straka, H. (2022). Transcardial injection and vascular distribution of microalgae in *Xenopus laevis* as means to supply the brain with photosynthetic oxygen. *STAR Protoc* 3, 1-20.
- Pfaff, C., Martin, T., and Ruf, I. (2015). Bony labyrinth morphometry indicates locomotor adaptations in the squirrel-related clade (Rodentia, Mammalia). *Proc Biol Sci* 282, 20150744.
- Pereira, M., Chen, X., Muller, N., Bovy, L., Lei, X., Chen, W., Ren, H., Song, C., Lewis, L.D., Dang-Vu, T.T., Czisch, M., Picchioni, D., Duyn, J., Peigneux, P., Tagliazucchi, E, and Dresler, M. (2022). Sleep Neuroimaging: past research, present challenges and future directions.
- Rajan, G., Lafaye, J., Faini, G., Carbo-Tano, M., Duroure, K., Tanese, D., Panier, T., Candelier, R., Henninger, J., Britz, R., Judkewitz, B., Gebhardt, C., Emiliani, V., Debregeas, G., Wyart, C., and Del Bene, F. (2022). Evolutionary divergence of locomotion in two related vertebrate species. *Cell Rep* 38, 110585.
- Ramlochansingh, C., Branoner, F., Chagnaud, B.P., and Straka, H. (2014). Tricaine methanesulfonate (MS-222) as an effective anesthetic agent for blocking sensory-motor responses in *Xenopus laevis* tadpoles. *PLoS ONE* 9, e101606.
- Rogers, S.W. (2005). Reconstructing the behaviors of extinct species: an excursion into comparative paleoneurology. *Am J Med Genet A* 134, 349-356.
- Schindelin, J., Arganda-Carreras, I., Frise, E., Kaynig, V., Longair, M., Pietzsch, T., Preibisch, S., Rueden, C., Saalfeld, S., Schmid, B., Tinevez, J.Y., White, D.J., Hartenstein, V., Eliceiri, K., Tomancak, P., and Cardona, A. (2012). Fiji: an open-source platform for biological-image analysis. *Nat Methods* 9, 676-682.
- Schwab, J.A., Kriwet, J., Weber, G.W., and Pfaff, C. (2019). Carnivoran hunting style and phylogeny reflected in bony labyrinth morphometry. *Sci Rep* 9, 70.
- Sillar, K.T., Combes, D., Ramanathan, S., Molinari, M., and Simmers, J. (2008). Neuromodulation and developmental plasticity in the locomotor system of anuran amphibians during metamorphosis. *Brain Res Rev* 57, 94-102.
- Soupiadou, P., Gordy, C., Forsthofer, M., Sanchez-Gonzalez, R., and Straka, H. (2020). Acute consequences of a unilateral VIIIth nerve transection on vestibulo-ocular and optokinetic reflexes in *Xenopus laevis* tadpoles. *J Neurol* 267, S62-S75.
- Spoor, F., Bajpai, S., Hussain, S.T., Kumar, K., and Thewissen, J.G. (2002). Vestibular evidence for the evolution of aquatic behaviour in early cetaceans. *Nature* 417, 163-166.
- Spoor, F., Garland Jr., T., Krovitz, G., Ryan, T.M., Silcox, M.T., and Walker, A. (2007). The primate semicircular canal system and locomotion. *Proc Natl Acad Sci U S A* 104, 10808-10812.

- Spoor, F., Wood, B., and Zonneveld, F. (1994). Implications of early hominid labyrinthine morphology for evolution of human bipedal locomotion. *Nature* 369, 645-648.
- Straka, H., and Baker, R. (2013). Vestibular blueprint in early vertebrates. *Front Neural Circuits* 7, 182.
- Straka, H., and Dieringer, N. (2004). Basic organization principles of the VOR: lessons from frogs. *Prog Neurobiol* 73, 259-309.
- Straka, H., Fritsch, B., and Glover, J.C. (2014). Connecting ears to eye muscles: evolution of a 'simple' reflex arc. *Brain Behav Evol* 83, 162-175.
- Straka, H., Lambert, F.M., and Simmers, J. (2022). Role of locomotor efference copy in vertebrate gaze stabilization. *Front Neural Circuits* 16, 1040070.
- Tomar, S. (2006). Converting video formats with FFmpeg. *Linux Journal* 146, 10.
- Wibble, T., Pansell, T., Grillner, S., and Pérez-Fernández, J. (2022). Conserved subcortical processing in visuo-vestibular gaze control. *Nat Commun* 13, 4699.

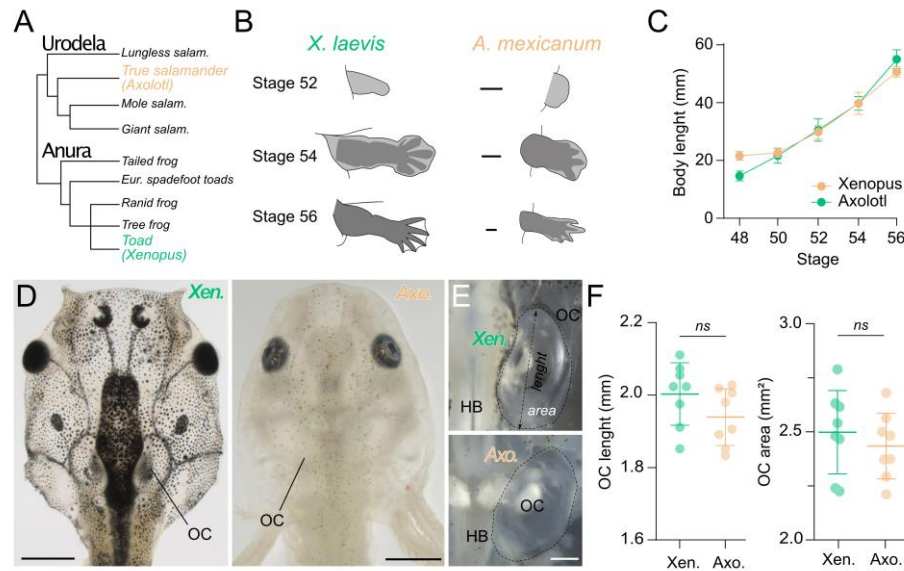


**Figure 1. Developmental pattern in *Xenopus* and *Axolotl* larvae.** (A) Phylogenetic tree of anurans and urodeles with a common ancestor about 220 million years ago. (B) Limb bud morphology in both *Xenopus* and *Axolotl* at stages 52, 54, and 56. (C) Growth curve measured as total body length in mm across stages 48 ( $n=8$  Xen.; 5 Axo.), 50 ( $n=8$  Xen.; 5 Axo.), 52 ( $n=6$  Xen.; 5 Axo.), 54 ( $n=6$  Xen.; 5 Axo.), and 56 ( $n=4$  Xen.; 5 Axo.). (D) Representative images of a *Xenopus* (Xen., left) and *Axolotl* (Axo., right) larval head at stage 54. (E) Magnification of the hindbrain (HB) and otic capsule (OC) in larval stage 54 *Xenopus* (top) and *Axolotl* (bottom). Dotted line indicates the selected region for otic capsule area calculations, dotted arrowhead lines indicate otic capsule length calculation axis. (F) Mean  $\pm$ SD for otic capsule length (left,  $n=8$  Xen.; 8 Axo.) and area (right,  $n=8$  Xen.; 8 Axo.) measured as indicated in (E). Statistical significance was calculated by the Mann-Whitney *U*-test, two-tailed,  $p=0.1049$  and  $p=0.5737$  respectively. Scale bar in B= 50  $\mu$ m; D= 2mm; E= 0.5 mm.

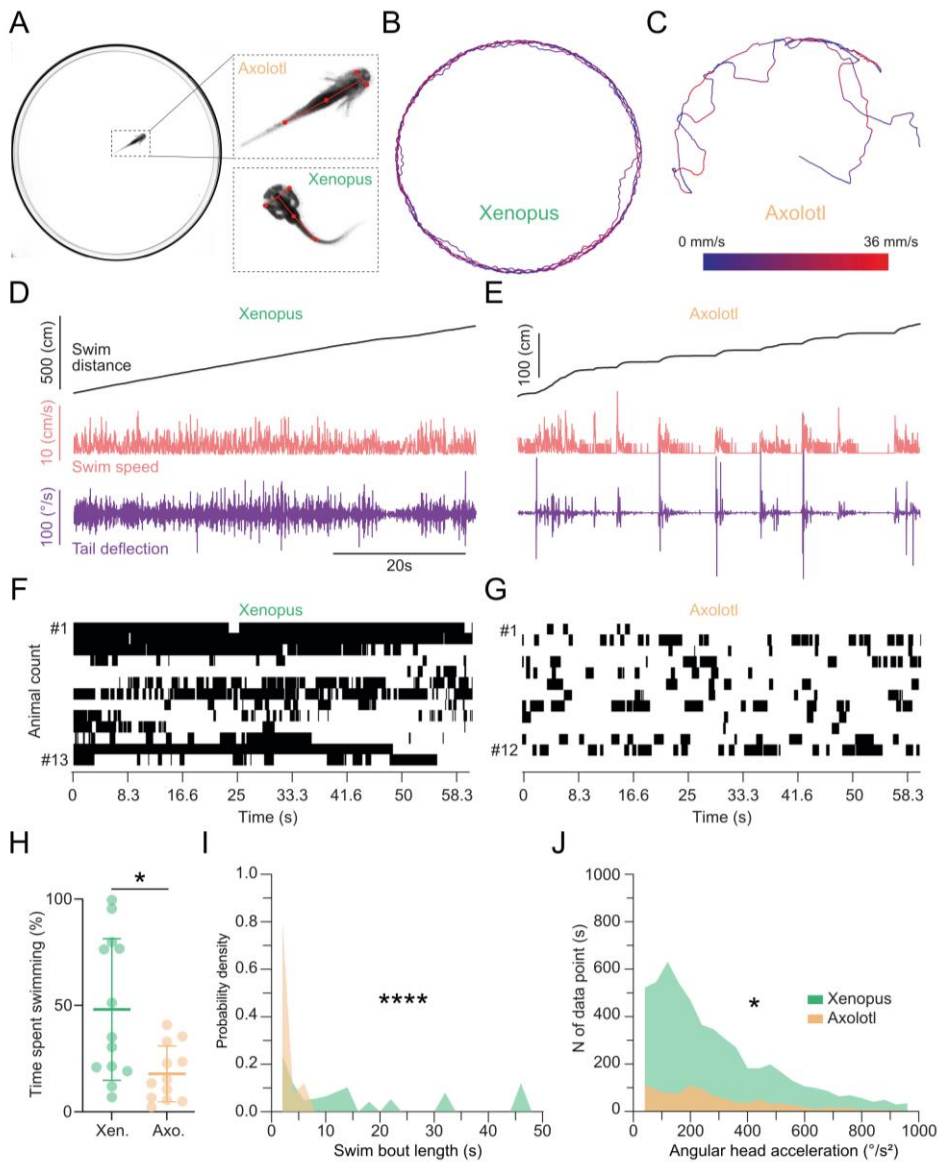


**Figure 2. Locomotor kinematics and patterns.** (A) Example of a salamander in the recording chamber. Magnification on the right side show the nodes fitted on the body of *Xenopus* (Xen.) and *Axolotl* (Axo.) to track head and tail movements. (B, C) Representative recording sessions showing displacement and speed of larval *Xenopus* (B) and *Axolotl* (C) during free swimming. (D, E) Representative examples (corresponding to recording sessions shown in B and C) of the overall swim distance, swim speed, and tail deflection in *Xenopus* (D) and *Axolotl* (E) respectively. (F, G) Event maps of each individual animal, over the whole recording session, indicating periods of swimming activity in black and non-swimming activity in white. (H) Percentage of time spent swimming over the recording session plotted as Mean  $\pm$ SD,  $p = 0.0188$ , Mann Whitney U-test, two-tailed. (I) Probability density of swim bout lengths illustrating the capacity to swim continuously over time,  $p < 0.0001$ , Kolmogorov-Smirnov test. (J) Distribution of angular head accelerations in *Xenopus* (green) and *Axolotl* (orange) during swimming,  $p = 0.012$ , Kolmogorov-Smirnov test.

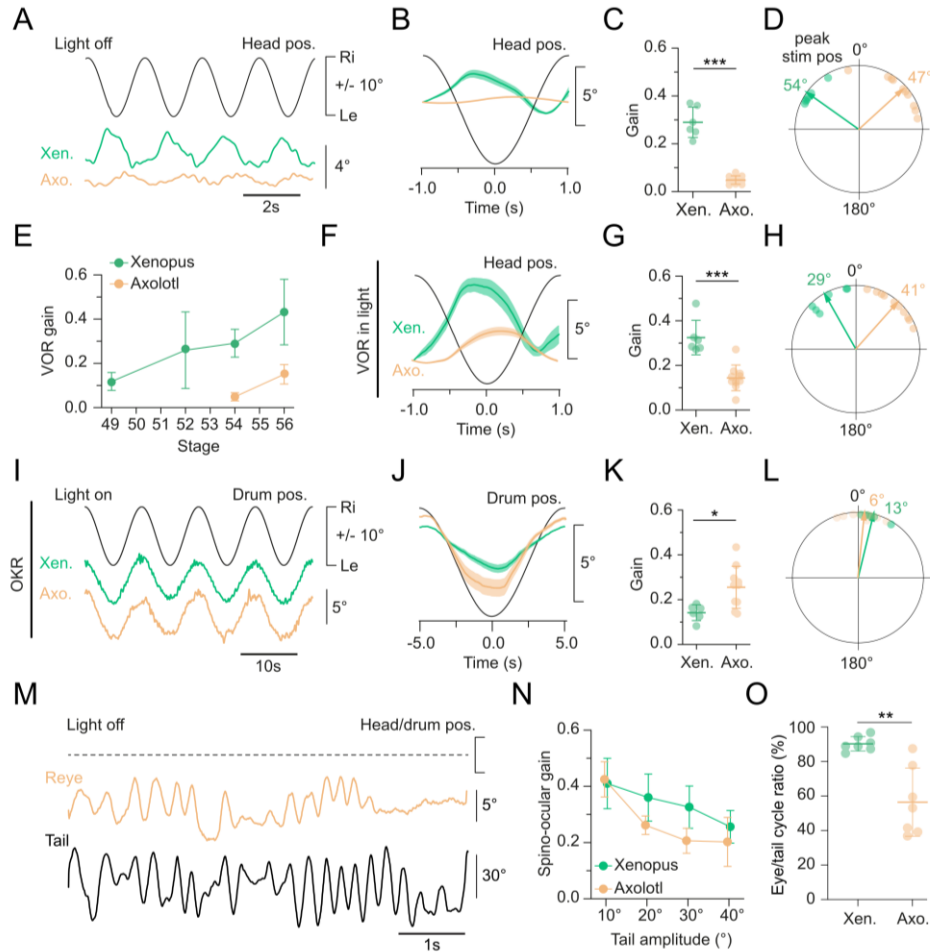


**Figure 3. Gaze-stabilizing eye movements.** (A-H) Reflexive eye movements evoked by the angular vestibulo-ocular reflex (aVOR) in response to horizontal head rotation in the dark (A-E) and in light (F-H). (A) Representative compensatory eye movements evoked by the aVOR during horizontal sinusoidal rotation of the head/table (0.5Hz; ± 31.4°/s). (B) Average response of the aVOR over a single head motion cycle (6-15 cycles averaged), black sine wave indicates stimulus position (head pos.; 0.5Hz; ± 31.4°/s). (C) Average gain (eye motion amplitude/stimulus amplitude; mean ± SD) of the aVOR at 0.5Hz (± 31.4°/s) for *Xenopus* (n= 6) and *Axolotl* (n=10) respectively. \*\*\*p < 0.001; Mann-Whitney U-test. (D) Polar plots illustrating aVOR phase relations to peak stimulus position (0°, peak stim pos) from 0° to ± 180°; arrows indicate the mean vector for *Xenopus* (green) and *Axolotl* (orange). (E) Averaged (± SD) gain of the aVOR through larval stages between *Xenopus* and *Axolotl*. (F) Average response of the aVOR over a single head motion cycle (10 cycles averaged), black sine wave indicates stimulus position (head pos.; 0.5Hz; ± 31.4°/s). (G) Average gain (eye motion amplitude/stimulus amplitude; mean ± SD) for aVOR at 0.5Hz; ± 31.4°/s for *Xenopus* (n= 6) and *Axolotl* (n=10,) respectively. \*\*\*p < 0.001; Mann-Whitney U-test. (H) Polar plots illustrating aVOR phase relations to peak stimulus position (0°, peak stim pos) from 0° to ± 180°; arrows indicate the mean vector for *Xenopus* (green) and *Axolotl* (orange). (I) Representative reflexive eye movements evoked by the optokinetic reflex (OKR) during horizontal sinusoidal rotation of a black and white striped pattern (0.1Hz; ± 31.4°/s). (J) Average response of OKR over a single head motion cycle (10 cycles averaged), black sine wave indicates stimulus position (drum pos.; 0.1Hz; ± 6.28°/s). (K) Average gain (eye motion amplitude/stimulus amplitude; mean ± SD) of the OKR at 0.1Hz; ± 6.28°/s for *Xenopus* (n= 6) and *Axolotl* (n=10,) respectively. \*p < 0.05; Mann-Whitney U-test. (L) Polar plots illustrating OKR phase relations to peak stimulus position (0°, peak stim pos) from 0° to ± 180°; arrows indicate the mean vector for *Xenopus* (green) and *Axolotl* (orange). (M) Representative reflexive eye movements evoked by the optokinetic reflex (OKR) during horizontal sinusoidal rotation of a black and white striped pattern (0.1Hz; ± 31.4°/s). (N) Spino-ocular gain vs Tail amplitude (°) for *Xenopus* (green) and *Axolotl* (orange). (O) Eye/tail cycle ratio (%) vs Tail amplitude (°) for *Xenopus* (green) and *Axolotl* (orange). \*\*p < 0.01; Mann-Whitney U-test.

arrows indicate the mean vector for *Xenopus* (green) and Axolotl (orange). (M) Representative compensatory eye movements evoked by the locomotor spino-ocular coupling during head-fixed swimming in the dark. (N) Average gain (eye motion amplitude/tail amplitude; mean  $\pm$  SD) vs tail amplitude for locomotor-induced eye movements between *Xenopus* ( $n= 7$ ) and Axolotl ( $n=8$ ) respectively. (O) Averaged ( $\pm$  SD) eye/tail cycle ratio (proportion of eye movement related to tail movement). \*\* $p < 0.001$ ; Mann-Whitney  $U$ -test.

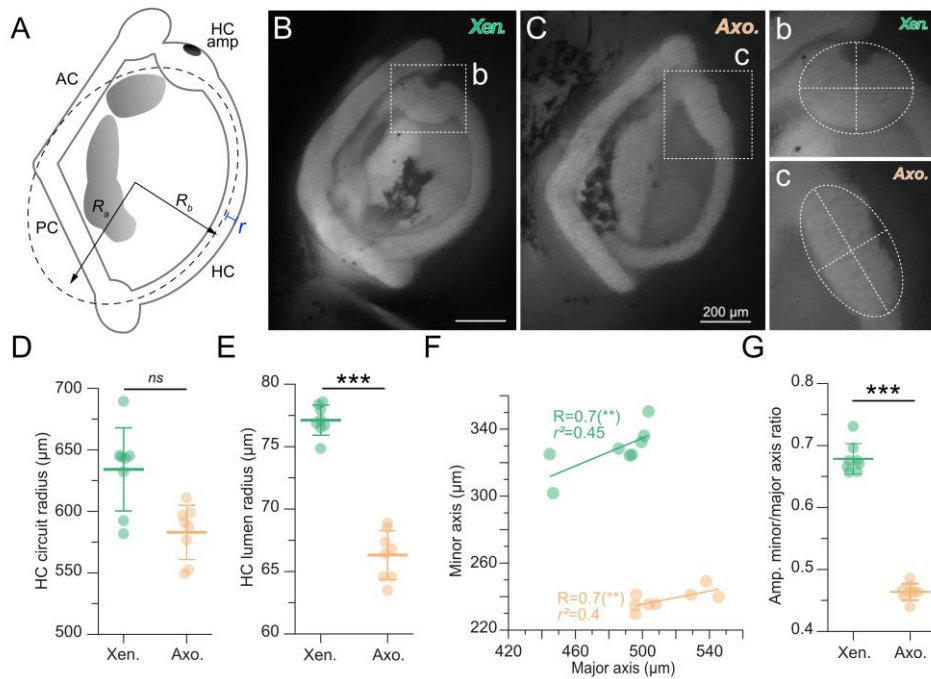


**Figure 4. Two-dimensional horizontal semicircular canal morphology.** (A) Top view schematic of the right semicircular canal spatial orientation showing the ellipse fitted (dotted line) to measure the circuit radius (calculated from the  $R_a$  and  $R_b$  ellipse radii) and the lumen radius (yellow " $r$ "). (B, C) Representative examples of stage 54 *Xenopus* (Xen.) and *Axolotl* (Axo.) labyrinth injected with Rhodamine dextran dye; (b,c) magnifications of the ampulla of the horizontal semicircular canals shown in B, C with an ellipse fit (white dotted line) to measure the ampulla size (see F and G). (D, E) Circuit (D) and lumen radii (E) of the horizontal canal (HC) depicted as mean  $\pm$  SD in *Xenopus* (green,  $n=8$ ) and *Axolotl* (orange,  $n=8$ );  $p=0.3282$ ,  $p=0.0002$ , respectively, Mann-Whitney U-test, two-tailed. (F) Correlation of the major and minor axis of the ellipse fitted on the ampulla (see b, c) in *Xenopus* (green) and *Axolotl* (orange). (G) Ratio of the major and minor axis of the HC canal depicted as mean  $\pm$  SD. \*\*\* $p < 0.001$ ; Mann-Whitney U-test.  $R_a$  major axis,  $R_b$  minor axis,  $r$  lumen radius. HC, PC, AC: horizontal, posterior, anterior canal, respectively; HC amp: HC ampulla. Scale bar in B & C = 200  $\mu\text{m}$ .

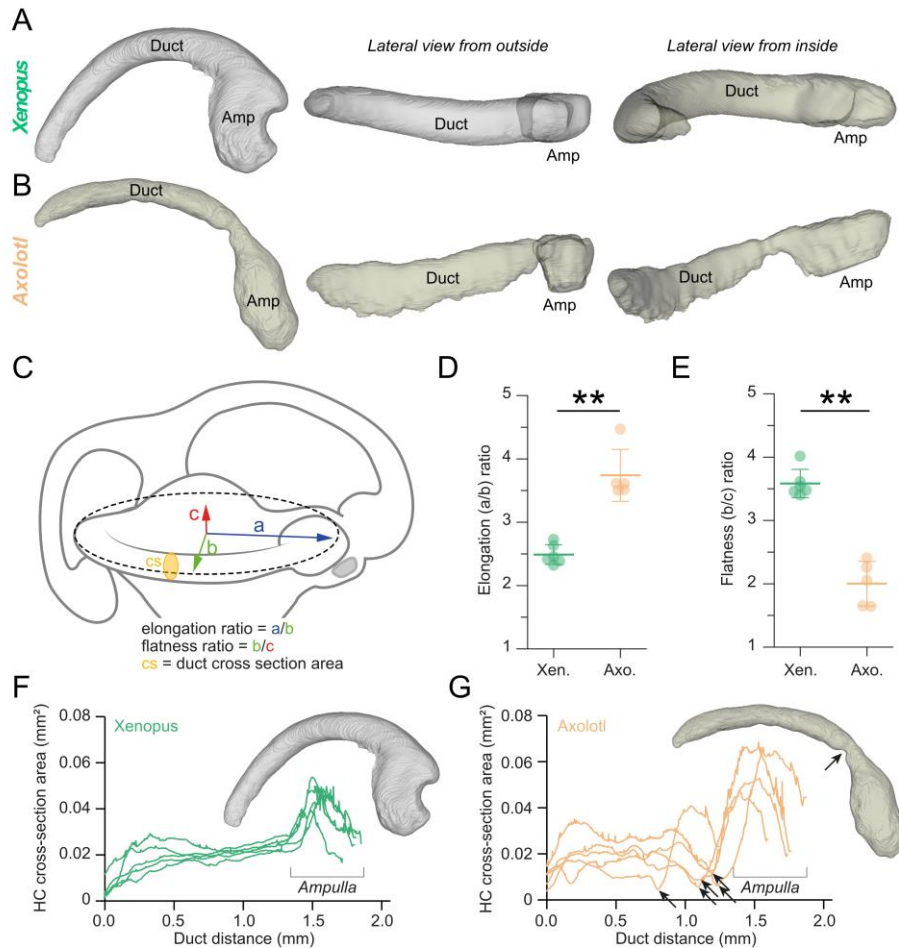


**Figure 5. Three-dimensional horizontal semicircular canal morphology.** (A, B) Representative reconstructed views of the 3D morphology of the horizontal canal in *Xenopus* (top row) and *Axolotl* (bottom row) at stage 54. (C) 3D Schematic of the vestibular canal system showing metrics for the 3D spatial measurements. Three oriented vectors are extracted from the 3D reconstruction; the “a” (blue) and “b” (green) vectors correspond to  $R_a$  and  $R_b$  of the fitted ellipse (like in Fig. 4), the “c” (red) vector corresponds to the vertical elevation component from the lowest to the highest detected limits of the canal. The yellow disk represents the duct cross section (cs) area measured all along the duct (see F and G). (D, E) Elongation (D, a/b) and Flatness (E, b/c) ratios of the horizontal canal depicted as mean  $\pm$  SD in *Xenopus* (green,  $n=6$ ) and *Axolotl* (orange,  $n=5$ );  $p=0.0043$ ,  $p=0.0043$ , respectively, Mann Whitney U-test, two-tailed. (F, G) Cross-section areas along the horizontal canal duct length in *Xenopus* (green,  $n=5$  in F) and *Axolotl* (orange,  $n=5$  in G); note the narrow canal lumen prior to the start of the ampulla in *Axolotl* indicated by a black arrow.

---

## CHAPTER III:

### ACUTE CONSEQUENCES OF A UNILATERAL VIIIITH NERVE TRANSECTION ON VESTIBULO-OCULAR AND OPTOKINETIC REFLEXES IN *XENOPUS LAEVIS* TADPOLES

---

**Parthena Soupiadou**<sup>1,2</sup>, Clayton Gordy<sup>1,2</sup>, Michael Forsthofer<sup>1,2</sup>, Rosario Sanchez-Gonzales<sup>1</sup>, Hans Straka<sup>1</sup>

<sup>1</sup> Faculty of Biology, Ludwig-Maximilians-University Munich, Großhaderner Str. 2, 82152 Planegg, Germany

<sup>2</sup> Graduate School of Systemic Neurosciences, Ludwig-Maximilians-University Munich, Großhaderner Str. 2, 82152 Planegg, Germany

\*Correspondence: straka@lmu.de (HS)

#### Contribution of authors:

Conceptualization: PS, CG, RSG, HS; Methodology: PS, CG, RSG, HS; Investigation: PS, HS; Formal analysis: PS, MF; Software: MF; Visualization: PS, HS; Writing-original draft: PS, HS; Writing-review & editing: PS, CG, MF, RSG, HS; Funding acquisition: HS.

#### My contributions to this manuscript:

I contributed to the design of experiments and the conceptualization of analysis scripts. I performed all experiments and analyses thereof. I created initial versions of the figures and supplemental figures and contributed to revisions on all figures. I took part in writing the initial version of the manuscript and contributed to the editing process.

The following manuscript is published in the *Journal of Neurology*. Permission for reuse in this thesis was granted to PS under the creative commons license CC BY 4.0.

For online access, please refer to: <https://doi-org.emedien.ub.uni-muenchen.de/10.1007/s00415-020-10205-x>



## Acute consequences of a unilateral VIIIth nerve transection on vestibulo-ocular and optokinetic reflexes in *Xenopus laevis* tadpoles

Parthena Soupiadou<sup>1,2</sup> · Clayton Gordy<sup>1,2</sup> · Michael Forsthofer<sup>1,2</sup> · Rosario Sanchez-Gonzalez<sup>1</sup> · Hans Straka<sup>1</sup>

Received: 10 June 2020 / Revised: 28 August 2020 / Accepted: 29 August 2020 / Published online: 11 September 2020  
© The Author(s) 2020

### Abstract

Loss of peripheral vestibular function provokes severe impairments of gaze and posture stabilization in humans and animals. However, relatively little is known about the extent of the instantaneous deficits. This is mostly due to the fact that in humans a spontaneous loss often goes unnoticed initially and targeted lesions in animals are performed under deep anesthesia, which prevents immediate evaluation of behavioral deficits. Here, we use isolated preparations of *Xenopus laevis* tadpoles with functionally intact vestibulo-ocular (VOR) and optokinetic reflexes (OKR) to evaluate the acute consequences of unilateral VIIIth nerve sections. Such in vitro preparations allow lesions to be performed in the absence of anesthetics with the advantage to instantly evaluate behavioral deficits. Eye movements, evoked by horizontal sinusoidal head/table rotation in darkness and in light, became reduced by 30% immediately after the lesion and were diminished by 50% at 1.5 h postlesion. In contrast, the sinusoidal horizontal OKR, evoked by large-field visual scene motion, remained unaltered instantaneously but was reduced by more than 50% from 1.5 h postlesion onwards. The further impairment of the VOR beyond the instantaneous effect, along with the delayed decrease of OKR performance, suggests that the immediate impact of the sensory loss is superseded by secondary consequences. These potentially involve homeostatic neuronal plasticity among shared VOR-OKR neuronal elements that are triggered by the ongoing asymmetric activity. Provided that this assumption is correct, a rehabilitative reduction of the vestibular asymmetry might restrict the extent of the secondary detrimental effect evoked by the principal peripheral impairment.

**Keywords** Vestibulo-ocular reflex · Semicircular canal · Extraocular motoneurons · Eye movements · Unilateral labyrinthectomy · Homeostatic plasticity · Optokinetic reflex

### Introduction

Unilateral loss of peripheral vestibular function causes severe and incapacitating symptoms [1]. These emerging deficits derive from either an impairment of inner ear structures or are commonly observed following damage to the statoacoustic (VIIIth) nerve. Well characterized impairments

of this nerve, such as neuritis, schwannoma, or surgical transection each provide some degree of peripheral vestibular loss that is usually accompanied by vertigo, dizziness, oscillopsia, and various cognitive deficits in orientation and navigation [2]. Furthermore, pathological motor reactions such as a nystagmus or postural asymmetries also occur following VIIIth nerve disfunction [2–7]. Human patients with impaired vestibular function presenting to a clinician, however, have usually suffered from such symptoms for many days prior to clinical assessment, with the more immediate and most severe impairments having often vanished. In addition, the presented symptoms are often superimposed with and influenced by, alterations that derive from vestibular compensation, a plasticity process thought to ameliorate lesion-induced deficits [1], which often encumbers diagnostic effectiveness.

Experimental reproduction of vestibular deficits in animal models also suffer from a general lack of detailed knowledge

**Electronic supplementary material** The online version of this article (<https://doi.org/10.1007/s00415-020-10205-x>) contains supplementary material, which is available to authorized users.

✉ Hans Straka  
straka@lmu.de

<sup>1</sup> Department Biology II, Ludwig-Maximilians-University Munich, Großhaderner Str. 2, 82152 Planegg, Germany

<sup>2</sup> Graduate School of Systemic Neurosciences, Ludwig-Maximilians-University Munich, Großhaderner Str. 2, 82152 Planegg, Germany

on the magnitude, variety, and progression of acute symptoms that appear instantaneously after an induced loss of peripheral vestibular function. This is mostly due to the fact that any peripheral vestibular lesion has to be performed in deeply anesthetized and analgesically treated animals that require a post-surgical recovery period until the behavioral impairments can be faithfully evaluated. During this period, the activity of the nervous system is considerably attenuated and thus unable to appropriately express immediate functional deficits [8]. Compared to typical patients with a vestibular syndrome that are seen by a clinician days and weeks after the incident, a planned tumor surgery of the VIIIth nerve [9] or a comparable experimental manipulation, e.g. in rabbits [10] or mice [11] are currently the closest conditions that allow an evaluation of the acute stage after a vestibular lesion. Nonetheless, all these studies suffer from the unavoidable temporal lag between the surgical lesion and the fully awake state of an animal, which is required to estimate the full spectrum of immediate behavioral consequences.

The difficulties of evaluating acute motor impairments after a unilateral peripheral vestibular nerve lesion can be circumvented, however, by employing the amphibian *Xenopus laevis* as a model system. In particular, an isolated in vitro whole-head preparation of *Xenopus laevis* tadpoles with intact sensory organs (eyes, inner ears) and motor effector organs (eye muscles) to execute visuo-vestibular motion-evoked eye movements allow an in vivo-like approach and manipulations under in vitro conditions [12]. Specifically, the isolated nature of the in vitro preparation allows a rapid surgical transection of the VIIIth nerve under visual guidance in the absence of anesthesia, providing the necessary condition to characterize and quantify the instantaneous behavioral consequences of a unilateral vestibular loss. To evaluate the impact of a VIIIth nerve transection, the current study directly assessed the behavioral output from ocular motor centers, where both vestibular and visual information converges. Accordingly, spontaneous eye position changes as well as vestibulo-ocular reflex (VOR) and visual image motion-evoked optokinetic reflex (OKR) performance during separate or combined horizontal visuo-vestibular motion stimulation [13, 14] were assessed.

In this study, static and motion-evoked eye movements were recorded with an infrared video camera prior to and immediately after a unilateral transection of the VIIIth nerve. The gain and phase magnitudes of evoked eye movements at four time points, over a period of up to 5 h postlesion, were analyzed to estimate the acute consequences of the lesion and to evaluate the plasticity of the ocular motor behavior.

## Material and methods

### Animals and experimental preparation

*Xenopus laevis* tadpoles of either sex ( $n = 7$ ) at developmental stages 53–55 [15] were obtained from the in-house animal breeding facility at the Biocenter-Martinsried of the Ludwig-Maximilians-University Munich. Tadpoles were maintained in tanks with non-chlorinated water (17–18 °C) at a 12/12 light/dark cycle. Experiments were performed in vitro on semi-intact preparations and comply with the "Principles of animal care", publication No. 86-23, revised 1985 of the National Institute of Health. Permission for these experiments was granted by the Regierung von Oberbayern (ROB-55.2–2532.Vet\_03-17-24).

Tadpoles were anesthetized in 0.05% 3-aminobenzoic acid ethyl ester methanesulfonate at room temperature (MS-222; Pharmaq Ltd. UK) for 3 min, transferred to ice-cold frog Ringer solution (75 mM NaCl, 25 mM NaHCO<sub>3</sub>, 2 mM CaCl<sub>2</sub>, 2 mM KCl, 0.1 mM MgCl<sub>2</sub>, and 11 mM glucose, pH 7.4), decapitated at the level of the upper spinal cord (Fig. 1a) and pinned to a Sylgard base with the ventral side up to remove the lower jaw and viscera under visual control. The skin was removed from the remaining tail and all spinal nerves were severed to prevent swim-related contractions of the most anterior axial muscles. The cartilaginous skull was opened from dorsal and the forebrain was removed. The hindbrain entrances of both VIIIth nerves were exposed by removal of connective tissue above and around the brain, as well as by removal of the choroid plexus overlaying the fourth ventricle. However, the remaining central nervous system, visual, and vestibular sensory periphery with afferent connections, and extraocular motor nerves were functionally preserved. This allowed the recording of eye movements during application of visual and vestibular motion stimuli. Following, the preparations were allowed to recover for ~2 h at 17 °C before commencing with the recording session [16]. During a recording session, preparations were mechanically secured in the center of a Sylgard-lined chamber and continuously superfused with oxygenated (Carbogen: 95% O<sub>2</sub>, 5% CO<sub>2</sub>) Ringer solution at a constant temperature of  $17.5 \pm 0.5$  °C.

Because of the maintained neuronal innervation of the extraocular muscles, the isolated preparation allowed the activation of eye movements by vestibular and visual motion stimulation. Natural activation of the vestibular endorgans was performed with a six degrees of freedom motion stimulator (PI H-840, Physik Instrumente, Karlsruhe, Germany). Vestibular motion stimuli consisted of sinusoidal horizontal rotations at 0.5 Hz and positional excursion of  $\pm 10^\circ$  that generated a peak

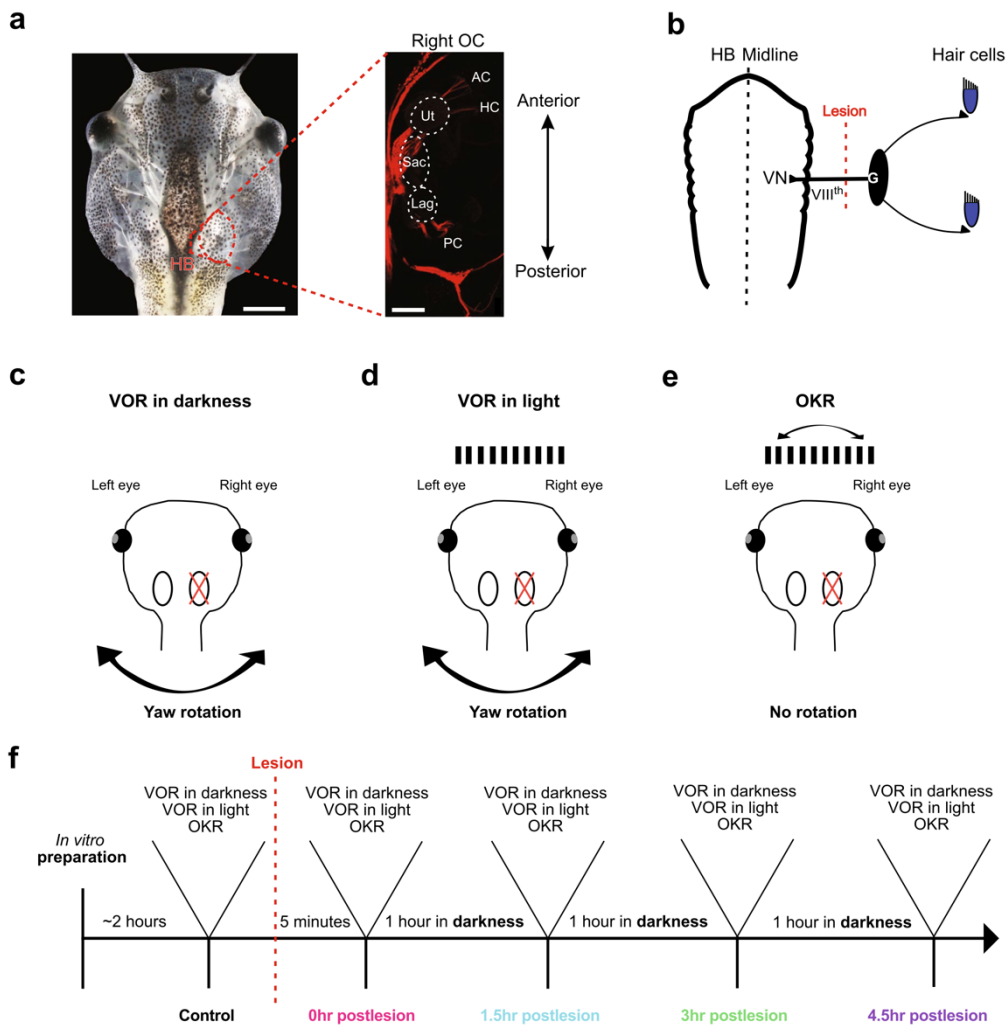


**Fig. 1** Experimental paradigm for evaluating acute consequences of a unilateral VIIIth nerve section on eye movements. **a** Isolated head preparation of a stage 55 *Xenopus laevis* tadpole with functional eyes, eye muscles, inner ears and neuronal circuits for ocular motor behavior; the inset on the right illustrates afferent innervation patterns of vestibular endorgans after tracer placement (Tetramethylrhodamine) into the vestibular nuclei. **b** Schematic of the vestibular hair cell—hindbrain vestibular nucleus (VN) connection depicting the VIIIth nerve, ganglion of *Scarpa* (G) and site of the postganglionic nerve

section (lesion). **c–e** Schematics illustrating the three experimental paradigms used to evaluate the impact of the unilateral lesion: vestibulo-ocular reflex in darkness (VOR in darkness; **c**), in light (VOR in light; **d**) and optokinetic reflex (OKR; **e**). **f** Flow chart illustrating the temporal sequence of prelesional control recordings, nerve transection, and postlesional recordings of visuo-vestibular motion-evoked eye movements. AC, PC, HC anterior, posterior vertical, horizontal semicircular canal, HB hindbrain, Lag lagena, OC otic capsule, Sac saccule, Ut utricle. Scale bars in a are 2 mm and 50  $\mu$ m, respectively

velocity of  $\pm 31.4^\circ/s$ . Visual pattern motion was provided in an open-loop virtual reality setting formed by an open cylindrical screen, encompassing  $275^\circ$  with a diameter of 8 cm and a height of 5 cm. Three digital light processing (DLP) video projectors (Aiptek V60), installed in  $90^\circ$  angles to each other were affixed to the table surrounding the screen and projected a visual pattern at a refresh rate of 60 Hz onto the screen [14]. The pattern consisted

of equally spaced, vertical, black and white stripes with a spatial size of  $16^\circ/16^\circ$ . The pattern motion consisted of horizontal sinusoidal oscillations at 0.2 Hz and positional excursions of  $\pm 10^\circ$  ( $\pm 12.6^\circ/s$  peak velocity). For all experiments, the Sylgard-lined recording chamber with the affixed preparation was placed in the center of the cylindrical screen that co-aligned with the vertical rotation axis of the motion stimulator. Visual and vestibular motion stimuli

were applied either separately or in combination to evoke a VOR in darkness, VOR in light (in the presence of world-stationary vertical black and white stripes) or an OKR (Fig. 1c–e). The temporal sequence of prelesional control recordings, nerve transection, and postlesional recordings of visuo-vestibular motion-evoked eye movements is illustrated in the flow chart of Fig. 1f.

Eye movements were recorded non-invasively with an infrared video camera (Grasshopper mono, Point Grey Research Inc., Canada) and a zoom objective (Optem Zoom 70XL, Qioptiq Photonics GmbH & Co. KG, Germany) with an adequate lens ( $M25 \times 0.75 + 0.25$ ) as previously described [16]. This system was mounted on top of the experimental setup to visualize the motion of both eyes from above during visual and vestibular motion stimulation at a video capture frame rate of 30 Hz with FlyCap2 software (v2.3.2.14.). Eye motion profiles and parameters were extracted from the captured video sequences using a custom video-processing algorithm written in C++ (for details see [17]). To calculate the motion of the eyes, an ellipse was drawn around each eyeball and the angle between the major axis of the ellipse and the longitudinal axis of the head was calculated in each frame of a given video sequence. Based on the frame rate (30 Hz), the change in eye position over time was then computed.

### Unilateral surgical transection of the VIIIth nerve

The plain visibility of the central nervous system (CNS) and cranial nerve roots facilitated a targeted transection of the right VIIIth nerve by cutting the nerve between its entrance into the hindbrain and the inner wall of the otic capsule with a microscissor under direct visual control. All procedures were completed under a binocular microscope, which allowed precise and complete transection of the entire nerve bundle with a single cut. Great care was taken to not damage the hindbrain, the otic capsule or other cranial nerves traversing ventrally in proximity to the VIIIth nerve. Based on the site of the transection, between the medial wall of the otic capsule (Fig. 1b) and the entry into the hindbrain, the lesion was postganglionic and accordingly disconnected the ganglion of *Scarpa* from the brain [18].

### Data analysis

Eye and stimulus positions were recorded in Spike2 (Cambridge Electronic Design, UK) for off-line analysis. For all subsequent analysis, eye and stimulus position data was re-sampled to 100 Hz using linear interpolation, and eye position traces were smoothed with a 0.05 s time constant with built-in Spike2 functions. Eye positions over a single head/table or visual image motion cycle were obtained from the recorded data using a custom Spike2 script for single-cycle

extraction and consolidated with a custom script written in Python 3. Average responses were calculated from 20–30 cycles. Respective magnitudes were computed from peak-to-peak amplitudes of “successful” VOR cycles (see “Results”). The phase relation of motion-induced eye movements with respect to the table position was obtained by comparing the timing of the average response peak with the timing of the maximal stimulus position or visual motion pattern deflection. To assess if the motion of both eyes was conjugated, bilateral eye positions were exported from Spike2 and plotted against each other. While exporting, a lower sampling rate of 10 Hz was used to avoid oversaturation of the plots. If data points did not have a corresponding value at each sampling interval, the nearest temporal point was used instead. To assess static eye position, average resting eye positions over 10 s were extracted from Spike2 prior to starting the first recording session in darkness. The data were further processed and analyzed statistically using Prism (GraphPad Software, Inc, USA). Responses were normalized and averaged ( $\pm$  SD; standard deviation) for comparison. Statistical differences were calculated with the Friedman test and Dunn’s multiple comparisons test (non-parametric, paired data; Prism, GraphPad Software, Inc, USA). Statistical analysis with the Friedman test will be reported only in the text while Dunn’s test will be reported also in the figures and/or legends.

### Dextran amine dye tracings

Fluorescent visualization of the VIIIth nerve was used to provide a pre-experimental visual reference of the distal entrance site of the nerve, ganglion cell bodies, and peripheral neurites within the otic capsule for subsequent experimental procedures requiring transection of unlabeled nerves. Tetramethylrhodamine (543 nm; 3000 MW; Invitrogen, D3308) crystals were dissolved until a viscous solution was produced. Pins affixed to glass micropipettes were placed in this viscous tracer solution, coated with a high concentration of tracer and inserted unilaterally into the vestibular nuclei of the hindbrain in an in vitro preparation. Tracer spread to neighboring structures was carefully avoided. The preparation was then transferred into 200 ml freshly-oxygenated Ringer solution and incubated at 17 °C for 24 h ( $n = 1$ ). Thereafter, the preparation was fixed in 4% paraformaldehyde (PFA) for 24 h and cleared using the uDISCO method [19]. In brief, the preparation was serially incubated in 30, 50, 70, 80, 90 and 96 vol% tert-butanol (2 h each; Sigma, 360538), and then cleared in a mixture of benzyl alcohol (Sigma, 24122-M), benzyl benzoate (Sigma, W213802) and diphenyl ether (Alpha Aesar, A15791) corresponding to BABB-D15 according to Pan et al. [19]. Subsequently, the tissue was mounted and coverslipped in BABB-D15

using a custom metal spacer before imaging on an Olympus Fluoview confocal microscope (FV 10-ASW 2.1 software).

## Results

The acute effects of unilateral vestibular nerve sections on static eye position and visuo-vestibular motion-induced eye movements were evaluated immediately and up to 5 h postlesion. The analysis of ocular motor performance in prelesional conditions for each experimental animal allowed reliable quantification of the behavioral impairment prior to and over the first few hours after the unilateral loss of peripheral vestibular function. Prelesional performance was first assessed to determine the range of unmanipulated responses and was subsequently followed by identical assessment after the VIIIth nerve lesion.

### Prelesional eye position and motion dynamics during visuo-vestibular stimulation

#### Resting eye position and stimulus-evoked eye movements

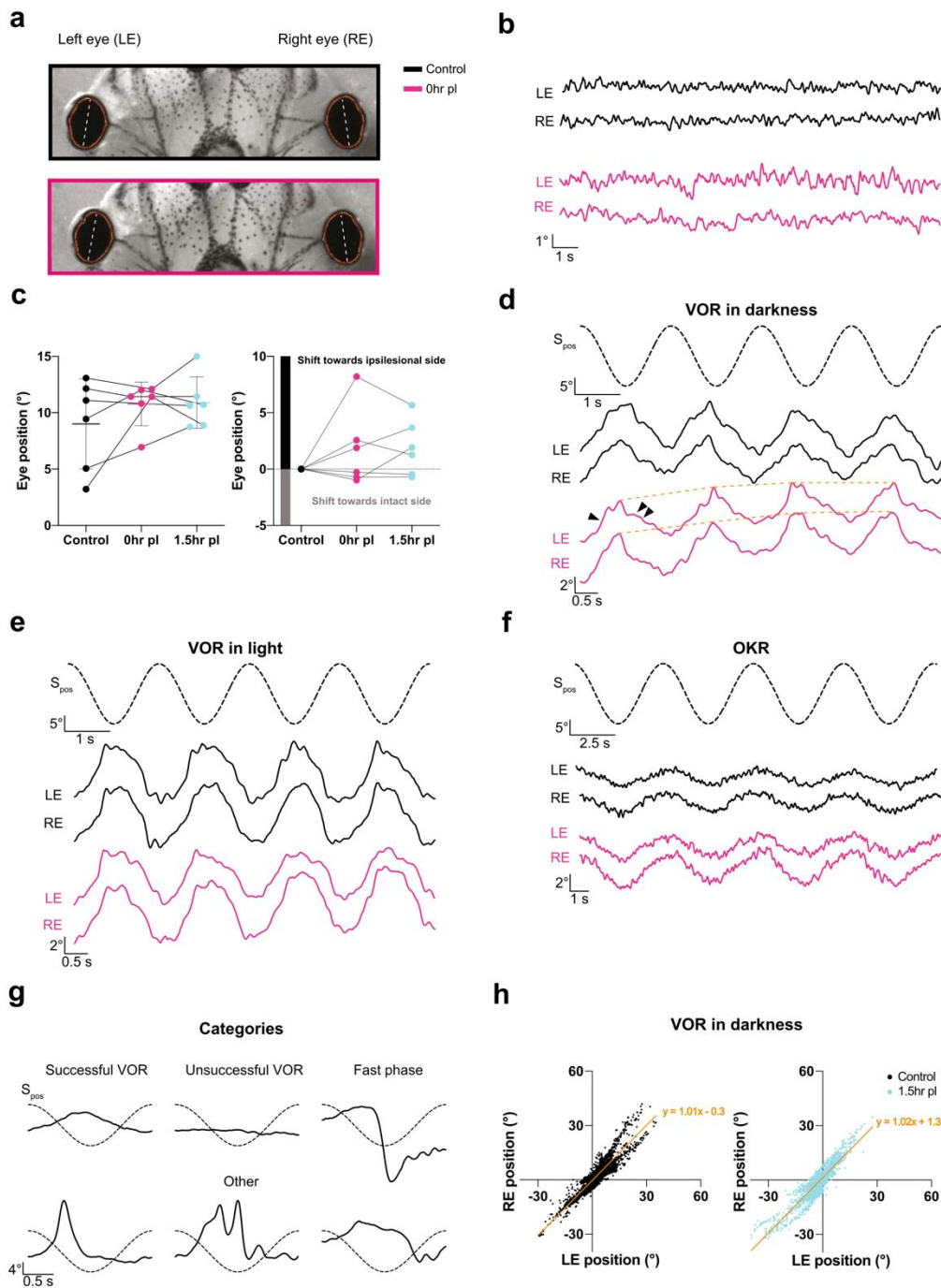
The eyes of *Xenopus laevis* tadpoles at mid-larval stages have a lateral position with a slightly nasal orientation of 5–10° relative to the longitudinal head/body axis (Figs. 1a, 2a) with an ocular motor range of ~20°, estimated by systematic analysis of the OKR performance [14]. In darkness, in the absence of visuo-vestibular motion stimulation, the position of both eyes remained relatively stable except for very small (~1°), horizontal oscillations (Fig. 2b) despite variability in absolute resting position between animals (Fig. 2c; black). The variability of the resting eye position between preparations likely derives from the combinatorial influence of potentially inconsistent horizontal placements of the latter within the recording chamber, variations in the electronic detection of the oval-shaped eyes by the tracking software and development-related differences of the eye position between animals at stage 53–55. Despite this variability, a consistent and most notable aspect was the absence of scanning saccadic eye movements, with the exception of infrequent locomotion-related fast horizontal eye deflections [20]. During prelesional control conditions, horizontal sinusoidal rotation in darkness (0.5 Hz; ±31.4°/s peak velocity;  $n=6$ ) evoked movements of both eyes that were directed in phase-opposition to the stimulus, indicative of a functional angular VOR (black traces in Fig. 2d). Eye movements during most cycles of the motion stimulus had waveforms and dynamics that matched well with the expectations of a “successful” VOR in *Xenopus* tadpoles (Fig. 2d,g) [13]. Other cyclic response types, although fewer, appeared to be “unsuccessful” attempts, as characterized mostly by negligible responses, “fast phases” of variable

kinetics and magnitudes [14] or were designated as “other” because of uncertain classification that did not allow reliable assignment to a particular category (Fig. 2g; Supplementary Fig. 2a). The common denominator of the latter class was an eye motion peak velocity that exceeded, in part considerably, stimulus peak velocity and thus did not meet the criteria of a VOR slow phase, which by definition can maximally adopt stimulus motion magnitudes [21].

A principally analogous pattern with similar dynamics of eye movements was evoked during horizontal sinusoidal motion stimulation in the presence of a black and white vertically striped, world-stationary visual pattern (VOR in light; black traces in Fig. 2e). The majority of eye movements were again designated as “successful” VOR, with responses that were generally more robust than the VOR in darkness (Figs. 2g, 3d). Likely due to the concurrent effect of the world-stationary visual pattern, “unsuccessful” attempts to stabilize gaze were almost completely absent (Supplementary Fig. 2b). In contrast, eye movements classified as “fast-phases” or “other” were found in similar proportions as during application of a sinusoidal motion stimulus in darkness. This indicates that vestibular motion stimulation evokes a qualitatively similar VOR in larval *Xenopus* under both illumination conditions, although, eye movements produced in the presence of a world-stationary black and white striped pattern were more robust. This enhanced robustness most likely derived from the synergistic performance of vestibular and optokinetic reflexes during turntable motion and concurrent relative motion of the visual pattern. To isolate the contribution of visual motion-induced eye movements during activation of the VOR in light, the OKR was separately elicited by visual pattern motion in the absence of turntable rotation. Horizontal sinusoidal motion of black and white vertical stripes (0.2 Hz; ±12.6°/s peak velocity;  $n=6$ ) evoked oscillatory movements of both eyes that aimed at following the stimulus (Fig. 2f), in correspondence with the spatio-temporal dynamics of a functional OKR in *Xenopus* tadpoles (see [13]). The responses were robust with no resetting “fast phases”. As described for the resting eye position in darkness (Fig. 2b), the eyes also remained relatively stationary in light, except for small irregular horizontal oscillations with magnitudes of ~1° (not shown).

#### Eye motion performance

All three different visuo-vestibular motion stimulus paradigms evoked horizontal movements of both eyes that were directionally coordinated (Fig. 2d–f). The extent of coordinated conjugation for the left and right eye was quantitatively evaluated by calculating the bilateral response coordination from 27–30 cycles of the VOR (in darkness), omitting twitch-like eye movements. Plotting eye position magnitudes of the left eye ( $x$ -axis) versus the right eye ( $y$ -axis)



confirmed that the positions of the two eyes during motion stimulation were strongly correlated with each other (VOR in darkness:  $\lambda = 1.015$ ;  $r^2 = 0.8567$ ;  $n = 6$ ), yielding a slope close to 1 (Fig. 2h, left panel). This close correspondence

indicated a strict conjugation of both eyes during stimulus-triggered motion, despite the lack of a fovea in these animals and the rather lateral position of the eyes. After averaging across multiple cycles (Fig. 3c–e), gain values *re* stimulus

**Fig. 2** Spontaneous and visuo-vestibular motion-evoked eye movements. **a, b** Infrared images (**a**) and static eye position of the left (LE) and right (RE) eye (**b**) before (upper image in **a**, black trace in **b**) and immediately after (0 h) transection of the right VIIIth nerve (lower image in **a**; magenta trace in **b**); dashed white lines in **a** indicate the major axis of the oval-shaped eyes, used to measure eye position and evoked motion. **c** Dot and whisker plot of the absolute eye position relative to the longitudinal body axis (left) and following subtraction of the prelesional eye position (right) in controls, immediately (0 h, magenta) and 1.5 h after transection of the right VIIIth nerve (cyan) in darkness. **d–f** Examples of movements of the left and right eye during four consecutive cycles of horizontal sinusoidal rotation of the head/table (0.5 Hz;  $\pm 31.4^\circ/\text{s}$ ) in darkness (VOR in darkness; **d**), in light (VOR in light; **e**), and of horizontal sinusoidal motion (0.2 Hz;  $\pm 12.6^\circ/\text{s}$ ) of a vertical black and white striped pattern (OKR; **f**) before (black traces) and immediately after (0 h) transection of the right VIIIth nerve (magenta traces); dashed sinusoids represent stimulus position profiles ( $S_{\text{pos}}$ ); arrowheads indicate eye movements evoked by head/table motion towards the intact (single arrowhead) and ipsilesional (two arrowheads) side; dotted orange line in **d** indicates the gradual shift in eye position towards the ipsilesional side with each rotation cycle. **g** Qualitative categorization of eye movements evoked by vestibular motion stimulation labeled as “successful”, “unsuccessful”, “fast phases” and “other”; dashed sinusoids represent the stimulus position ( $\pm 10^\circ$ ) profiles of the head/table motion cycle at 0.5 Hz. **h** Conjugation correlation plots of the position of the left and right eye during horizontal sinusoidal head/table rotation (VOR in darkness) before (black) and 1.5 h (cyan) after transection of the right VIIIth nerve; note that the position of both eyes is closely correlated indicating strict conjugation during the horizontal angular VOR before and after the lesion

were calculated for “successful” VOR and OKR responses, respectively (Fig. 3f–h). Under control conditions, i.e., prior to the unilateral section of the VIIIth nerve, this analysis yielded a gain value (eye motion/stimulus motion) for the VOR in darkness of  $0.29 \pm 0.1$ , for the VOR in light of  $0.32 \pm 0.08$  and for the OKR during sinusoidal motion stimulation of  $0.14 \pm 0.04$  (all values are mean  $\pm$  SD;  $n = 6$ , respectively). Peak responses *re* stimulus position had phase leads of  $-54^\circ$  ( $-54.3^\circ \pm 12.34^\circ$ ) and  $-29^\circ$  ( $-29.4^\circ \pm 18.2^\circ$ ) for the VOR in darkness and in light, respectively. For the OKR, the peak response was nearly phase-aligned with stimulus position ( $13.4^\circ \pm 10.1^\circ$ ; values are mean  $\pm$  SD;  $n = 6$ , respectively). These values complied with those reported earlier for *Xenopus* tadpoles at this developmental stage [13, 14].

### Postlesional effects following unilateral transection of the VIIIth nerve

#### Transection of the VIIIth nerve

The plain visibility of the hindbrain and cranial nerve roots allowed a rapid, targeted transection of the right VIIIth nerve by a single cut with a microscissor between the nerve entrance and *Scarpa's* ganglion (Fig. 1b). This controlled surgical intervention ensured that no other cranial nerve traversing in close vicinity such as the abducens nerve was

unintentionally harmed. Since the transections were made in vitro in the absence of neuronal activity-suppressing anesthetic agents, the consequences on eye position and evoked eye motion could be evaluated immediately after the lesion.

#### Impact on resting eye position

The impact of the unilateral peripheral vestibular impairment on resting eye position in darkness was evaluated immediately (0 h) and 1.5 h after the nerve section. Most notably, a spontaneous nystagmus, as present for instance in mammalian species [11, 22] including human patients [1], was not observed in any preparation. Instead, both eyes continued to remain relatively stable except for horizontal oscillations with similarly small magnitudes as those observed in controls (compare magenta and black traces in Fig. 2b). Even though the prelesional resting position was variable across animals (black in Fig. 2c), the average resting position of both eyes tended to shift towards the ipsilesional side immediately after the lesion (lower image in Fig. 2a at 0h; magenta in Fig. 2c). This more eccentric position was maintained at similar values at 1.5 h postlesion in 4 out of 6 animals (cyan in Fig. 2c). The postlesional alteration of individual resting eye position at the first two tested time points is more clearly illustrated in Fig. 2c, right plot, following subtraction of the individual control resting position, respectively. This average tentative shift in eye position across preparations complies with the induced asymmetry in bilateral vestibular afferent resting discharge rates following the nerve section, known to consequently cause a sustained, ipsilesionally directed excitatory drive of extraocular motoneurons [23].

#### Impact on VOR performance

VOR responses were elicited by sinusoidal head motion in darkness and in light as under control conditions. Responses were found again to be heterogenous (magenta traces in Fig. 2d,e; Supplementary Fig. 2a, b) across stimulus cycles and repetitions but in general continued to adhere to the four categories established for the control condition (see Fig. 2g). Immediately after the VIIIth nerve section, “successful” VOR responses during sinusoidal motion in darkness decreased in occurrence (magenta in Fig. 3a) but significantly more so after 1.5 h (cyan in Fig. 3a;  $p = 0.1416$  Friedman test; control versus 0 h  $p = 0.5637$ ; control versus 1.5 h  $p = 0.0433$  Dunn's multiple comparisons test). In contrast, the number of “successful” VOR responses during sinusoidal motion in light remained largely unchanged compared to control responses (magenta and cyan in Fig. 3b;  $p = 0.7402$  Friedman test; control versus 0 h  $p > 0.9999$ ; control versus 1.5 h  $p = 0.3865$  Dunn's multiple comparisons test),

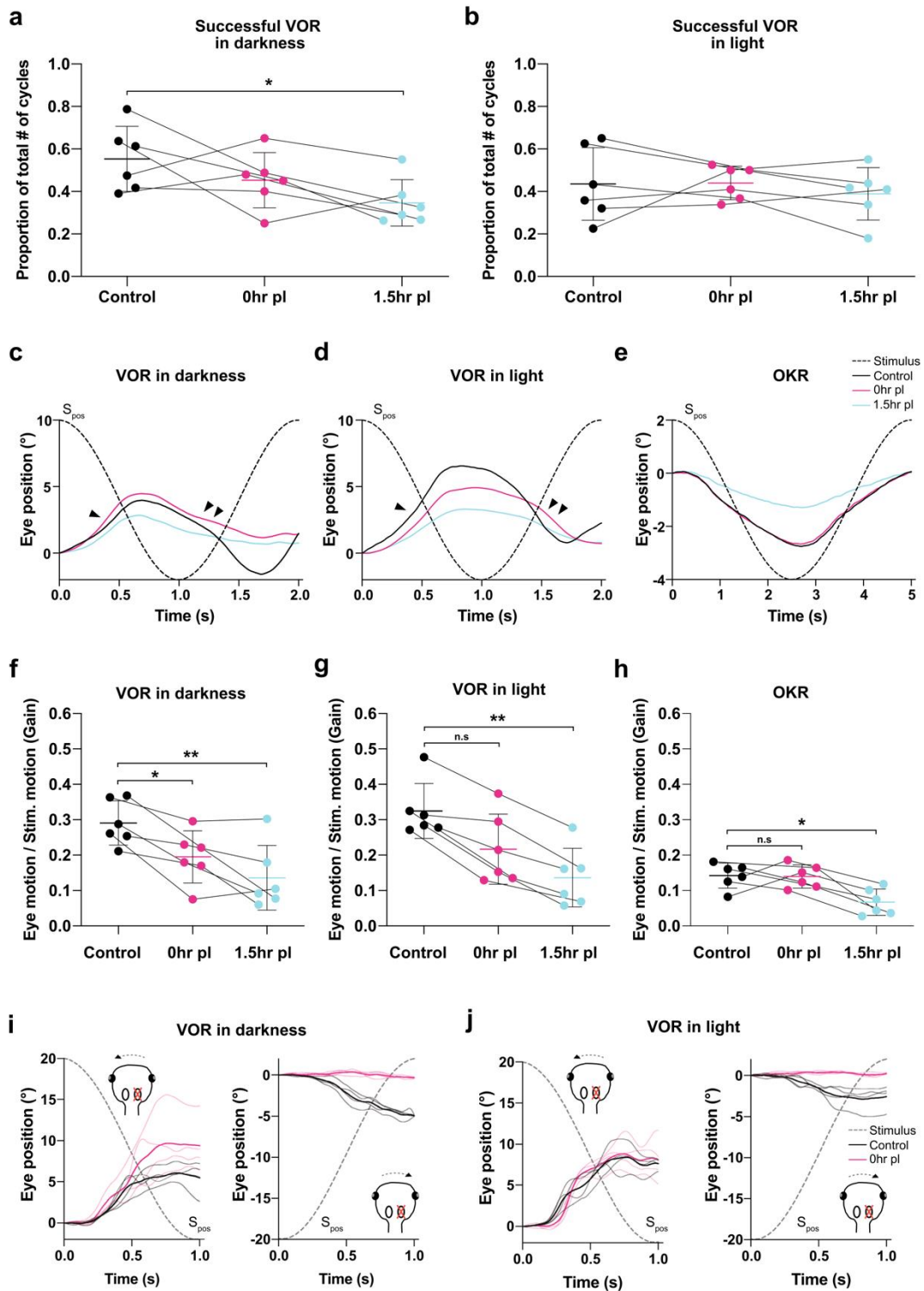


**Fig. 3** Immediate effects of a unilateral VIIIth nerve section on eye movement dynamics. **a, b** Relative proportion of “successful” VOR responses before (black), immediately (0 h, magenta) and 1.5 h postlesion (cyan) during sinusoidal rotation in darkness (**a**) and in light (**b**). **c–e** Averages of “successful” VOR responses in darkness (**c**), in light (**d**) and OKR responses (**e**) over a single sinusoidal stimulus motion cycle; averages are the mean of the responses from all preparations ( $n=6$ ), respectively; dashed sinusoids represent the stimulus position profile ( $S_{\text{pos}}$ ); arrowheads indicate eye movements evoked by head/table motion towards the intact (single arrowhead) and ipsilesional (two arrowheads) side, respectively. **f–h** Response gains (eye motion / stimulus motion) before, at 0 h and 1.5 h after the lesion for the VOR in darkness (**f**), in light (**g**) and the OKR (**h**). **i–j** Representative example traces of sinusoidal VOR eye movements over the first half cycle during head/table motion in darkness (**i**) and in light (**j**) directed towards the intact (left) and ipsilesional side (right) before (black traces) and immediately after the VIIIth nerve section (0 h, magenta traces); thin and thick lines represent individual and average responses, respectively. \* $p < 0.05$ ; \*\* $p < 0.01$ ; Dunn’s multiple comparisons test with respect to control values

suggesting that the additional presence of a world-stationary black and white striped visual pattern that activates concurrent visuo-motor responses during vestibular motion stimulation in light might offset the unilateral lack of head rotational sensory signals.

In a complementary manner, the category of “unsuccessful” VOR response attempts, which was rather low in occurrence during prelesional control conditions, increased following VIIIth nerve transection (Supplementary Fig. 2a, b). While this was particularly pronounced for the VOR in darkness ( $p=0.0009$  Friedman test), the occurrence of this category was not significantly increased for VOR in light ( $p=0.4244$  Friedman test). This is likely due to the fact that this category is virtually absent in all preparations under prelesional control conditions (Supplementary Fig. 2b) and only mildly increased in reciprocal correspondence to the tendency of reduced “successful” VOR response attempts after the lesion.

At variance with the complementary postlesional alterations of the “successful” and “unsuccessful” VOR response categories, the average occurrence of “fast phases” and “other” was largely unaffected by the VIIIth nerve section during both table motion in darkness and in light (Supplementary Fig. 2a,b; Friedman test in darkness  $p=0.6922$  and in light  $p=0.2537$  for “fast phases”;  $p=0.8781$  in darkness and  $p=0.4247$  in light for “other”). The lack of an increase in the number of fast phases during motion stimulation also complies with the absence of a VIIIth nerve lesion-induced nystagmus during static head position both in light and in darkness (see above). The unchanged frequency of occurrence of eye movements during motion stimulation designated as “other” before and after the nerve section (Supplementary Fig. 2a,b) suggests that this category of jerky ocular motor behavior is independent of vestibular signals

and potentially driven by spontaneous episodes of activity in brainstem or spinal locomotor circuits [20].

### Impact on VOR response gain and phase

An VIIIth nerve section appeared to cause the evoked cyclic eye movements during sinusoidal rotation in darkness to decrease in magnitude (magenta traces in Fig. 2d) immediately after the unilateral loss of vestibular signals (0 h). The reduced responses of the VOR, although rather variable between preparations, yielded an average gain of  $0.20 \pm 0.10$  (mean  $\pm$  SD;  $n=6$ ) as indicated by the mean responses over a single motion cycle (Fig. 3c, f). The bidirectional eye motion components of the VOR during horizontal sinusoidal motion stimulation, however, were differentially affected. Instead of symmetric responses in both head motion directions (Fig. 2d black traces), eye movements evoked by rotation towards the side of the lesion became considerably slower and smaller in magnitude (magenta traces; two arrowheads in Fig. 2d). In contrast, eye movements evoked by rotation towards the intact side appeared to be unchanged compared to controls in terms of dynamics and amplitude (magenta traces; arrowhead in Fig. 2d). This asymmetric performance caused the position of both eyes to gradually but constantly shift with each successive motion cycle towards the side of lesion (orange dotted line, connecting peak responses in Fig. 2d). The directionally different dynamics of eye movement components during repetitive motion cycles was confirmed by evaluating the responses during the first half cycle in either direction starting from the resting table position (Fig. 3i, j). A typical example of directionally different eye movements immediately after the lesion (0 h) is illustrated in Fig. 3i, j. Peak-to-peak amplitudes and velocities of the eye movements in response to ipsilesionally directed head/table motion in darkness (Fig. 3i) dropped immediately after the nerve section (Fig. 3i, right) to rather negligible values, while eye movements evoked by head/table motion towards the intact (contralesional) side remained unaltered or even increased slightly in amplitude and dynamics compared to those recorded in controls (Fig. 3i, left).

Despite concurrent visuo-vestibular stimulation during the VOR in light, i.e. in the presence of a world-stationary vertical striped pattern, a considerable reduction of the response amplitude was observed, with a drop in gain from  $0.32 \pm 0.08$  (mean  $\pm$  SD;  $n=6$ ) in controls to a value of  $0.22 \pm 0.10$  (mean  $\pm$  SD;  $n=6$ ; Figs. 2e, 3d, g) immediately after the VIIIth nerve section (0 h). Even though vestibular-evoked eye movements in light appeared to be less asymmetric than in darkness, the reduction in response amplitude was similar for the VOR in darkness and in light. Thus, concurrently evoked visuo-motor responses during the VOR in light were unable to attenuate a full gain reduction immediately after the VIIIth nerve section; however, visual motion

signals appeared to have allowed to at least partially offset the impaired eye motion dynamics during rotation in the ipsilesional direction. Nonetheless, eye movements evoked by head/table motion towards the ipsi- and contralesional (intact) side in light were as asymmetric in amplitude and dynamics (Fig. 3j) as those evoked during rotation in darkness (compare with left and right in Fig. 3i).

During the postlesional period, the VOR in darkness and in light continued to deteriorate further after the instantaneous recordings following the nerve section (0 h) to reach even lower values at 1.5 h postlesion. The gain of both VOR in darkness and in light dropped to  $0.14 \pm 0.10$  (mean  $\pm$  SD;  $n=6$ ; Fig. 3f, g), respectively. This further impairment derived largely from the eye motion component that was elicited during the stimulus half-cycle directed towards the ipsilesional side and was independent if a world-stationary visual pattern was present or not (compare plots in Fig. 3c, d). Most noticeably, however, the eye motion component during rotation towards the intact side also became considerably smaller at 1.5 h postlesion (cyan traces in Fig. 3c, d), suggesting a secondary effect as the origin for this severe impairment of the VOR gain. Despite the overall gain impairment, the response phase *re* stimulus position after the lesion remained largely unaltered at both time points for the VOR in darkness. In contrast, the smaller phase leads *re* stimulus position for the VOR in light after the transection of the VIII<sup>th</sup> nerve remained and likely derived from a reweighted contribution of visual response components during rotation towards the ipsilesional side that were generally more in phase with the optokinetic stimulus (compare Fig. 3d, e; magenta and cyan traces). In addition, despite the loss of unilateral vestibular signals, the movements of both eyes were still highly conjugated (right plot in Fig. 2h;  $\lambda=1.019$ ;  $r^2=0.8419$ ; linear regression;  $n=6$ ), lending support to the decisive role of abducens internuclear neurons as substrate for this ocular motor behavior [19].

### Impact on OKR performance

Immediately after the section of the VIII<sup>th</sup> nerve (0 h), horizontal sinusoidal rotation of a black and white vertical striped visual pattern provoked typical phase-coupled oscillatory eye movements with similar dynamics, bilateral symmetry, phase relation and amplitude as those recorded before the lesion. This is illustrated by the eye movements over four cycles (Fig. 2f) as well as by the averaged responses over a single motion cycle (Fig. 3e). Statistical comparison confirmed the impression that the response gains immediately after the lesion (0 h) remained unaltered or even increased, although only slightly with respect to control values, to a mean gain of  $0.14 \pm 0.03$  with a phase lag *re* stimulus of  $\sim 11^\circ$  ( $10.6^\circ \pm 13.3^\circ$ ; mean  $\pm$  SD;  $n=6$ ; Fig. 3h). In contrast and most surprisingly, the OKR gain severely

deteriorated at 1.5 h postlesion to a magnitude of  $0.07 \pm 0.04$  (mean  $\pm$  SD;  $n=6$ ; Fig. 3h; Supplementary Fig. 2e), corresponding to a loss of 50% of the initial prelesional value. The severe reduction of the OKR gain at 1.5 h postlesion was unsuspected and comparable in magnitude to the overall gain reduction of the VOR in darkness and in light at the same postlesional time point. The delayed reduction in the amplitude of visuo-motor responses that were not immediately impaired by the unilateral lesion of the VIII<sup>th</sup> nerve, but rather occurred only at a time point 1.5 h past the initial lesion, further corroborates the likely presence of extended secondary lesion-related effects. Plastic alterations in central areas which are potentially concerned with shared VOR-OKR circuit components, such as extraocular motoneurons or cerebellar elements, could be the *loci* of such a secondary effect.

### Amelioration or maintenance of VIII<sup>th</sup> nerve lesion-induced deficits

Given the striking decrease in response performance 1.5 h postlesion, and to better evaluate the temporal progression of the ocular motor deficits, the performance of visuo-vestibular reflexes was further characterized at 3 and 4.5 h postlesion. These time points are often still inaccessible for a systematic evaluation of the VOR and OKR because of the slowly fading anesthesia and/or the presence of a roaring nystagmus in many animal species. At both time points (3 and 4.5 h postlesion) the number of “successful” attempts of the VOR in light and in darkness remained considerably lower than in controls (Supplementary Fig. 2a, b; Friedman test  $p=0.2942$  VOR in darkness,  $p=0.6492$  VOR in light), despite a slight, yet non-significant augmentation of “successful” episodes of the VOR in darkness at 4.5 h postlesion. In a complementary fashion, “unsuccessful” cycles of both visuo-vestibulo-motor responses after the VIII<sup>th</sup> nerve section remained at an elevated frequency compared to controls (Supplementary Fig. 2a, b; Friedman test  $p=0.0009$  VOR in darkness,  $p=0.4244$  VOR in light), while the number of “fast phases” or eye movements designated “other” remained unaltered at all time points before and after the lesion (Supplementary Fig. 2a, b; Friedman test in darkness  $p=0.6922$  and in light  $p=0.2537$  for “fast phases”;  $p=0.8781$  in darkness and  $p=0.4247$  in light for “other”). This suggests again that the latter two categories of ocular motor behaviors are independent of vestibular activity.

In a corresponding manner, the respective gains of the VOR in darkness and in light as well as the OKR continued to remain severely depressed at 3 and 4.5 h postlesion (Supplementary Fig. 2c–e; Friedman test  $p=0.0054$  for VOR in darkness,  $p=0.0041$  for VOR in light;  $p=0.0138$  for OKR) with a tendency for a slight, yet non-significant amelioration at the latter time point. The phase of the responses

remained largely unaltered (not shown) with the exception of those responses that included a visuo-motor component, that by definition was more in phase with stimulus position as already indicated by the control responses of the OKR (see above). The apparent slight amelioration of visuo-vestibular eye movements beginning at 4.5 h postlesion, however, resulted from a differential recovery of the ocular motor components during head/table motion in ipsi- and contralesional direction as indicated by the averages over a single motion cycle (see color-coded traces in Supplementary Fig. 1p–r). Accordingly, eye movements evoked by head/table motion towards the intact side, both in light and in darkness generated amplitudes and dynamics at 4.5 h postlesion that approached, though slowly, again those of prelesional controls (Supplementary Fig. 1p, q). In contrast, eye movements evoked by head/table rotation towards the ipsilesional side in light and in darkness continued to remain absent or had only very small amplitudes with very low dynamics (Supplementary Fig. 1p, q). These residual eye movements likely derived from a disfacilitation of the vestibular activity on the intact side during a head/table motion towards the ipsilesional side. The general amelioration after 4.5 h postlesion for vestibulo- and visuo-motor responses suggests that the improvement of eye motion magnitudes at this time point results from a gradually reestablished efficacy of cellular and circuit elements of the shared visuo-vestibulo-motor pathway.

## Discussion

Unilateral transection of the VIIIth nerve immediately provoked a severe impairment of the VOR in darkness with a smaller effect in light, which further deteriorated 1.5 h later to remain more or less unchanged for the next 3 h. In contrast, the OKR remained functionally intact and unaltered immediately after the vestibular loss (0 h) but experienced a considerable reduction starting at 1.5 h postlesion. The time course and occurrence of detrimental events at later time points suggest that the immediate impact by the loss of vestibular sensory signals is followed by secondary neuronal consequences involving shared VOR-OKR cellular and/or circuit components.

### Targeted transection of the VIIIth nerve and immediate impact on static eye position

The advantage of employing isolated head preparations of *Xenopus* tadpoles is the possibility to transect the VIIIth nerve under direct visual control, which thus ensures that other cranial nerves, the brainstem, or cerebellar structures remain entirely unaffected. Furthermore, bleeding or undesired tissue damage is completely avoided as it is

potentially observed during comparable surgical interventions when performing a postganglionic neurectomy e.g. in mice [11]. Following control recordings, the section of the VIIIth nerve was complete and the preparation ready again for postlesional eye motion recordings within a few minutes, outcompeting other experimental models in terms of acute recordings. Moreover, the absence of any anesthetics during the surgical process in the isolated, yet functional, preparation circumvented all critical issues associated with anesthesia in an intact animal [11]. Most importantly, however, the employment of such an isolated preparation allowed an immediate evaluation of the impact of the unilateral vestibular loss on the behavioral consequences once the VIIIth nerve has been sectioned. This is not possible in any in vivo experiment to our knowledge, given the necessity to use anesthetics for the surgery and the difficulty to determine a clear time point when the effects of the anesthesia on neuronal activity have completely faded.

Immediately after the VIIIth nerve section in the current experiments, on average both eyes shift their resting position towards the side of the lesion, consistent with the imbalance in resting activity between the bilateral vestibular nuclei and the consequently asymmetric activation of extraocular motoneuronal pools [24, 25]. The lack of an acute spontaneous nystagmus after the unilateral vestibular lesion (see Fig. 2b) is likely an amphibian-specific particularity, related to the rather low resting activity in vestibular circuits in these animals [13, 26] and the corresponding small asymmetry of bilateral vestibular resting rates. The relatively variable shift in resting eye position between different preparations might be related to the specific magnitude of the bilateral vestibular firing rate asymmetry after the lesion and/or reflect a dependency of the postlesional shift on the prelesional eye position as suggested from the data plotted in Fig. 2c. In correspondence, the presence of a spontaneous nystagmus in mammalian species [27–29] is likely related to larger bilateral vestibular firing rate asymmetries after a unilateral loss due to generally higher vestibular discharge rates in these animals.

### Acute impact of VIIIth nerve transection on visuo-vestibular motion-evoked eye movements

Immediately after the VIIIth nerve section (0 h), the gain of the horizontal angular VOR in darkness decreased by ~30% (Fig. 3f, g). This instantaneous deterioration directly derives from the disconnection of the respective semicircular canal signals on the ipsilesional side, which as expected, substantially contribute to the excitatory drive for extraocular motoneurons. A gain reduction of the VOR in light is also noticeable even though vestibular and visual motion signals are concurrently activated during horizontal head rotation in the presence of a world-stationary vertical black and white

striped pattern. This suggests that simultaneously activated visuo-motor reflexes are unable to acutely substitute the unilaterally disconnected vestibular signals. This also complies with the finding that the gain of the OKR remained largely unaltered immediately after the VIIIth nerve section (0 h; Figs. 2f, 3h). Following the initial reduction of VOR amplitudes, response gains showed no recovery but instead deteriorated further over the first few hours after the nerve section to remain low, in compliance with the many reports indicating severely impaired eye movements for many days after the lesion [11, 22, 25, 28].

Unexpectedly, however, the performance of the OKR at 1.5 h postlesion was also severely impaired (Fig. 3e, h) with a gain reduction by ~50% comparable to the impairment of the VOR at this time point. This delayed deterioration of the OKR is surprising because the underlying short-latency direct pathway, known to mediate this reflex in amphibians [30], was per se not affected by the vestibular lesion. The severe reduction in OKR performance along with the equally drastic impairment of the VOR at 1.5 h postlesion could, however, result from an initiation of a secondary effect by the ongoing bilateral asymmetric neuronal activity in vestibulo-motor circuits. The resulting persistence of higher firing rates in vestibular circuits on the intact side after the lesion, reinforced by commissural inhibitory connections [31], may have induced a homeostatic plasticity [32] that caused a reduction of the respective synaptic gains within the shared OKR-VOR circuit elements. Such an adaptive process has, in fact, been described for extraocular motor discharge of *Xenopus* tadpoles after continuous (> 20 min) excessive sinusoidal vestibular motion stimulation [33]. This plasticity depended on an intact cerebellum and caused an attenuation of the extraocular motor output. Because cerebellar circuits integrate vestibular inputs and residual retinal image slip signals to adequately adjust eye motion magnitudes [34], the vestibular imbalance after a unilateral VIIIth nerve lesion might have also prompted the circuitry to down-regulate the gains of the ocular motor output during both OKR and VOR.

While homeostatic plasticity processes are known to occur during long-term recalibration of vestibular deficits [25, 35], such plasticity processes could also be triggered during the initial phase after a unilateral vestibular lesion. This assumption allows the generation of testable hypotheses, which probe the possibility that the impairment of vestibulo-motor reflexes is a combinatorial effect of the unilateral loss of vestibular signals followed by an attenuation of central vestibulo-motor signal processing as part of an adaptive plasticity response, prior to and even unrelated to the process of “vestibular compensation”. Comparison of the outcome of studies when the animals remain in darkness between the recordings (current study), or in light with a stationary striped pattern providing a continuous visual reference allows testing the hypothesis that the delayed deterioration

of visuo-motor reflexes is a result of an ongoing homeostatic plasticity after a VIIIth nerve section. Moreover, gaze stabilization by visuo-vestibular sensory signals is supplemented in most vertebrates by neck/body/limb proprioceptive signals [34] and even supplanted by spinal locomotor efference copies in amphibians [20]. While it is known that the contribution of such signals to gaze stabilization collectively increases at the extended, chronic, time period after a VIIIth nerve lesion [36], it would be highly interesting to test the efficacy of the respective ocular motor responses immediately after the lesion. Accordingly, recordings of eye movements during fictive locomotion in *Xenopus* tadpoles [20] before and after transection of the VIIIth nerve would reveal if the respective ocular motor performance is also subjected to a delayed gain diminishment as shown for the OKR. Alternatively, locomotor efference copy-evoked eye movements might remain unaltered after the lesion, potentially because of the direct pathway connections between the spinal central pattern generator and extraocular motoneurons, which bypass central vestibular nuclei and the cerebellum [20].

### Clinical implications

The current findings in *Xenopus* tadpoles specifically highlight the fact that the spectrum of observed symptoms after a unilateral peripheral vestibular lesion [28, 29, 37] might not exclusively reflect the bilateral imbalance in resting activity of the vestibular circuitry. Rather, the observed static and dynamic syndromes, also present in human patients, could be a combinatorial effect that results from the sudden unilateral loss of peripheral vestibular bulk discharge and a secondary consequence that causes an extreme form of housekeeping-related plasticity reactions, which normally aim at consolidating the synaptic gain at a preset value [32]. Such a process would assist the initial step of restituting the excessive activity. The asymmetric activity is integrated and interpreted as a single ongoing motion percept. As a resultant consequence, the synaptic efficacy along shared visuo-vestibulo-motor pathways is reduced and eye movement magnitudes are attenuated, despite being behaviorally inappropriate. Even though this hypothesis derived from results in amphibians without a roaring nystagmus after the VIIIth nerve lesion, it is likely that a comparable neuronal plasticity is also induced in mammals, including humans. In fact, the generally higher vestibular resting activity in mammalian species [34] provokes an even larger bilateral asymmetry after a unilateral loss of peripheral sensory inputs. Such a pathophysiological condition is interpreted as constant rotation towards the intact side, hence the nystagmus in mammals, which as a consequence should also trigger a diminishment of the gain because of the continuous excessive motion signaling in the vestibular system (see [33]).

Unilateral VIIIth nerve section in mammals thus creates an even larger necessity to diminish the excessive activity by a homeostatic mechanism. Therefore, differences in the immediate consequences of a VIIIth nerve lesion between amphibians and mammals should be quantitative rather than qualitative. Provided that this assumption is correct, an immediate reduction of the initial asymmetric vestibular activity after a planned surgery in humans through, for example, hyperpolarizing galvanic vestibular stimulation of the intact side [38] or by directionally appropriate constant velocity visual motion stimulation might be beneficial for a faster recovery from the static deficits after a peripheral vestibular lesion. Visual image motion, and in particular in the framework of the OKR, play, in fact, an important role for gaze stabilization and motion perception given the integration with vestibular signals under normal conditions, and even more so under pathophysiological conditions (e.g. [39]). After the acute phase of a unilateral vestibular loss, visual motion has been employed in rehabilitation treatments of vestibular patients [39, 40], and such motion signals are likely also part of a general sensory substitution strategy, potentially leading to a long-term increase in the contribution and magnitude of the OKR to image stabilization [4, 5, 7].

**Acknowledgements** The authors thank Felix Schneider and Dr. Tobias Kohl for their help with the scripts for eye motion analysis. The authors acknowledge financial support from the German Science Foundation (CRC 870; STR 478/3-1; RTG 2175) and the German Federal Ministry of Education and Research under the Grant code 01 EO 0901.

**Funding** Open Access funding provided by Projekt DEAL.

### Compliance with ethical standards

**Conflicts of interest** The authors declare no competing financial interests.

**Ethical standards** Experiments complied with the publication No. 86-23, revised 1985 of the National Institute of Health. Approval for these experiments was granted by the liable governmental institution of Upper Bavaria (ROB-55.2-2532.Vet\_03-17-24).

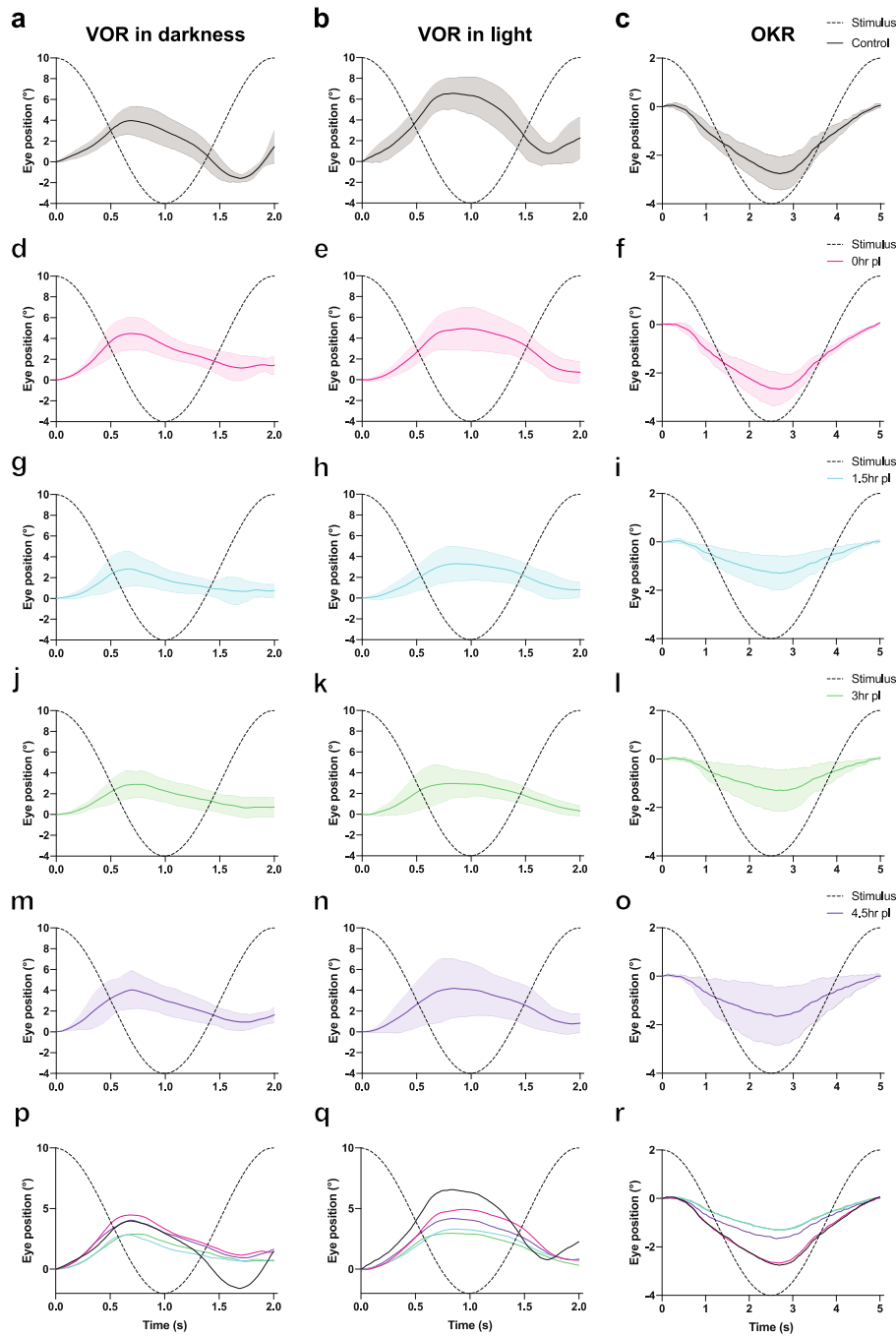
**Open Access** This article is licensed under a Creative Commons Attribution 4.0 International License, which permits use, sharing, adaptation, distribution and reproduction in any medium or format, as long as you give appropriate credit to the original author(s) and the source, provide a link to the Creative Commons licence, and indicate if changes were made. The images or other third party material in this article are included in the article's Creative Commons licence, unless indicated otherwise in a credit line to the material. If material is not included in the article's Creative Commons licence and your intended use is not permitted by statutory regulation or exceeds the permitted use, you will need to obtain permission directly from the copyright holder. To view a copy of this licence, visit <http://creativecommons.org/licenses/by/4.0/>.

### References

1. Strupp M, Brandt T (2013) Peripheral vestibular disorders. *Curr Opin Neurol* 26:81–89
2. Brandt T, Strupp M, Dieterich M (2014) Five keys for diagnosing most vertigo, dizziness, and balance syndromes: an expert opinion. *J Neurol* 261:229–231
3. Curthoys IS (1988) Neuronal activity in the ipsilateral medial vestibular nucleus of the guinea pig following unilateral labyrinthectomy. *Brain Res* 444:308–319
4. Smith PF, Curthoys IS (1989) Mechanisms of recovery following unilateral labyrinthectomy: a review. *Brain Res Rev* 14:155–180
5. Curthoys IS, Halmagyi GM (1995) Vestibular compensation: A review of the oculomotor, neural, and clinical consequences of unilateral vestibular loss. *J Vestib Res* 5:67–107
6. Dieterich M, Brandt T (2015) The bilateral central vestibular system: its pathways, functions, and disorders. *Ann N Y Acad Sci* 1343:10–26
7. Lambert FM, Straka H (2012) The frog vestibular system as a model for lesion-induced plasticity: basic neural principles and implications for posture control. *Front Neurol* 3:42
8. Fàbregas N, Bruder N (2007) Recovery and neurological evaluation. *Best Pract Res Clin Anaesthesiol* 21:431–447
9. Schubert MC, Mantokoudis G, Xie L, Agrawal Y (2014) Acute VOR gain differences for outward vs. inward head impulses. *J Vestib Res* 24:397–402
10. Park BR, Suh JS, Kim MS, Jeong JY, Chun SW, Lee JH (1995) Effect of sensory deprivation or electrical stimulation on acute vestibular symptoms following unilateral labyrinthectomy in rabbit. *Acta Otolaryngol Suppl* 519:162–167
11. Simon F, Pericat D, Djian C, Fricker D, Denoyelle F, Beranek M (2020) Surgical techniques and functional evaluation for vestibular lesions in the mouse: unilateral labyrinthectomy (UL) and unilateral vestibular neurectomy (UVN). *J Neurol*. <https://doi.org/10.1007/s00415-020-09960-8>
12. Straka H, Simmers J (2012) *Xenopus laevis*: an ideal experimental model for studying the developmental dynamics of neural assembly and sensory motor computations. *Dev Neurobiol* 72:649–663
13. Gensberger KD, Kaufmann AK, Dietrich H, Branoner F, Banchi R, Chagnaud BP, Straka H (2016) Galvanic vestibular stimulation: cellular substrates and response patterns of neurons in the vestibulo-ocular network. *J Neurosci* 36:9097–9110
14. Gravot CM, Knorr AG, Glasauer S, Straka H (2017) It's not all black and white: Visual scene parameters influence optokinetic reflex performance in *Xenopus laevis* tadpoles. *J Exp Biol* 220:4213–4224
15. Nieuwkoop PD, Faber J (1994) Normal Table of *Xenopus laevis* (Daudin): A Systematical and Chronological Survey of the Development from the Fertilized Egg Till the End of Metamorphosis. Garland Pub, New York
16. Ramlochansingh C, Branoner F, Chagnaud BP, Straka H (2014) Tricaine methanesulfonate (MS-222) as an effective anesthetic agent for blocking sensory-motor responses in *Xenopus laevis* tadpoles. *PLoS ONE* 9:e101606
17. Knorr AG, Gravot CM, Gordy C, Glasauer S, Straka H (2018) I spy with my little eye: a simple behavioral assay to test color sensitivity on digital displays. *Biol Open* 7:bio035725
18. Kunkel A, Dieringer N (1994) Morphological and electrophysiological consequences of unilateral pre- versus postganglionic vestibular lesions in the frog. *J Comp Physiol A* 174:621–632
19. Pan C, Cai R, Quacquarelli FP, Ghasemigharagoz A, Lourdopoulos A, Matryba P, Plesnila N, Dichgans M, Hellal F, Ertürk A (2016) Shrinkage-mediated imaging of entire organs and organisms using uDISCO. *Nat Methods* 13:859–867

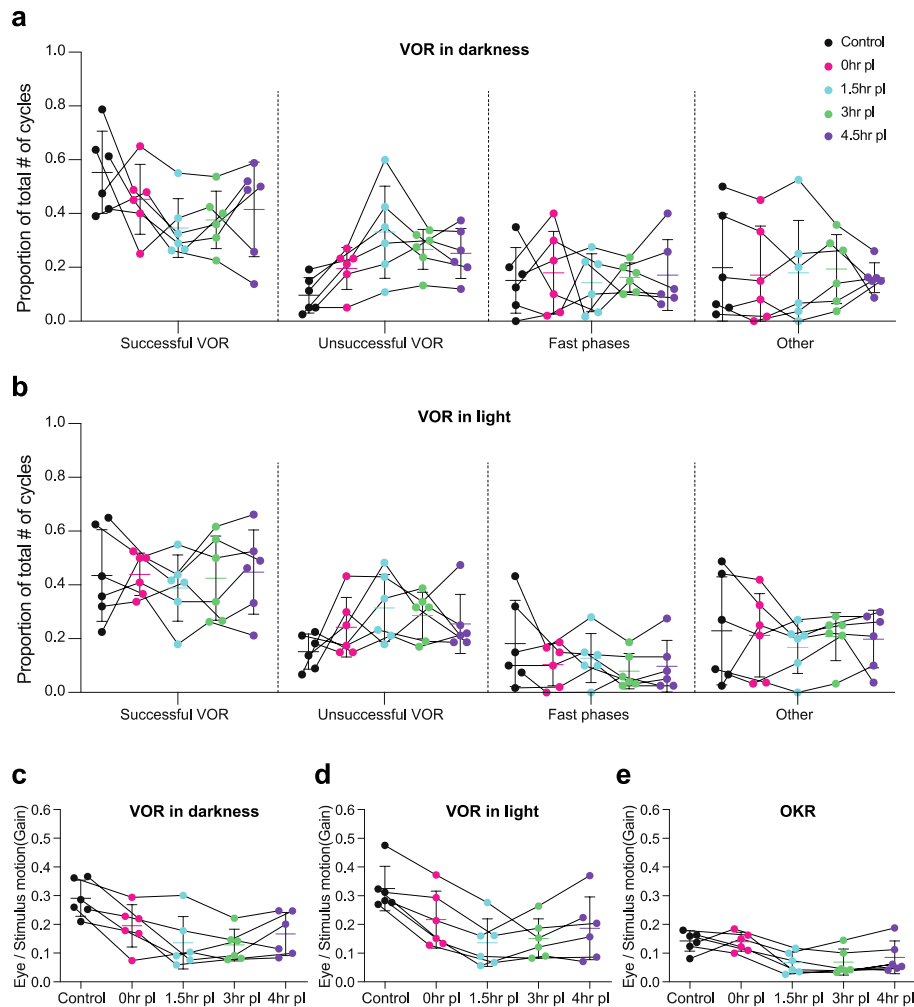
20. Lambert FM, Combes D, Simmers J, Straka H (2012) Gaze stabilization by efference copy signaling without sensory feedback during vertebrate locomotion. *Curr Biol* 22:1649–1658
21. Straka H, Dieringer N (2004) Basic organization principles of the VOR: lessons from frogs. *Prog Neurobiol* 73:259–309
22. Dieringer N (1995) ‘Vestibular compensation’: Neuronal plasticity and its relation to functional recovery after labyrinthine lesions in frogs and other vertebrates. *Progr Neurobiol* 46:97–129
23. Lambert FM, Malinvaud D, Gratacap M, Straka H, Vidal PP (2013) Restricted neural plasticity in vestibulo-spinal pathways after unilateral labyrinthectomy as the origin for scoliotic deformations. *J Neurosci* 33:6845–6856
24. Straka H, Vibert N, Vidal PP, Moore LE, Dutia MB (2005) Intrinsic properties of vertebrate vestibular neurons: function, development and plasticity. *Prog Neurobiol* 76:349–392
25. Beraneck M, Idoux E (2012) Reconsidering the role of neuronal intrinsic properties and neuromodulation in vestibular homeostasis. *Front Neur* 3:25. <https://doi.org/10.3389/fneur.2012.00025>
26. Blanks RHI, Precht W (1976) Functional characterization of primary vestibular afferents in the frog. *Exp Brain Res* 25:369–390
27. Strupp M, Arbusow V (2001) Acute vestibulopathy. *Curr Opin Neurol* 14:11–20
28. Dutia MB (2010) Mechanisms of vestibular compensation: recent advances. *Curr Opin Otolaryngol Head Neck Surg* 18:420–424
29. Fetter M (2016) Acute unilateral loss of vestibular function. *Handb Clin Neurol* 137:219–229
30. Cochran SL, Dieringer N, Precht W (1984) Basic optokinetic-ocular reflex pathways in the frog. *J Neurosci* 4:43–57
31. Malinvaud D, Vassias I, Reichenberger I, Rössert C, Straka H (2010) Functional organization of vestibular commissural connections in frog. *J Neurosci* 30:3310–3325
32. Turrigiano G (2012) Homeostatic synaptic plasticity: local and global mechanisms for stabilizing neuronal function. *Cold Spring Harb Perspect Biol* 4:a005736
33. Dietrich H, Straka H (2016) Prolonged vestibular stimulation induces homeostatic plasticity of the vestibulo-ocular reflex in larval *Xenopus laevis*. *Eur J Neurosci* 44:1787–1796
34. Cullen KE (2016) Physiology of central pathways. *Handb Clin Neurol* 137:17–40
35. Beraneck M, Hachemaoui M, Idoux E, Ris L, Uno A, Godaux E, Vidal PP, Moore LE, Vibert N (2003) Long-term plasticity of ipsilesional medial vestibular nucleus neurons after unilateral labyrinthectomy. *J Neurophysiol* 90:184–203
36. Sadeghi SG, Minor LB, Cullen KE (2010) Neural correlates of motor learning in the vestibulo-ocular reflex: dynamic regulation of multimodal integration in the macaque vestibular system. *J Neurosci* 30:10158–10168
37. Strupp M, Magnusson M (2015) Acute unilateral vestibulopathy. *Neurol Clin* 33:669–685
38. Długaiczek J, Gensberger KD, Straka H (2019) Galvanic vestibular stimulation: from basic concepts to clinical applications. *J Neurophysiol* 121:2237–2255
39. Bronstein AM (2016) Multisensory integration in balance control. *Handb Clin Neurol* 137:57–66
40. Bronstein AM (2004) Vision and vertigo: some visual aspects of vestibular disorders. *J Neurol* 251:381–387

Supplementary figure 1, Soupiadou et al.



**Supplementary Fig.1** Visuo-vestibular motion-evoked eye movements before and after a section of the VIIIth nerve. **a-o** Average responses (color-coded solid lines)  $\pm$  SD (color-coded areas) over a single cycle of sinusoidal head/table motion in darkness (VOR in darkness), in light (VOR in light) and visual pattern motion (OKR) separately before the lesion (**a-c**), immediately after (0 hours; **d-f**), at 1.5 hours (**g-i**), 3 hours (**j-l**) and 4.5 hours postlesion (**m-o**) from all recorded preparations ( $n = 6$ ), respectively; dashed sinusoids represent stimulus position profiles ( $S_{pos}$ ); note that the stimulus frequency and peak velocity for head/table motion is 0.5 Hz and  $31.4^\circ/s$  and for the visual pattern motion 0.2 Hz and  $12.6^\circ/s$ . **p-r** Overlay of average responses over single motion cycles shown in **a-o** from all time points (SDs were omitted).

Supplementary figure 2, Soupiadou et al.



**Supplementary Fig.2** Proportional distribution and performance of motion-evoked eye movements before and after a section of the VIIIth nerve. **a, b** Relative proportions of the categories “successful”, “unsuccessful”, “fast phases” and “other” during head/table motion in darkness (VOR in darkness, **a**) and in light (VOR in light, **b**) before the lesion, immediately after (0 hours) and at 1.5 hours, 3 hours and 4.5 hours postlesion. **c-e** Progression of the response gain (eye motion / stimulus motion) before the lesion, immediately after (0 hours) and at 1.5 hours, 3 hours and 4.5 hours postlesion for the VOR in darkness (**c**), in light (**d**) and OKR (**e**); the time points in all plots are color-coded and specified in the right upper corner of **a**.

---

## CHAPTER IV:

### DISCUSSION & FUTURE DIRECTIONS

---

Dynamic and complex environments necessitate species to undergo adaptive changes, which can manifest in multiple ways and degrees, surpassing functionalities established during development. This dissertation aimed to explore adaptations of the oculomotor system ensuring gaze stabilization during self-motion. For this, I made use of well-defined, reproducible, and easily modifiable eye-stabilizing behaviors as a readout to gain a more profound understanding of plasticity mechanisms that potentially take place in the CNS. The data chapters presented above focused on understanding how motor performances may be altered or improved in phylogenetically related species with different eco-physiological characteristics and under pathological conditions, acutely after a severe loss of vestibular sensory input. More precisely, my experiments tried to investigate how different anatomical and neuronal elements contribute to plasticity, in two amphibian species, namely *Xenopus* and Axolotl larvae, which share various morphophysiological similarities but also clear differences (Chapter II, Schneider-Soupiadis et al., unpublished manuscript). In the following paragraphs, I will summarize the main findings discovered in this thesis. Firstly, after exploring the main characteristics of their gaze stabilizing behaviors, and finding that Axolotls of similar body size, anatomy, and age have worse VOR performances compared to *Xenopus*, I took a closer look at their locomotion patterns which represents the main trigger for the need to stabilize one's gaze. Video recordings of both species made two distinct modes of locomotion apparent. Both species make use of undulatory tail-based swimming, but while *Xenopus* tadpoles are generally in continuous motion, Axolotl larvae move significantly less and, if they commence swimming, then it is characterized by a short active forward propulsion followed by a passive glide (bout). Moreover, a difference in sensor morphology was also taken into consideration as a potential cause of the worse vestibular gaze stabilizing performance in Axolotl. Bright-field and confocal microscopy of fluorescent dye-injected inner ears revealed significant differences in canal diameter, curvature, elongation, and flatness which all have a major impact on the endolymph flow within the canal and therefore the mechano-sensory transduction of motion on vestibular hair cells. These results suggest, taking into consideration data from older staged animals, that the morphology of the horizontal canal is limiting the performance of the vestibulo-ocular reflex (VOR) in Axolotl. Moreover, the lower locomotion performance which comes along with a less profound acceleration of the head might be correlated with the differences observed in canal morphology.

After investigating visuo-vestibular reflexes under normal, healthy conditions I also examined how *Xenopus* tadpoles acutely cope with a sudden loss of unilateral sensory input (Chapter III, Soupiadou et al., 2020). While compensation of such injuries has been explored already extensively in various species, the novelty of my experiments involved *in vitro* whole

head preparations which allow a targeted nerve transection with a direct evaluation of its impact within minutes after the surgery. As expected, immediately after the unilateral transection, the VOR was significantly impaired. However, the further decline in VOR performance with the delayed reduction of the OKR at 1.5 hours after the lesion, which persisted for the following 3 hours was surprising. This led to the conclusion that the sensory loss was intensified by secondary neuronal effects that likely involve homeostatic plasticity triggered by the ongoing asymmetric activity in the shared VOR-OKR pathway. In the following, I will discuss the above-mentioned results in more depth and put them in context to the currently known literature.

## XENOPUS LAEVIS & AXOLOTL LARVAE: IDEAL EXPERIMENTAL MODELS FOR STUDYING PLASTICITY IN SENSORIMOTOR CIRCUITS

To gain a deeper insight into the mechanisms and constraints of functional plasticity in the CNS, reproducible and defined behavioral motor outputs are required to be able to draw robust conclusions. Present in all vertebrates, the reflexive oculomotor systems mediating vestibulo-ocular and optokinetic responses are phylogenetically the oldest type of eye movements (Spencer and Porter, 2006). Moreover, the remarkably preserved sensory endorgans and functional principles of these reflexes, along with the relatively short neural circuits allow us to draw general conclusions which are applicable to wider phylogenetic considerations (Straka et al., 2016). These reflexes have been therefore extensively investigated in various species ranging from fish to mammals to gain a better understanding of the structure and computational characteristics of vestibular and visual motion processing (Goldberg, 2000; Masseck and Hoffmann, 2009). Despite the robust behavioral outcomes of these reflexes in minimizing image slip on the retina, they must also possess the ability to adapt to species-specific features related to locomotion style, eco-physiology, and lifestyles to maintain their functionality (Straka et al., 2016; Goyens, 2019). Moreover, they must be able to adapt during ontogeny as the organisms are growing (Rinaudo et al., 2019), varying their speed of locomotion and being exposed to changing environments. Amphibians combine many of these challenging features for adaptive and functional plasticity as their development includes metamorphosis from a swimming larval lifestyle to adult terrestrial locomotion (Combes, 2019). The similar developmental patterns and comparable morphological features as presented in Fig.1 of Chapter II, combined with the methodological advantages of semi-intact preparations (see Introduction), allowed for diverse investigations of sensory-motor plasticity under normal, healthy conditions and after the acute, unilateral sensory loss of vestibular input.

## SELF-MOTION & ITS CONSEQUENCES

While the salamander Axolotl is a sit-and-wait predator and is not known to be an active locomotor (Hoff et al., 1989), anurans such as *Xenopus laevis* tadpoles are filter feeders and almost constantly in motion (Sillar et al., 2008; Currie and Sillar, 2018). In the absence of a flexible neck, as is the case in both species, swimming related trunk/tail movements tightly influence the motion kinematics of the head and as a consequence the activation of visuo-vestibular components (Chagnaud et al., 2012). During periods of swimming, both Axolotl and *Xenopus* swim at speed ranges that are consistent with the values reported for fish and aquatic larvae (Budick and O'Malley, 2000; Hännzi and Straka, 2017). Despite Axolotl swimming at higher velocities, a striking difference was observed in their swimming mode. The more or less continuous locomotion of *Xenopus* (Fig.2, Chapter II, Schneider-Soupiadis et al., unpublished manuscript; Currie and Sillar, 2018) contrasts with the swim style in Axolotl, who utilizes short, high velocity forward thrusts followed by a passive glide. These distinct swimming modes have previously been also compared and reported in two related freshwater fish. Herein, zebrafish employ bouts, while *Danionella* displays slow and sustained locomotion that has been associated with reduced levels of dissolved oxygen availability and delayed swim bladder development in the latter case (Rajan et al., 2022). Moreover, the data presented in Chapter II confirm previous analyses of swimming kinematics in adult Axolotls, which similarly observed that they exhibit less efficient swimming than anuran tadpoles and most fishes, linking that to differences in their ecological niche (D'août and Aerts, 1997). A plausible explanation is given by the fact that ambystomatid salamanders are endemic in shallow lakes in Mexico, where they sit at the bottom of the lake with dense vegetation, features that would favor maneuverability and fast escape behaviors. In addition, as *Xenopus* transition their locomotion from tail-based swimming to limb-based kick propulsion, the swimming frequency decreases (Combes et al., 2012; Hännzi and Straka, 2017). This switch in locomotion strategy is in contrast to Axolotls, which as neotenic amphibians maintain their juvenile features throughout ontogeny (Adamson et al., 2022) and undergo changes mainly in body length. Analysis of kinematic variables of larval stages to adults showed that the swimming style remains remarkably similar throughout ontogeny (D'août and Aerts, 1999). Therefore, the observed lower locomotion performance in Axolotl might be also linked to different locomotor control strategies. While in *Xenopus* the axial undulatory swimming switches to appendicular locomotion control, both systems co-exist into adulthood in salamanders (Sillar et al., 2023).

Swimming in an undulatory manner produces rhythmic oscillations of the head, creating angular acceleration stimuli and thereby activating the horizontal semicircular canal. Semicircular canals of stage 54 *Xenopus* tadpoles experience on average peak angular accelerations around  $150\text{-}200^\circ/\text{s}^2$  (Lambert et al., 2020; Chapter II, Schneider-Soupiadis et al., unpublished manuscript). Although the peak angular accelerations in Axolotl were higher compared to *Xenopus*, on average head accelerations were lower, consistent with their lower swimming performance. Despite being temporarily exposed to high angular

accelerations, these stimuli may prove ineffective for activating an aVOR, given that canal morphology has been demonstrated to be a limiting factor (Lambert et al., 2008). Overall, the differences observed in swimming characteristics, along with the varying exposure to angular acceleration regimes between the two species during self-motion, prompt consideration of how this may influence sensory-motor plasticity in gaze stabilizing systems.

## VISUO-VESTIBULAR & EC PLASTICITY UNDER HEALTHY CONDITIONS

The observed difference in locomotor regimes along with its influence on semicircular canal activation imposed multiple interesting questions. Among those, one particularly evident query was whether *Xenopus* and Axolotl interpret sensory information related to motion differently, and if so, how such distinctions are manifested in their gaze stabilizing circuits. In order to address this question effectively, I had to ensure the utilization of the appropriate developmental stages, as gaze stabilizing performances undergo significant changes throughout metamorphosis as proven by extensive investigations in anurans (Straka and Dieringer, 2004; von Uckermann et al., 2013; Branoner et al., 2016). Herein, otolith (gVOR), optokinetic (OKR), and efference copy (EC) driven gaze stabilization becomes operational immediately after hatching when tadpoles commence swimming (Horn et al., 1986; Bacqué-Cazenave et al., 2022). In contrast, angular derived responses (aVOR) first emerge at stage 49, showing an improvement in performance until it diminishes beyond stage 60. At this point, tadpoles start metamorphosing into frogs which rely on compensatory head movements rather than eye movements to offset retinal image slip (Dieringer and Precht, 1982; Dieringer, 1987). In combination with the fact that the OKR also starts declining after stage 52 (Bacqué-Cazenave et al., 2022), I chose stage 54 animals for the comparative investigations in *Xenopus* and Axolotl.

The adaptability of visuo-vestibular responses during anuran ontogeny is not restricted to developmental processes, nor is it unique to amphibians. A plethora of studies have demonstrated the enduring plasticity of gaze stabilizing reflexes throughout an animal's lifespan triggered by changes of the usually perceived stimuli in the environment (Faulstich et al., 2004; Dietrich and Straka, 2016; França de Barros et al., 2020; Forsthofer and Straka, 2023). In that regard, the assessment of gaze stabilizing performances is made based on two widely used metrics: gain, defined as the ratio of the amplitude/velocity of the eye motion and the stimulus amplitude/velocity, and phase, which constitutes the temporal difference between the maximum eye response and the maximum stimulus response (Gordy and Straka, 2022; Panichi et al., 2022). Moreover, adaptive changes are mainly reflected as changes in response gain and have aimed to investigate the sites of shared VOR and OKR plasticity. Hence, I used those metrics as the primary determinants to assess gaze stabilizing performances in *Xenopus* and Axolotl.

Given the observed distinctions in locomotion characteristics, it was not a big surprise that there were significant differences observed in eye-stabilizing performances in

response to visuo-vestibular stimulation. However, the extremely low response gain of the VOR in Axolotl with an almost 100° phase shift was not expected (Fig.3, Chapter II, Schneider-Soupiadis et al., unpublished manuscript). This very low gain together with the severely delayed peak eye motion amplitude suggests that Axolotls are barely capable of an appropriate response during angular rotations in the horizontal plane at the tested frequency. While the gain was significantly higher during rotations with a stationary striped pattern, in comparison to the vestibular-only experimental paradigm, it was still significantly lower compared to *Xenopus* (Fig.3, Chapter II, Schneider-Soupiadis et al., unpublished manuscript; Fig.3 Chapter III, Soupiadou et al., 2020). Despite that, the phase, which should overlap with the maximal stimulus velocity, was unaffected during the co-activation of visuo-vestibular reflexes suggesting that the sensation of rotational movements is extremely deficient.

As the VOR and OKR operate synergistically and converge on central targets (Horn and Straka, 2021), it was interesting to investigate if the OKR would be higher in Axolotl to compensate for the reduced vestibular output. Indeed, the OKR phase was very similar between the two species, overlapping with the peak stimulus position, while the gain was significantly higher in Axolotl. The increased OKR performance could be explained by plasticity mechanisms which have been observed in various studies in response to alterations of visuo-vestibular sensation. Such changes can be induced for instance by telescopic goggles that double the size of the seen world, which in primates leads to parallel changes in VOR and OKR gains (Lisberger et al., 1981). In contrast, in mice as in rabbits, adaptive stimuli that reduce the VOR gain result in an increased OKR gain (Collewyn and Grootendorst, 1979; Faulstich et al., 2004). The shared components of this type of oculomotor plasticity seem to reside within the vestibular nuclei and the cerebellum (du Lac et al., 1995; Highstein et al., 1997; Forsthofer and Straka, 2022). Moreover, despite the variance in outcomes of adaptive plasticity among vertebrates, these examples highlight a key feature of visuo-vestibular reflexes: maintain efficacy throughout life.

The tight functional link between gaze stabilization and self-motion becomes apparent in precocial animals such as fish that start locomotion immediately after birth/hatching and have been shown to already obtain significant eye motion gains (Beck et al., 2004; Straka, 2010). In contrast, the offspring of altricial animals like mice are relatively immature and immobile after birth with low VOR gains (Faulstich et al., 2004), presumably correlating with the maturation of vestibular system elements. Nevertheless, semicircular canal-evoked motor responses are also absent immediately after hatching in fish (Beck et al., 2004) and *Xenopus* (Lambert et al., 2008), the presence of which correlates with substantial growth in body and canal size. To partly compensate for the delayed aVOR onset in small vertebrates, intrinsic efference copy signals during rhythmic locomotion have been shown to assist poor or absent sensory feedback-driven image stabilization (Combes et al., 2008; Lambert et al., 2023). Therefore, it was of particular interest to investigate to what extent this signaling may supplement the very low VOR gain in Axolotl. As previously shown in *Xenopus* (Bacqué-Cazenave et al., 2022), Axolotl also exhibited tail phase coupled eye

movements. However, the spico-ocular gain values were comparable, indicating no higher significant role of spinal ECs (Chapter II, Schneider-Soupiadis et al., unpublished manuscript). Taken together, the increased gain under stimulation with visual feedback, which is not sufficient to restore the missing VOR component during co-activation of both reflexes, along with the phase-lagged response under both experimental conditions with vestibular stimulation point to a vestibular sensor limitation which will be addressed in more depth in the following section.

## SEMICIRCULAR CANAL SENSITIVITY IS CONSTRAINED BY MORPHOLOGY

As already pointed out above, semicircular canal morphology is key for the execution and onset of an angular VOR. Despite the evolutionary conservation of the basic design and physiology of vestibular endorgans among vertebrates, semicircular canals in particular, show a large anatomical variability (Platt and Straka, 2020). This variability concerns parameters such as canal/lumen radius, circularity, and length (Muller, 1999; Yang and Hullar, 2007). The reason why these parameters affect the sensitivity of the respective canal is the following: canals are filled with endolymph, which during head rotations and due to fluid inertia causes a pressure force opposite to the direction of head motion. This in turn leads to a deflection of the cupula, the gelatinous structure inside the ampulla that contains the hair cells (Steinhausen, 1931). As a result, depending on the direction of angular acceleration, the hair cells of the respective horizontal semicircular canal will be depolarized while its matching planar pair will be hyperpolarized (for more details please refer to Chapter I). Moreover, studies taking into consideration fluid mechanics have shown that parameters such as canal radius and length influence significantly the fluid/endolymph resistance (Essner et al., 2022). In summary, the conversion of endolymph displacements into neural signals depends on the biomechanics of the canal and influences the subsequent outcome on downstream vestibular neural circuit elements/functions.

Although studies in a number of vertebrates have tried to draw correlations between canal size and vestibular function (mouse: Curthoys, 1979; toadfish: Yamauchi et al., 2002; squamates: Goyens 2019), amphibian species present, apart from the previously mentioned benefits, a tremendous advantage: their inner ear is easily accessible and visually discernible during their larval stages (Fig. 1, Chapter II, Schneider-Soupiadis et al., unpublished manuscript). While quantification of the semicircular canal radius of *Xenopus* was in line with previous analyses (Lambert et al. 2008), Axolotl radii were significantly lower in comparison (Fig.4, Chapter II, Schneider-Soupiadis et al., unpublished manuscript). Moreover, the fact that the otic capsule length and area were comparable between the two species was another strong support for the argument that the ears/otic capsules themselves are not differently scaled. Yet another distinction was that the shape of the ampulla was much more elliptic in contrast to the relatively round shape of *Xenopus* canals. These two notable differences lead to the assumption that endolymph flow is more favorable in the latter case.

Going a step further and analyzing the 3D structure of the canals revealed more intriguing distinctions: a stenosis of the canal lumen just before the start of the ampulla in Axolotl along with the much flatter, rounder, and more homogeneous cross-section area of the *Xenopus* canal. These data are in agreement with previous findings which tried to combine morphological measurements from the Axolotl *Ambystoma tigrinum* with mathematical models to determine canal sensitivity (Muller and Verhagen, 2002; Vega et al., 2008). The authors concluded that the calculated relationships of duct radii and circuit radii speak for a low sensitivity of the canals. While size differences of minimal scale are usually uncritical for vertebrates above the size of rodents, in aquatic animals such as fishes, and amphibians, which start with very small body sizes after hatching, canal dimensions changes are highly relevant (Straka, 2010). This was also observed in our study where an increase in body size (stage 56) led to a much better aVOR, reaching gain values comparable to the onset of the aVOR in *Xenopus* (Fig.3, Chapter II, Schneider-Soupiadis et al., unpublished manuscript).

## VISUO-VESTIBULAR PLASTICITY UNDER PATHOLOGICAL CONDITIONS

Under normal, healthy conditions balanced neuronal activity in the bilateral vestibular circuits is maintained (Curthoys, 2020; Deans, 2021). Symmetric activity levels, which can be dynamically modulated during head rotations, are observed at all stages of vestibular signal processing, from afferent fibers to central vestibular neurons and as a consequence in extraocular motoneurons (Fetter, 2007; Beraneck and Idoux, 2012). Under stationary conditions, spontaneous neurotransmitter release causes a resting discharge of the postsynaptic vestibular afferents which during head motions either facilitates or disfacilitates the activity of the downstream circuit, transmitted centrally via the VIIIth cranial nerve of which the afferents compose (Jones et al., 2008; Lambert and Bacqué-Cazenave, 2020). Plasticity mechanisms following lesions in the oculomotor system ensuring gaze stabilization have been an extensive subject of investigations and shown to be partly capable of restoring its function after injuries (Smith and Curthoys, 1989; Vibert et al., 1999; Curthoys, 2000; Cullen et al., 2009; Lambert and Straka, 2012). However, according to my knowledge, all the so far utilized animal models lacked the ability to test the immediate behavioral effect on static and dynamic symptoms caused by a complete unilateral loss of vestibular input. This limitation arises from surgical manipulations, which go along with anesthesia and analgesics (Faulstich et al., 2006) that may influence and mask plasticity processes in the immediate time past the insult. This is an important factor to consider as plasticity is a continuous process involving multiple sites and mechanisms, each exhibiting distinct time courses (Beraneck and Idoux, 2012). Therefore, I employed whole head preparations of *Xenopus laevis* tadpoles to address this question (Chapter III, Soupiadou et al., 2020) as they not only provide many experimental advantages (elaborated in Chapter I) but also allow one to address the immediate effect of an VIIIth nerve transection, which can

be introduced with ease and investigated within a very short timeframe after the lesion and long after cessation of anesthesia.

Under stationary conditions, acute abolishment of unilateral vestibular input caused a shift of resting eye position towards the lesioned side. This shift was induced by the imbalance in the basic discharge between the bilateral vestibular nuclei (Darlington et al., 2002; Beraneck and Idoux, 2012). Unlike lesions in other sensory systems, where loss of sensory information is not causing any sensation, abolishment of vestibular input is interpreted as motion towards the intact side due to the relatively higher resting activity in the contralesional side. In the case of the visual system, for instance, lesion of the optic nerve leads to a complete loss of sensory information from the affected eye (Atkins et al., 2008; Forsthofer et al., 2023). Apart from this eye position shift, a spontaneous nystagmus, which is typically observed in other species (Newlands et al., 2005; Vidal et al., 2016; Zwergal et al., 2022), was not present. As a fundamental feature of vestibular encoding relies on fluctuations in afferent resting activity from baseline levels (Gensberger et al., 2016), a possible explanation for this could be the relatively low resting rates of less than 10 Hz in amphibian vestibular circuits (Blanks and Precht, 1976; Gensberger et al., 2016). This is in contrast to other vertebrates that possess tenfold higher discharges, thereby exhibiting a greater imbalance between the bilateral vestibular nuclei after a unilateral lesion (Anastasio et al., 1985; Goldberg, 2000; Forbes et al., 2022; Gordy and Straka, 2022).

Horizontal rotations in the dark showed a significant decrease of the aVOR gain within minutes after the lesion as a consequence of the missing semicircular canal excitatory drive (Gordy and Straka, 2022). This reduction in gain was also observed under vestibular stimulation with a world-stationary striped pattern, thus co-activating an optokinetic response which was acutely not able to compensate for the missing vestibular component. Moreover, investigation of the OKR in isolation revealed no discernible impact on its execution, as anticipated, given that a lesion of the vestibular nerve should not directly influence visually induced gaze stabilization. Similar findings were observed in animals raised with only one ear which were investigated at the same developmental stages (Gordy and Straka, 2022).

Over the first two hours after the lesion, aVOR gains decreased further to remain low with no signs of recovery. This is not unexpected given that numerous previous studies have demonstrated that dynamic responses only partly recover, and if so, only after a considerable time ranging from days to weeks after the lesion (Curthoys, 2000; Dutia, 2010; Simon et al., 2020). Surprisingly, the OKR gain also severely declined at 1.5 hours following the neurectomy, reaching a level comparable to aVOR gain values and remaining relatively unchanged for the subsequent hours. This delayed and significant gain mitigation of both reflexes might stem from secondary neuronal consequences in the shared VOR-OKR circuit elements, triggered by the ongoing asymmetric activity resulting from the high firing rates on the contralesional side which are reinforced by the lack of commissural inhibitory connections from the ipsilesional side (Yagi and Markham, 1984; Straka et al., 2005;

Malinvaud et al., 2010). Therefore, as one of the hallmarks of the vestibular system is to maintain homeostatic activity levels, aiming to re-balance the activity in ipsi- and contralesional vestibular nuclei, might be a plausible explanation (Beraneck et al., 2003; Straka et al., 2005; Dutia, 2010; Turrigiano, 2012; Gordy and Straka, 2022). Moreover, adaptive changes in oculomotor performance have already been observed in *Xenopus* tadpoles after prolonged vestibular and visual stimulation, a type of plasticity that depends on intact cerebellar functioning (Dietrich and Straka, 2016; Forsthofer and Straka, 2023). The rationale behind this lies in the fact that Purkinje cells (neurons in the cerebellum) receive input from vestibular neurons (De Zeeuw and Yeo, 2005; Sadeghi and Beraneck, 2020). Additionally, through the inferior olive, they also receive information about optic flow (du Lac et al., 1995), making them a site of convergence for visuo-vestibular sensory information. In fact, in mice which lacked adequate cerebellar input, compensation processes were heavily impaired (Faulstich et al., 2006; Beraneck et al., 2008). However, cerebellum independent plasticity mechanisms, induced by changes in intrinsic properties of second order vestibular neurons (Cameron and Dutia, 1997), modified commissural inhibition (Berquist et al., 2008), and reorganization of the vestibular circuit (Rohregger and Dieringer, 2003) might also provide plausible explanations.

## CONCLUSIONS & FUTURE DIRECTIONS

Overall, the data presented in this thesis have helped to expand our current knowledge of sensorimotor plasticity in gaze stabilizing systems. Investigation of such performances in two phylogenetically related amphibian species, with shared similarities in body plan, natural environments, and the ability to utilize *in vitro* preparations allowed for versatile comparative investigations shedding light on vertebrate functional and adaptive plasticity mechanisms. Robust semicircular canal driven (aVOR) and optokinetic (OKR) responses were recorded in *Xenopus* tadpoles with distinct differences observed in Axolotl larvae. The latter had almost absent aVOR gains at similar developmental stages, under identical experimental conditions, while they exhibited higher gains under optic flow-induced conditions. This increased performance under optokinetic stimulation might be the result of adaptive plasticity in the shared visuo-vestibular circuit. Investigation of these reflexes in older staged Axolotls showed significantly higher gains which met the magnitude of the aVOR onset in *Xenopus*, indicating a delayed ontogenetic execution of semicircular canal evoked reflexes. Based on these results it would be interesting to investigate otolith-derived compensatory eye movements at stage 54 Axolotls as they have been found to be already functional immediately after hatching in fish and *Xenopus* (Horn et al., 1986; Bacqué-Cazenave et al., 2022). Despite the conserved nature of visuo-vestibular systems (Masseck and Hoffmann, 2009; Straka and Baker, 2013; Lipovsek and Wingate, 2018), differences in circuitry components cannot be excluded. It has been shown for instance that urodeles possess, unlike anurans, a mixed and non-purely motor trochlear nerve with a larger number of motoneurons (Firtzsch and Sonntag, 1987). Additionally, urodeles have a lower number of

retinal cells and a less myelinated optic nerve (Roth et al., 1992). Another interesting study would be the comparative investigation of the impact of an optic nerve lesion in salamander and frog larvae, under the same experimental conditions as described in Chapters II and III. This approach aims to provide a more comprehensive understanding of the shared underlying circuitry. In addition, profiling of the extraocular motor responses in the following days after the neurectomy might lead to an increased gain in aVOR responses as part of adaptive plasticity processes. Furthermore, a combination of VIIIth cranial nerve transections with an ablation of the cerebellum (Blazquez et al., 2004; Kassardjian et al., 2005) might shed more light on the origin of secondary vestibular consequences observed in Chapter III. As a result of such an investigation, the observed decrease in OKR gain might not be induced.

Research in various vertebrates has led to the conclusion that the development and maturation of the vestibular system plays a crucial role in determining an animal's posture and locomotion capabilities as being evident in the offspring of precocial versus altricial species (Straka, 2010; Gordy and Straka, 2020). Moreover, eco-physiological factors have also been speculated to influence an animal's behavioral plasticity (Straka and Dieringer, 2004; Masseck and Hoffmann, 2009). The observed difference in locomotor strategies of *Xenopus* and Axolotl might be a combination of all these factors. The almost constant locomotion of *Xenopus* goes along with their filter-feeding behavior, while the short, high velocity swim mode in Axolotl might be the result of insufficiently sized semicircular canals as well as stem from living in shallow lakes with dense vegetation (D'août and Aerts, 1997; Lambert et al., 2008). Apart from thinner horizontal semicircular canals in Axolotls, the distinct differences observed in canal characteristics strongly indicate a more advantageous endolymph flow in *Xenopus*.

As Dieringer already suggested in 1991, locomotion seems to be an important evolutionary driving force for the adaptation of gaze-stabilizing performances (Frýdlová et al., 2019). Moreover, locomotion is strongly linked to an animal's fitness, such as the escape response from predators, thus shaping an organism's body plan (Dickinson et al., 2000). This fast escaping response that is dictated by the dense environments in which Axolotls reside may favor the adoption of the bout mode of locomotion, subsequently influencing the acceleration kinematics of the head. Furthermore, anuran species with different ecologies have been found to exhibit different swimming kinematics (Robovska-Havelkova et al., 2014). Thereby, the differences observed in semicircular canal geometry, which constrain hair cell activation in Axolotls, may stem from adaptation to living in their natural environment and as a result to the locomotion strategy.

As the VOR and OKR operate synergistically with each sensory system covering a particular frequency range determined by the temporal resolution of the respective motion sensors (Beraneck and Straka, 2011) it cannot be excluded that the tested frequency of 0.5 Hz is not optimal for Axolotls. In foveate animals, the VOR bandwidth is in the range of 1-50 Hz (Eatock and Songer, 2011), whereas for afoveate anurans sensitivities are below 1 Hz

(Gensberger et al., 2016). However, the fact that the gain significantly increases at later developmental stages favors the hypothesis that there is a developmental and morphological constraint other than a difference in tuning. Moreover, to gain further insights into the observed correlations in Chapter II, expanding the diversity of species would be a logical next step. An intriguing candidate in this regard could be lampreys, as they not only exhibit undulatory swimming but also possess an OKR and EC-derived gaze stabilization (Wibble et al., 2022).

In conclusion, amphibian species provide attractive animal models to investigate visuo-vestibular plasticity mechanisms. The easy accessibility of neuronal circuit components and sensory periphery, surgical manipulations without effects of anesthesia together with ideal optical properties provided by tissue transparency are only some of the many experimental advantages. Moreover, the plasticity framework provided by metamorphosis in which animals switch their locomotion strategies and natural habitat offers unique testable hypothesis within the same organism. Investigations in further species belonging to the amphibian group might shed more light into the interactions of gaze stabilizing reflexes and their interplay with sensory morphology and locomotor strategies under physiological and pathological conditions. Such comparisons might bridge the gap between biology and technology and find practical use given the prevalence of vestibular disorders in humans. Research in this direction would also significantly contribute to therapeutic measures. Furthermore, industrial applications, including advancements in sophisticated robotics, virtual reality technologies, and the finetuning of motion sensors in self-driving car technologies, stand to benefit from basic neurobiological research.

---

## REFERENCES

---

- Adamson, C.J., Morrison-Welch, N., and Rogers, C.D. (2022). The amazing and anomalous axolotls as scientific models. *Dev Dyn* 251, 922-933.
- Anastasio, T.J., Correia, M.J., and Perachio, A.A. (1985). Spontaneous and driven responses of semicircular canal primary afferents in the unanesthetized pigeon. *J Neurophysiol* 54, 335-347.
- Anastasopoulos, D., Gianna, C., Bronstein, A.M., and Gresty, M.A. (1996). The interaction of the human linear otolith-ocular and angular horizontal vestibule-ocular reflexes in darkness. *Ann N Y Acad Sci* 781, 580-582.
- Angelaki, D.E., and Cullen, K. E. (2008). Vestibular system: the many facets of a multimodal sense. *Annu Rev Neurosci* 31, 125-150.
- Angelaki, D.E., Gu, Y., and DeAngelis, G.C. (2009). Multisensory integration: psychophysics, neurophysiology, and computation. *Curr Opin Neurobiol* 19, 452–458.
- Atkins, E.J., Newman, N.J., and Biousse, V. (2008). Post-Traumatic Visual Loss. *Rev Neurol Dis* 5, 73-81.
- Bacqué –Cazenave, J., Courtand, G., Beraneck, M., Straka, H, Combes, D., and Lambert, F.M. (2022). Locomotion-induced ocular motor behavior in larval *Xenopus* is developmentally tuned by visuo-vestibular reflexes. *Nat Commun* 13, 2957.
- Baker, R., Evinger, C., and McCrea, R.A. (1981). Some thoughts about the three neurons in the vestibular ocular reflex. *Ann N Y Acad Sci* 374, 171-188.
- Baker, R., and Highstein, S.M. (1975). Physiological identification of interneurons and motoneurons in the abducens nucleus. *Brain Res* 91, 292-298.
- Barlow, H.B., and Hill, R.M. (1963). Selective sensitivity to direction of movement in ganglion cells of the rabbit retina. *Science* 139, 412-414.
- Barnes, G.R. (1983). Physiology of visuo-vestibular interaction: discussion paper. *J R Soc Med* 9, 747-754.
- Beck, J.C., Gilland, E., Tank, D.W., and Baker, R. (2004). Quantifying the ontogeny of optokinetic and vestibuloocular behaviors in zebrafish, medaka, and goldfish. *J Neurophysiol* 92, 3546-3561.
- Benfey, N., Foubert, D., and Ruthazer, E.S. (2022). Glia Regulate the Development, Function, and Plasticity of the Visual System From Retina to Cortex. *Front Neural Circuits* 16, 826664.
- Beraneck, M., Hachemaoui, M., Idoux, E., Ris, L., Uno, A., Godaux, E., Vidal, P.P., Moore, L. E., and Vibert, N. (2003). Long-term plasticity of ipsilesional medial vestibular nucleus neurons after unilateral labyrinthectomy. *J Neurophysiol* 90, 184-203.
- Beraneck, M., McKee, J.L., Aleisa, M., and Cullen, K.E. (2008). Asymmetric recovery in cerebellar-deficient mice following unilateral labyrinthectomy. *J Neurophysiol* 100, 945-958.

- Beraneck, M., and Straka, H. (2011). Vestibular signal processing by separate sets of neuronal filters. *J Vestib Res* 21, 5-19.
- Bergquist, F., Ludwig, M., and Dutia, M.B. (2008). Role of the commissural inhibitory system in vestibular compensation in the rat. *J Physiol* 586, 4441-4452.
- Blanks, R.H., Estes, M.S., and Markham, C.H. (1975). Physiologic characteristics of vestibular first-order canal neurons in the cat. II. Response to constant angular acceleration. *J Neurophysiol* 38, 1250-1268.
- Blanks, R.H., and Precht, W. (1976). Functional characterization of primary vestibular afferents in the frog. *Exp Brain Res* 25, 369-390.
- Blazquez, P.M., Hirata, Y., and Highstein, S.M. The vestibulo-ocular reflex as a model system for motor learning: what is the role of the cerebellum? *Cerebellum* 3, 188-192.
- Borst, A., and Egelhaaf, M. (1993). Detecting visual motion: theory and models. *Rev Oculomot Res* 5, 3-27.
- Branoner, F., Chagnaud, B.P., and Straka, H. (2016). Ontogenetic Development of Vestibulo-Ocular Reflexes in Amphibians. *Front Neural Circuits* 10, 91.
- Budick, S.A., and O'Malley, D.M. (2000). Locomotor repertoire of the larval zebrafish: swimming, turning and prey capture. *J Exp Biol* 203, 2565-2579.
- Büttner-Ennever, J.A. (2006). The extraocular motor nuclei: organization and functional neuroanatomy. *Prog Brain Res* 151, 95-125.
- Büttner, U., and Büttner-Ennever, J.A. (2006). Present concepts of oculomotor organization. *Prog Brain Res* 151, 1-42.
- Cameron, S.A., and Dutia, M.B. (1997). Cellular basis of vestibular compensation: changes in intrinsic excitability of MVN neurons. *Neuroreport* 8, 2595-2599.
- Campos, J.L., and Bühlhoff, H.H. (2012). Multimodal Integration during Self-Motion in Virtual Reality. In *The Neural Bases of Multisensory Processes*, Chapter 30, Murray, M.M., Wallace, M.T. eds (CRC Press/Taylor & Francis), PMID: 22593878.
- Chagnaud, B.P., Simmers, J., and Straka, H. (2012). Predictability of visual perturbation during locomotion: implications for corrective efference copy signaling. *Biol Cybern* 106, 669-679.
- Cochran, S.L., Dieringer, N., and Precht, W. (1984). Basic optokinetic-ocular reflex pathways in the frog. *J Neurosci* 4, 43-57.
- Collewijn, H., and Grootendorst, A.F. (1979). Adaptation of optokinetic and vestibulo-ocular reflexes to modified visual input in the rabbit. *Pro Brain Res* 50, 771-781.
- Combes, D. (2019). Metamorphosing motor networks. *Curr Biol* 29, R557-R561.

Combes, D., Le Ray, D., Lambert, F.M., Simmers, J., and Straka, H. (2008). An intrinsic feed-forward mechanism for vertebrate gaze stabilization. *Curr Biol* 18, R241-243.

Combes, D., Sillar, K.T., and Simmers, J. (2012). A switch in aminergic modulation of locomotor CPG output during amphibian metamorphosis. *Front Biosci (Schol Ed)* 4, 1364-1374.

Cohen, B., Suzuki, J.I., and Bender, M.B. (1964). EYE MOVEMENTS FROM SEMICIRCULAR CANAL NERVE STIMULATION IN THE CAT. *Ann Otol Rhinol Laryngol* 73, 153-169.

Cramer, S.C., Sur, M., Dobkin, B.H., O'Brien, C., Sanger, T.D., Trojanowski, J.Q., Rumsey, J.M., Hicks, R., Cameron, J., Chen, D., Chen, W.G., Cohen, L.G., deCharms, C., Duffy, C.J., Eden, G.F., Fetz, E.E., Filart, R., Freund, M., Grant, S.J., Haber, S., Kalivas, P.W., Kolb, B., Kramer, A.F., Lynch, M., Mayberg, H.S., McQuillen, P.S., Nitkin, R., Pascual-Leone, A., Reuter-Lorenz, P., Schiff, N., Sharma, A., Shekim, L., Stryker, M., Sullivan, E.V., and Vinogradov, S. (2011). Harnessing neuroplasticity for clinical applications. *Brain* 134, 1591-1609.

Cullen, K.E. (2019). Vestibular processing during natural self-motion: implications for perception and action. *Nat Rev Neurosci* 20, 346–363.

Cullen, K.E., Sadeghi, S.G., Beraneck, M., and Minor, L.B. (2009). Neural substrates underlying vestibular compensation: Contribution of peripheral versus central processing. *J Vestib Res* 19, 171-182.

Cullen, K.E., and Zobeiri, O.A. (2021). Proprioception and the predictive sensing of active self-motion. *Curr Opin Physiol* 20, 29-38.

Currie, S.P., and Sillar, K.T. (2018). Developmental changes in spinal neuronal properties, motor network configuration, and neuromodulation at free-swimming stages of *Xenopus* tadpoles. *J Neurophysiol* 119, 786-795.

Curthoys, I.S. (1979). The development of function of horizontal semicircular canal primary neurons in the rat. *Brain Res* 167, 41-52.

Curthoys, I.S. (1981). Scarpa's ganglion in the rat and guinea pig. *Acta Otolaryngol* 92, 107-113.

Curthoys, I.S. (2000). Vestibular compensation and substitution. *Curr Opin Neurol* 13, 27-30.

Curthoys, I.S. (2020). The Anatomical and Physiological Basis of Clinical Tests of Otolith Function. A Tribute to Yoshio Uchino. *Font Neurol* 11, 566895.

Curthoys, I.S. (2021). The Neural Basis of Skull Vibration Induced Nystagmus (SVIN). *Audiol Res* 11, 557-566.

D'août, K., and Aerts, P. (1997). Kinematics and Efficiency of Steady Swimming in Adult Axolotls (*Ambystoma Mexicanum*). *J Exp Biol* 200, 1863-1871.

D'août, K., and Aerts, P. (1999). The kinematics of voluntary steady swimming of hatchling and adult axolotls. *Belg J Zool* 129, 305-316.

- Darlington, C.L., Dutia, M.B., and Smith, P.F. (2002). The contribution of the intrinsic excitability of vestibular nucleus neurons to recovery from vestibular damage. *Eur J Neurosci* 15, 1719-1727.
- Day, B.L., and Fitzpatrick, R.C. (2005). The vestibular system. *Curr Biol* 15, R583-R586.
- DeAngelis, G.C., and Angelaki, D.E. (2012). Visual-Vestibular Integration for Self-Motion Perception. In *The Neural Bases of Multisensory Processes*, Chapter 31, Murray, M.M., Wallace, M.T. eds (CRC Press/Taylor & Francis).
- Deans, M.R. (2021). Conserved and Divergent Principles of Planar Polarity Revealed by Hair Cell Development and Function. *Front Neurosci* 15, 742391.
- de Burel H. M. (1929). Zur vergleichenden Anatomie der Labyrinthinnervation. *J Comp Neurol* 47, 155–169.
- De Zeeuw, C.I., and Yeo, C.H. (2005). Time and tide in cerebellar memory formation. *Curr Opin Neurobiol* 15, 667-674.
- Dichgans, J., and Brandt, T. (1978). Visual-Vestibular Interaction: Effects on Self-Motion Perception and Postural Control. In *Perception*, Held, R., Leibowitz, H.W., and Teuber, H.L. eds. (Berlin, Heidelberg: Springer Berlin Heidelberg), pp. 755-804.
- Dickinson, M.H., Farley, C.T., Koehl, M.A., Kram, R., Lehman, S. (2000). How animals move: an integrative view. *Science* 288, 100-106.
- Dieringer, N. (1987). The role of compensatory eye and head movements for gaze stabilization in the unrestrained frog. *Brain Res* 404, 33-38.
- Dieringer, N. (1991). Comparative aspects of gaze stabilization in vertebrates. *Zool Jahrb Physiol* 95, 369-377.
- Dieringer, N. (1995). 'Vestibular compensation': neural plasticity and its relations to functional recovery after labyrinthine lesions in frogs and other vertebrates. *Prog Neurobiol* 46, 97-129.
- Dieringer, N., and Precht, W. (1982). Compensatory head and eye movements in the frog and their contribution to stabilization of gaze. *Exp Brain Res* 47, 394-406.
- Dieringer, N., Reichenberger, I., and Graf, W. (1992). Differences in optokinetic and vestibular ocular reflex performance in teleosts and their relationship to different life styles. *Brain Behav Evol* 39, 289-304.
- Dietrich, H., and Straka, H. (2016). Prolonged vestibular stimulation induces homeostatic plasticity of the vestibulo-ocular reflex in larval *Xenopus laevis*. *Eur J Neurosci* 44, 1787-1796.
- Distler, C., and Hoffmann, K.P. (2011). The optokinetic reflex. In *The Oxford Handbook on Eye Movements*, Liversedge, S.P., Gilchrist, I.D., and Everling, S., eds (Oxford University Press), pp. 65-83.
- du Lac, S., Raymond, J.L., Sejnowski, T.J., and Lisberger, S.G. (1995). Learning and memory in the vestibulo-ocular reflex. *Annu Rev Neurosci* 18, 409-441.

- Dutia, M.B. (2010). Mechanisms of vestibular compensation: recent advances. *Curr Opin Otolaryngol Head Neck Surg* 18, 420-424.
- Eatock, R.A., and Songer, J.E. (2011). Vestibular hair cells and afferents: two channels for head motion signals. *Annu Rev Neurosci* 34, 501-534.
- Erskine, L., and Herrera, E. (2014). Connecting the retina to the brain. *ASN Neuro* 6, 1759091414562107.
- Essner, R.L.Jr., Pereira, R.E.E., Blackburn, D.C., Singh, A.L., Stanley, E.L., Moura, M.O., Confetti, A.E., and Pie, M.R. (2022). Semicircular canal size constrains vestibular function in miniaturized frogs. *Sci Adv* 8, eabn1104.
- Fetter, M. (2007). Vestibulo-ocular reflex. *Dev Ophthalmol* 40, 35-51.
- Fetter, M. (2016). Acute unilateral loss of vestibular function. *Handb Clin Neurol* 137, 219-229.
- Faulstich, B.M., Onori, K.A., and du Lac, S. (2004). Comparison of plasticity and development of mouse optokinetic and vestibulo-ocular reflexes suggests differential gain control mechanisms. *Vision Res* 44, 3419-3427.
- Faulstich, M., van Alphen, A.M., Luo, C., du Lac, S., and De Zeeuw, C.I. (2006). Oculomotor plasticity during vestibular compensation does not depend on cerebellar LTP. *J Neurophysiol* 96, 1187-1195.
- Forbes, P.A., Kwan, A., Rasman, B.G., Mitchell, D.E., Cullen, K.E., and Blouin, J.S. (2022). Neural Mechanisms Underlying High-Frequency Vestibulocollic Reflexes In Humans And Monkeys. *J Neurosci* 40, 1874-1887.
- Forsthofer, M., Gordy, C., Kolluri, M., and Straka, H. (2023). Bilateral retinofugal pathfinding impairments limit behavioral compensation in near-congenital one-eyed *Xenopus laevis*. *eNeuro*, in press.
- Forsthofer, M., and Straka, H. (2023). Homeostatic plasticity of eye movement performance in *Xenopus* tadpoles following prolonged visual image motion stimulation. *J Neurol* 270, 57-70.
- França de Barros, F., Schenberg, L., Tagliabue, M., and Beraneck, M. (2020). Long term visuo-vestibular mismatch in freely behaving mice differentially affects gaze stabilizing reflexes. *Sci Rep* 10, 20018.
- Fritsch, B. (1998). Evolution of the vestibulo-ocular system. *Otolaryngol Head Neck Surg* 119, 182-192.
- Fritsch, B., and Sonntag, R. (1987). The trochlear nerve of amphibians and its relation to proprioceptive fibers: a qualitative and quantitative HRP study. *Anat Embryol (Berl)* 177, 105-114.

Fritzsch, B., and Straka, H. (2014). Evolution of vertebrate mechanosensory hair cells and inner ears: toward identifying stimuli that select mutation driven altered morphologies. *J Comp Physiol A Neuroethol Sens Neural Behav Physiol* 200, 5-18.

Frydlová, P., Sedláčková, K., Žampachová, B., Kurali, A., Hýbl, J., Škoda, D., Kutílek, P., Landová, E., Černý, R., Frynta, D. (2019). A gyroscopic advantage: phylogenetic patterns of compensatory movements in frogs. *J Exp Biol* 222, jeb186544.

Gensberger, K. D., Kaufmann, A.K., Dietrich, H., Branoner, F., Banchi, R., Chagnaud, B.P., and Straka, H. (2016). Galvanic Vestibular Stimulation: Cellular Substrates and Response Patterns of Neurons in the Vestibulo-Ocular Network. *J Neurosci* 36, 9097-9110.

Ghysen, A., and Dambly-Chaudière, C. (2004). Development of the zebrafish lateral line. *Curr Opin Neurobiol* 14, 67-73.

Goldberg, JM. (2000). Afferent diversity and the organization of central vestibular pathways. *Exp Brain Res* 130, 277-297.

Gollisch, T., and Meister, M. (2010). Eye smarter than scientists believed: neural computations in circuits of the retina. *Neuron* 65, 150-164.

Gordy, C., and Straka, H. (2022). Developmental eye motion plasticity after unilateral embryonic ear removal in *Xenopus laevis*. *iScience* 25, 105165.

Goyens, J. (2019). High ellipticity reduces semi-circular canal sensitivity in squamates compared to mammals. *Sci Rep* 9, 16428.

Goyens, J., Pourquoi, M.J.B.M., Poelma, C., and Westerweel, J. (2019). Asymmetric cupula displacement due to endolymph vortex in the human semicircular canal. *Biomech Model Mechanobiol* 6, PMID: 31069593.

Graf, W., and Baker, R. (1983). Adaptive changes of the vestibulo-ocular reflex in flatfish are achieved by reorganization of central nervous pathways. *Science* 221, 777-779.

Grillner, S. (2003). The motor infrastructure: from ion channels to neuronal networks. *Nat Rev Neurosci* 4, 573-586.

Groves, A.K., and Fekete, D.M. (2012). Shaping sound in space: the regulation of inner ear patterning. *Development* 139, 245-257.

Gruberg, E.R., and Grasse, K.L. (1984). Basal optic complex in the frog (*Rana pipiens*): a physiological and HRP study. *J Neurophysiol* 51, 998-1010.

Hänzi, S., and Strak, H. (2017). Developmental changes in head movement kinematics during swimming in *Xenopus laevis* tadpoles. *J Exp Biol* 220, 227-236.

Hellmer, C.B., Hall, L.M., Bohl, J.M., Sharpe, Z.J., Smith, R.G., and Ichinose, T. (2021). Cholinergic feedback to bipolar cells contributes to motion detection in the mouse retina. *Cell Rep* 37, 110106.

- Highstein, S.M., Partsalis, A., and Arkan, R. (1997). Role of the Y-group of the vestibular nuclei and flocculus of the cerebellum in motor learning of the vertical vestibulo-ocular reflex. *Prog Brain Res* 114, 383-397.
- Hodos, W., and Butler, A.B. (1997). Evolution of Sensory Pathways in Vertebrates. *Brain Behav Evol* 50, 189-197.
- Hoff, K.V., Hug, N., King, V.A., and Wassersug, R.J. (1989). The kinematics of larval salamander swimming (Ambystomatidae: Caudata). *Can J Zool* 67, 2756-2761.
- Horn, A.K.E. (2020). Neuroanatomy of Central Vestibular Connections. In *The Senses: A Comprehensive Reference*, Vol 6, Fritzsche, B., Straka, H., eds (Elsevier), pp. 21-37.
- Horn, A.K.E, and Straka, H. (2021). Functional Organization of Extraocular Motoneurons and Eye Muscles. *Annu Rev Vis Sci* 7, 793-825.
- Hudspeth, A.J. (2005). How the ear's works work: mechano-electrical transduction and amplification by hair cells. *C R Biol* 328, 155-162.
- Hullar, T.E. (2006). Semicircular canal geometry, afferent sensitivity, and animal behavior. *Anat Rec A Discov Mol Cell Evol Biol* 288, 466-472.
- Huterer, M., and Cullen, K.E. (2002). Vestibuloocular reflex dynamics during high-frequency and high-acceleration rotations of the head on body in rhesus monkey. *J Neurophysiol* 88, 13-28.
- Ingram, N.T., Sampath, A.P., and Fain, G.L. (2016). Why are rods more sensitive than cones? *J Physiol* 594, 5415-5426.
- Jones, T.A., Jones, S.M., and Hoffman, L.F. (2008). Resting Discharge Patterns of Macular Primary Afferents in Otoconia-Deficient Mice. *J Assoc Res Otolaryngol* 9, 490-505.
- Kassardjian, C.D., Tan, Y.F., Chung, J.Y., Heskin, R., Peterson, M.J., and Broussard, D.M. (2005). The site of a motor memory shifts with consolidation. *J Neurosci* 25, 7979-7985.
- Kawamura, S. (1994). Molecular mechanism of light-adaptation in retinal photoreceptors. *Keio J Med* 43, 149-154.
- Kawamura, S., and Tachibanaki, S. (2022). Molecular bases of rod and cone differences. *Prog Retin Eye Res* 90, 101040.
- Knorr, A.G., Gravot, C.M., Gordy, C., Glasauer, S., and Straka, H. (2018). I spy with my little eye: a simple behavioral assay to test color sensitivity on digital displays. *Biol Open* 7, bio035725.
- Koundakjian, E.J., Appler, J.L., and Goodrich, L.V. (2007). Auditory neurons make stereotyped wiring decisions before maturation of their targets. *J Neurosci* 27, 14078-14088.
- Lacour, M., and Tighilet, B. (2010). Plastic events in the vestibular nuclei during vestibular compensation: the brain orchestration of a "deafferentation" code. *Restor Neurol Neurosci* 28, 19-35.

- Lambert, F.M., and Bacqué-Cazenave, J. (2020). Rules and Mechanistic Principles for the Ontogenetic Establishment of Vestibular Function. In *The Senses: A Comprehensive Reference*, Vol 6, Fritzsche, B., Straka, H., eds (Elsevier), pp. 162-172.
- Lambert, F.M., Bacqué-Cazenave, J., Le Seach, A., Arama, J., Courtand, G., Tagliabue, M., Eskiizmirli, S., Straka, H., and Beraneck, M. (2020). Stabilization of Gaze during Early *Xenopus* Development by Swimming-Related Utricular Signals. *Curr Biol* 30, 746-753.
- Lambert, F.M., Beck, J.C., Baker, R., and Straka, H. (2008). Semicircular canal size determines the developmental onset of angular vestibuloocular reflexes in larval *Xenopus*. *J Neurosci* 28, 8086-8095.
- Lambert, F.M., Beraneck, M., Straka, H., and Simmers, J. (2023). Locomotor efference copy signaling and gaze control: An evolutionary perspective. *Curr Opin Neurobiol* 82, 102761.
- Lambert, F.M., Combes, D., Simmers, J., and Straka, H. (2012). Gaze stabilization by efference copy signaling without sensory feedback during vertebrate locomotion. *Curr Biol* 22, 1649-1658.
- Lambert, F.M., and Straka, H. (2012). The Frog Vestibular System as a Model for Lesion-Induced Plasticity: Basic Neural Principles and Implications for Posture Control. *Front Neurol* 3, 42.
- Lindeman, H.H. (1969). Studies on the morphology of the sensory regions of the vestibular apparatus with 45 figures. *Ergeb Anat Entwicklungsgesch* 42, 1-113.
- Linford, N.J., Kuo, T.H., Chan, T.P., and Pletcher, S.D. (2011). Sensory perception and aging in model systems: from the outside in. *Annu Rev Cell Dev Biol* 27, 759-785.
- Lipovsek, M., and Wingate, R.J. (2018). Conserved and divergent development of brainstem vestibular and auditory nuclei. *elife* 7, e40232.
- Lisberger, S.G., Miles, F.A., Optican, L.M., and Eighmy, B.B. (1981). Optokinetic response in monkey: underlying mechanisms and their sensitivity to long-term adaptive changes in vestibuloocular reflex. *J Neurophysiol* 45, 869-890.
- Lysakowski, A., and Goldberg, J.M. (2004). Morphophysiology of the Vestibular Periphery. In *The Vestibular System*, Vol 19, Highstein, S.M., Fay, R.R., Popper, A.N. eds (Springer, NY), pp. 57-152.
- Mackowetzky, K., Yoon, K.H., Mackowetzky, E.J., and Waskiewicz, A.J. (2021). Development and evolution of the vestibular apparatuses of the inner ear. *J Anat* 4, 801-828.
- Maklad, A., and Fritzsche, B. (2003). Development of vestibular afferent projections into the hindbrain and their central targets. *Brain Res Bull* 60, 497-510.
- Malinvald, D., Vassias, I., Reichenberger, I., Rössert, C., and Straka, H. (2010). Functional organization of vestibular commissural connections in frog. *J Neurosci* 30, 3310-3325.
- Mauss, A.S., Vlasits, A., Borst, A., and Feller, M. (2018). Visual Circuits for Direction Selectivity. *Annu Rev Neurosci* 40, 211-230.

- Mauss, A.S., and Borst, A. (2020). Optic flow-based course control in insects. *Curr Opin Neurobiol* 60, 21-27.
- Marder, E., and Calabrese, R.L. (1996). Principles of rhythmic motor pattern generation. *Physiol Rev* 76, 687-717.
- Masseck, O.A., and Hoffmann, K.P. (2009). Comparative neurobiology of the optokinetic reflex. *Ann N Y Acad Sci* 1164, 430-439.
- Mateos-Aparicio, P., and Rodríguez-Moreno, A. (2019). The Impact of Studying Brain Plasticity. *Front Cell Neurosci* 13:66.
- Matsumoto, A., Briggman, K.L., and Yonehara, K. (2019). Spatiotemporally Asymmetric Excitation Supports Mammalian Retinal Motion Sensitivity. *Curr Biol* 29, 3277-3288.
- McKenna, O.C., and Wallman, J. (1985). Accessory optic system and pretectum of birds: comparisons with those of other vertebrates. *Brain Behav Evol* 26, 91-116.
- Meehan, C.F., Grondahl, L., Nielsen, J.B., and Hultborn, H. (2012). Fictive locomotion in the adult decerebrate and spinal mouse *in vivo*. *J Physiol* 590, 289-300.
- Meredith, F.L., and Rennie, K.J. (2016). Channeling your inner ear potassium: K(+) channels in vestibular hair cells. *Hear Res* 338, 40-51.
- Miles, F.A., and Lisberger, S.G. (1981). Plasticity in the vestibulo-ocular reflex: a new hypothesis. *Annu Rev Neurosci* 4, 273-299.
- Mouritsen, H. (2015). Magnetoreception in Birds and Its Use for Long-Distance Migration. In *Sturkie's Avian Physiology, Sixth Edition*, Scanes CG ed (Academic Press), pp. 113-133.
- Mukhopadhyay, M., and Pangrsic, T. (2022). Synaptic transmission at the vestibular hair cells of amniotes. *Mol Cell Neurosci* 121, PMID: 103749.
- Muller, M. (1999). Size limitations in semicircular duct systems. *J Theor Biol* 198, 405-437.
- Muller, M., and Verhagen, J.H.G. (2002). Optimization of the mechanical performance of a two-duct semicircular duct system-part 2: excitation of endolymph movements. *J Theor Biol* 216, 425-442.
- Newlands, S.D., Dara, S., and Kaufman, G.D. (2005). Relationship of static and dynamic mechanisms in vestibuloocular reflex compensation. *Laryngoscope* 115, 191-204.
- Nieuwkoop, P.D., and Faber, J. (1994). *Normal Table of Xenopus laevis (Daudin): A Systematical and Chronological Survey of the Development from the Fertilized Egg Till the End of Metamorphosis*. Garland Pub., New York.
- Nye, H.L., Cameron, J.A., Chernoff, E.A., and Stocum, D.L. (2003). Extending the table of stages of normal development of the axolotl: limb development. *Dev Dyn* 226, 555-560.

- Panichi, R., Dieni, C.V., Sullivan, J.A., Biscarini, A., Contemoni, S., Faralli, M., and Pettorossi, V.E. (2022). Inhibition of androgenic pathway impairs encoding of cerebellar-dependent motor learning in male rats. *J Comp Neurol* 530, 2014-2032.
- Pascual-Leone, A., Amedi, A., Fregni, F., and Merabet, L.B. (2005). The plastic human brain cortex. *Annu Rev Neurosci* 28, 377-401.
- Paterson, J., Menzies, J., Bergquist, F., and Dutia, M.B. (2005). Cellular Mechanisms of Vestibular Compensation. *Neuroembryol Aging* 3, 183-193.
- Platt, C., and Straka, H. (2020). Vestibular Endorgans in Vertebrates and Adequate Sensory Stimuli. In *The Senses: A Comprehensive Reference*, Vol 6, Fritzsche, B., Straka, H., eds (Elsevier), pp. 108-128.
- Popper, A.N., Ramcharitar, J., and Campana, S.E. (2005). Why otoliths? Insights from inner ear physiology and fisheries biology. *Mar Freshw Res* 56, 497-504.
- Precht, W. (1979). Vestibular Mechanisms. *Ann Rev Neurosci* 2, 265-289.
- Rajan, G., Lafaye, J., Faini, G., Carbo-Tano, M., Duroure, K., Tanese, D., Panier, T., Candelier, R., Henninger, J., Britz, R., Judkewitz, B., Gebhardt, C., Emiliani, V., Debregeas, G., Wyart, C., and Del Bene, F. (2022). Evolutionary divergence of locomotion in two related vertebrate species. *Cell Rep* 38, 110585.
- Rillich, J., Stevenson, P.A., and Pflueger, H.J. (2013). Flight and Walking in Locusts-Cholinergic Co-Activation, Temporal Coupling and Its Modulation by Biogenic Amines. *PLoS One* 8, e62899.
- Rinaudo, C.N., Schubert, M.C., Figtree, W.V., Todd, C.J. and Migliaccio, A.A. (2019). Human vestibulo-ocular reflex adaptation is frequency selective. *J Neurophysiol* 122, 984-993.
- Roberts, B.L., and Russell, I.J. (1972). The activity of lateral-line afferent neurons in stationary and swimming dogfish. *J Exp Biol* 57, 435-448.
- Robovska-Havelkova, P., Aerts, P., Rocek, Z., Prikryl, T., Fabre, A.C., and Herrel, A. (2014). Do all frogs swim alike? The effect of ecological specialization on swimming kinematics in frogs. *J Exp Biol* 217, 3637-3644.
- Rohregger, M., and Dieringer, N. (2003). Postlesional vestibular reorganization improves the gain but impairs the spatial tuning of the maculo-ocular reflex in frogs. *J Neurophysiol* 90, 3736-3749.
- Roth, G., Dicke, U., and Nishikawa, K. (1992). How do Ontogeny, Morphology, and Physiology of Sensory Systems Constrain and Direct the Evolution of Amphibians? *Am Nat* 139, 105-124.
- Sadeghi, S.G., and Beraneck, M. (2020). Task-Specific Differentiation of Central Vestibular Neurons and Plasticity During Vestibular Compensation. In *The Senses: A Comprehensive Reference*, Vol 6, Fritzsche, B., Straka, H. eds (Elsevier), pp. 290-308.
- Sadeghi, S.G., Minor, L.B., and Cullen, K.E. (2012). Neural Correlates of Sensory Substitution in Vestibular Pathways Following Complete Vestibular Loss. *J Neurosci* 32, 14685-14695.

- Schreckenberg, G.M., and Jacobson, A.G. (1975). Normal stages of development of the axolotl. *Ambystoma mexicanum*. *Dev Biol* 42, 391-400.
- Schroeder, D.M., and Loop, M.S. (1976). Trigeminal projections in snakes possessing infrared sensitivity. *J Comp Neurol* 169, 1-11.
- Schweigart, G., Mergner, T., and Becker, W. (1995). Eye Stabilization by Vestibulo-ocular Reflex (VOR) and Optokinetic Reflex (OKR) in Macaque Monkey: Which Helps Which?. *Acta Otolaryngol* 115, 19-25.
- Schweigart, G., Mergner, T., Evdokimidis, I., Morand, S., and Becker, W. (1997). Gaze stabilization by optokinetic reflex (OKR) and vestibulo-ocular reflex (VOR) during active head rotation in man. *Vision Res* 37, 1643-1652.
- Sillar, K.T., Combes, D., Ramanathan, S., Molinari, M., and Simmers, J. (2008). Neuromodulation and developmental plasticity in the locomotor system of anuran amphibians during metamorphosis. *Brain Res Rev* 57, 94-102.
- Sillar, K.T., Simmers, J., and Combes, D. (2023). From tadpole to adult frog locomotion. *Curr Opin Neurobiol* 82, 102753.
- Simon, F., Pericat, D., Djian, C., Fricker, D., Denoyelle, F., and Beraneck, M. (2020). Surgical techniques and functional evaluation for vestibular lesions in the mouse: unilateral labyrinthectomy (UL) and unilateral vestibular neurectomy (UVN). *J Neurol* 267, 51-61.
- Simpson, J.I., Leonard, C.S., and Soodak, R.E. (1988). The accessory optic system. Analyzer of self-motion. *Ann N Y Acad Sci* 545, 170-179.
- Smith, P.F., and Curthoys, I.S. (1989). Mechanisms of recovery following unilateral labyrinthectomy: a review. *Brain Res Rev* 14, 155-180.
- Spencer, R.F., and Porter, J.D. (2006) Biological organization of the extraocular muscles. *Prog Brain Res* 151, 43-80.
- Spoor, F., Bajpai, S., Hussain, S.T., Kumar, K., and Thewissen, J.G.M. (2002). Vestibular evidence for the evolution of aquatic behaviour in early cetaceans. *Nature* 417, 163-166.
- Spoor, F., Garland Jr., T., Krovitz, G., Ryan, T.M., Silcox, M.T., and Walker, A. (2007). The primate semicircular canal system and locomotion. *Proc Natl Acad Sci U S A* 104, 10808-10812.
- Stehouwer, D.J. (1987). Compensatory eye movements produced during fictive swimming of a deafferented, reduced preparation in vitro. *Brain Res* 410, 264-268.
- Steinhausen, W. (1931). Über den Nachweis der Bewegung der Cupula in der intakten Bogengansampulle des Labyrinthes bei der natürlichen rotatorischen und calorischen Reizung. *Pflügers Archiv* 228, 322-328.
- Stenkamp, D.L. (2015). Development of the Vertebrate Eye and Retina. *Prog Mol Biol Transl Sci* 134, 397-414.

- Straka, H. (2010). Ontogenetic rules and constraints of vestibulo-ocular reflex development. *Curr Opin Neurobiol* 20, 689-695.
- Straka, H., and Baker, R. (2013). Vestibular blueprint in early vertebrates. *Front Neural Circuits* 7, 182.
- Straka, H., and Dieringer, N. (1991). Internuclear neurons in the ocular motor system of frogs. *J Comp Neurol* 312, 537-548.
- Straka, H., and Dieringer, N. (2004). Basic organization principles of the VOR: lessons from frogs. *Prog Neurobiol* 73, 259-309.
- Straka, H., Fritzschn, B., and Glover, J.C. (2014). Connecting ears to eye muscles: evolution of a 'simple' reflex arc. *Brain Behav Evol* 83, 162-175.
- Straka, H., and Gordy, C. (2020). The Vestibular System: The “Leatherman™” Among Sensory Systems. In *The Senses: A Comprehensive Reference*, Vol 6, Fritzschn, B., Straka, H., eds (Elsevier), pp. 708-720.
- Straka, H., and Simmers, J. (2012). *Xenopus laevis*: an ideal experimental model for studying the developmental dynamics of neural network assembly and sensory-motor computations. *Dev Neurobiol* 72, 649-663.
- Straka, H., Simmers, J., and Chagnaud, B.P. (2018). A New Perspective on Predictive Motor Signaling. *Curr Biol* 28, R232-R243.
- Straka, H., Lambert, F.M., and Simmers, J. (2022). Role of locomotor efference copy in vertebrate gaze stabilization. *Front Neural Circuits* 16, 1040070.
- Straka, H., Paulin, M.G., and Hoffman, L.F. (2021). Translations of Steinhausen’s Publications Provide Insight Into Their Contributions to Peripheral Vestibular Neuroscience. *Front Neurol* 12, PMID: 34149604
- Straka, H., Vibert, N., Vidal, P.P., Moore, L.E., and Dutia, M.B. (2005). Intrinsic membrane properties of vertebrate vestibular neurons: function, development, and plasticity. *Prog Neurobiol* 76, 349-392.
- Straka, H., Zwergal, A., and Cullen, K.E. (2016). Vestibular animal models: contributions to understanding physiology and disease. *J Neurol* 263 Suppl 1, S10-23.
- Sung, C.H, Makino, C., Baylor, D., and Nathans, J. (1994). A rhodopsin gene mutation responsible for autosomal dominant retinitis pigmentosa results in a protein that is defective in localization to the photoreceptor outer segment. *J Neurosci* 14, 5818-5833.
- Tanahashi, S., Ashihara, K., and Ujike, H. (2015). Effects of auditory information on self-motion perception during simultaneous presentation of visual shearing motion. *Front Psychol* 6, 749.
- Taylor, W.R., and Smith, R.G. (2012). The role of starburst amacrine cells in visual signal processing. *Vis Neurosci* 29, 73-81.

- Turrigiano, G. (2012). Homeostatic synaptic plasticity: local and global mechanisms for stabilizing neuronal function. *Cold Spring Harb Perspect Biol* 4, a005736.
- Vega, R., Alexandrov, V.V., Alexandrova, T.B., and Soto, E. (2008). Mathematical Model of the Cupula-Endolymph System with Morphological Parameters for the Axolotl (*Ambystoma tigrinum*) Semicircular Canals. *Open Med Inform J* 2, 138-148.
- Vibert, N., Bantikyan, A., Babalian, A., Serafin, M., Mühlethaler, M., and Vidal, P.P. (1999). Post-lesional plasticity in the central nervous system of the guinea-pig: a “top-down” adaptation process? *Neuroscience* 94, 1-5.
- Vidal, P.P., de Waele, C., and Mühlethaler, M. (2016). Vestibular compensation revisited. *Otolaryngol Head Neck Surg* 119, 34-42.
- von Uckermann, G., Le Ray, D., Combes, D., Straka, H., and Simmers, J. (2013). Spinal efference copy signaling and gaze stabilization during locomotion in juvenile *Xenopus* frogs. *J Neurosci* 33, 4253-4264.
- Wibble, T., Pansell, T., Grillner, S., and Pérez-Fernández, J. (2022). Conserved subcortical processing in visuo-vestibular gaze control. *Nat Commun* 13, 4699.
- Yagi, T., and Markham, C.H. (1984). Neural correlates of compensation after hemilabyrinthectomy. *Exp Neurol* 84, 98-108.
- Yang, A., and Hullar, T.E. (2007). Relationship of semicircular canal size to vestibular-nerve afferent sensitivity in mammals. *J Neurophysiol* 98, 3197-3205.
- Zwergal, A., Lindner, M., Grosch, M., and Dieterich, M. (2022). In vivo neuroplasticity in vestibular animal models. *Mol Cell Neurosci* 120, 103721.

---

## ACKNOWLEDGMENTS

---

What an incredible adventure the past few years have been! It's unbelievable that this chapter of my life has come to a close. Herewith I would like to express my gratitude to all the people who accompanied me on this PhD journey, contributing to my personal and professional growth.

First off, my supervisor and mentor Prof. Dr. Hans Straka. Hans, I am incredibly sad that you will never be able to witness the outcome of the many years you accompanied me throughout my academic life, starting from my early days of studying. I truly appreciated your excitement for science, creativity, and immense support in both personal and professional matters. Your consistent availability for your students, and the ability to walk to your office to share any scientific success or failure at any time, kept me motivated to move on. Your high standards for writing have certainly made a lasting impact. Antje and Veronika, thank you for following my progress and meeting with us to process the shock of Hans' unexpected loss. It helped and felt good to still have some connection to Hans' life.

I would also like to greatly thank Prof. Dr. med. Andreas Zwergal for taking over my supervision without a second thought. I really appreciate that you took over this role despite your very busy schedule and without knowing me personally before. Thank you for your interest in my research and for your support.

I especially would like to express my gratitude to Dr. François M Lambert, my dream boss from France. Thanks to you, I rediscovered the joy of doing science! Completing my project and this thesis became truly enjoyable, and this would have been impossible without your guidance and patience.

My profound thanks are due to all the members of the Straka lab for all the support throughout the years. Rosario, thank you for your help, teaching, and influence on my scientific standards during the initial stages of my PhD. Clayton and Michi, expressing my gratitude fully is a challenge! Thank you for the countless laughs, support, discussions, and unforgettable moments in and outside the lab. I am grateful for having you on my side!

Further I would like to thank Prof. Dr. Benedikt Grothe, Prof. Dr. Laura Busse, PD Dr. Lars Kunz, PD Dr. Michael Pecka, Prof. Dr. Oliver Behrend, Dr. Pepe Alcami, and PD Dr. Conny Kopp-Scheinflug for their guidance, particularly during the final phase of my PhD. Laura and Conny, I am immensely grateful for your support and help during a very difficult time of my doctoral journey.

I would also like to thank my TAC committee members, Prof. Dr. Silvia Cappello and Prof. Dr. Marianne Dieterich for fruitful discussions, and Prof. Dr. Ansgar Büschges for reviewing this thesis.

Additional gratitude goes to the GSN and to Verena Winkler, Stefanie Bosse, Dr. Raluca Goron, Katrin Birner, Yamei Li, and Nadine Hamze for their efforts, help and kindness.

Finally, heartfelt thanks to my family and friends. Listing each one of you would require a thesis of its own. Thanks for your love, always being there for me when I needed it and belief in me! Felix, words cannot express my gratitude for having you on my side! Your love, support and encouragement sustained me throughout the challenging journey of my PhD.

---

## LIST OF PUBLICATIONS

---

**Schneider-Soupiadis, P.**, Forsthofer, M., Courtand, G., Schneider-Soupiadis, F., Sanchez-Gonzalez, R., Lambert, F.M., and Straka, H. (in preparation). A functional comparison between inner ear morphology, gaze stabilization, and locomotion in larval amphibians.

Gordy, C., Forsthofer, M., **Soupiadou, P.**, Özugur, S., and Straka, H. (2022). Functional neurobiology in *Xenopus* provides insights into health and disease. In: Moody, S., Fainsod, A. (Eds.), *Xenopus, from basic biology to disease models in the genomic era*. CRC Press. 277-288. doi.org/10.1201/9781003050230-22.

**Soupiadou, P.**, Gordy, C., Forsthofer, M., Sanchez-Gonzalez, R., and Straka, H. (2020). Acute consequences of a unilateral VIIIth nerve transection on vestibulo-ocular and optokinetic reflexes in *Xenopus laevis* tadpoles. *J Neurol* 267, 62-65. doi.org/10.1007/s00415-020-10205-x.

**Soupiadou, P.**, Branoner, F., and Straka, H. (2018). Pharmacological profile of vestibular inhibitory inputs to superior oblique motoneurons. *J Neurol* 265, 18-25. doi.org/10.1007/s00415-018-8829-4.

---

## AI DISCLOSURE

---

During the preparation of this work, I used ChatGPT and Grammarly to improve readability and to verify grammar and spelling. Despite the grammatical and structural changes suggested by these tools, the intellectual content of this dissertation remains unchanged from original versions provided to the tools and is thus wholly the product of the author. I, the author, take full responsibility for the content produced therein.

Munich, 06.02.2024

---

Place, Date

Parthena Schneider-Soupiadis

---

Unterschrift / Signature

---

## AFFIDAVIT/EIDESTÄTLICHE ERKLÄRUNG

---

Eidesstattliche Versicherung/Affidavit

Hiermit versichere ich an Eides statt, dass ich die vorliegende Dissertation **Visuo-vestibular sensorimotor plasticity in Xenopus and Axolotl larvae** selbstständig angefertigt habe, mich außer der angegebenen keiner weiteren Hilfsmittel bedient und alle Erkenntnisse, die aus dem Schrifttum ganz oder annähernd übernommen sind, als solche kenntlich gemacht und nach ihrer Herkunft unter Bezeichnung der Fundstelle einzeln nachgewiesen habe.

I hereby confirm that the dissertation **Visuo-vestibular sensorimotor plasticity in Xenopus and Axolotl larvae** is the result of my own work and that I have only used sources or materials listed and specified in the dissertation.

Munich, 06.02.2024

Parthena Schneider-Soupiadis

---

Place, Date

---

Unterschrift / Signature

---

## DECLARATION OF AUTHOR CONTRIBUTIONS

---

### Chapter II:

A functional comparison between inner ear morphology, gaze stabilization, and locomotion in larval amphibians.

**Parthena Schneider-Soupiadis**, Michael Forsthofer, Gilles Courtand, Rosario Sanchez-Gonzales, François M. Lambert and Hans Straka

(Unpublished manuscript)

#### Contribution of authors:

Conceptualization: PS, MF, RSG, FML, HS; Methodology: PS, MF, GC, FML, HS; Investigation: PS, MF, FML, HS; Formal analysis: PS, MF, GC, FML; Software: MF, GC, FML; Visualization: PS, FML; Writing-original draft: PS, MF, FML, HS; Writing-review & editing: PS, MF, RSG, FML; Funding acquisition: FML, HS.

#### My contributions to this manuscript:

I contributed to the design of experiments and the conceptualization of analysis scripts. I performed all experiments and analyzed the anatomical comparisons of *Xenopus* and Axolotl larvae, visuo-vestibular eye tracking data, and 2D canal injection data. I created initial versions of the figures and contributed to revisions on all figures. I wrote the initial version of the manuscript and contributed to the editing process.

I hereby confirm the accuracy of the above author contributions.

---

Place, Date

---

Parthena Schneider-Soupiadis

---

Place, Date

---

Dr. François M Lambert

---

Place, Date

---

Prof. Dr. med. Andreas Zwergal

### Chapter III:

Acute consequences of a unilateral VIIIth nerve transection on vestibulo-ocular and optokinetic reflexes in *Xenopus laevis* tadpoles.

**Parthena Soupiadou**, Clayton Gordy, Michael Forsthofer, Rosario Sanchez-Gonzales, Hans Straka

(Published paper, *Journal of Neurology*, 2020)

#### Contribution of authors:

Conceptualization: PS, CG, RSG, HS; Methodology: PS, CG, RSG, HS; Investigation: PS, HS; Formal analysis: PS, MF; Software: MF; Visualization: PS, HS; Writing-original draft: PS, HS; Writing-review & editing: PS, CG, MF, RSG, HS; Funding acquisition: HS.

#### My contributions to this manuscript:

I contributed to the design of experiments and the conceptualization of analysis scripts. I performed all experiments and analyses thereof. I created initial versions of the figures and supplemental figures and contributed to revisions on all figures. I took part in writing the initial version of the manuscript and contributed to the editing process.

I hereby confirm the accuracy of the above author contributions.

---

Place, Date

---

Parthena Schneider-Soupiadis

---

Place, Date

---

Dr. Clayton Gordy

---

Place, Date

---

Michael Forsthofer

---

Place, Date

---

Dr. Rosario Sanchez-Gonzalez

---

Place, Date

---

Prof. Dr. med. Andreas Zwergal